Power Electronic Based Active Protection for Worksite Accidental Energization

by

Tianyi Hou

A thesis submitted in partial fulfillment of the requirements for the degree of

Master of Science

in

Energy Systems

Department of Electrical and Computer Engineering
University of Alberta

Abstract

Worksite safety is a major concern for utility companies maintaining distribution systems. Electric hazards often occur when worksite equipment accidentally contacts a live power line. This leads to dangerous ground potential rise, touch voltage or step voltage in surrounding areas. A number of approaches have been adopted by utility companies to ensure electrical safety on worksites. One of these involves trip grounding. Trip grounding is realized by connecting the equipment with a grounding rod. Once the equipment is energized, a relay at a substation will operate and trip the power supply due to the large fault current. Frequently however, when worksite grounding resistance or system impedance is high, the fault current will be low. This may result in a long fault clearing time or a tripping failure.

In order to overcome the above limitations, this study proposes and tests a new approach to actively generate signals with specific patterns from an energized worksite using power electronic devices. Once these specific signals, transmitted through the power line itself, are recognized by a signal detector at the closest upstream recloser, the recloser trips the power supply and protects the worksite safety. The proposed method is first implemented using a diode-based signal generator scheme, which has a simple configuration but restricted application range. Then the approach is further refined using a thyristor-based signal generator scheme to fit a wide range of worksite conditions. As a result,

worksite safety can be improved in a short time despite wide system parameter variations, such as high grounding resistance and long feeder distance.

Practical considerations for prototype designs and parameter settings of the proposed active protection schemes are presented in this thesis. Simulation studies and sensitivity analysis are conducted to evaluate tripping performance. Comparative studies with conventional relay protection reveal that the proposed schemes offer better response speed and adapt to various worksite conditions.

Acknowledgement

First and foremost, I would like to express my most sincere gratitude to my supervisor, Dr. Wilsun Xu for his tireless guidance and continuous support in my M.Sc. study and related research. Throughout these more than two years' studies, Dr. Xu supervised me on scientific research approaches, pointed my research direction with a vision for Power Systems issues, and served as my role model in pursuing high standards in both academic and industry projects. All these endeavors help me build logical thinking abilities, practical trouble shooting skills, and rigorous research methods which will make an assuring positive difference to my future career.

I would like to show my special appreciation to Dr. Jing Yong for her great contribution to this thesis through inspired discussions on proposed ideas, productive suggestion on implementation methods, and consistent guidance in report writings. I am also pleased to thank Dr. Xiangguo Yang for the efficient cooperation in lab experiments. Thanks to Tianyu Ding for imparting his extensive knowledge in Power System studies. I would also like to thank everyone working in PDS-LAB for all the support and friendship in the last two years.

Finally and most importantly, I would like to express gratitude to my parents Mr. Yuesheng Hou and Mrs. Yan Yang for their ceaselessly encouragement and unconditional love.

Contents

List of Tables

List of Figures

Chapter 1
Introduction

A variety of construction activities often occur near the overhead distribution lines. At worksites, large and heavy mobile equipment, such as cranes, excavators and concrete pumps, are commonly operated nearby the power lines and thus the live power lines can be contacted or hit by those equipment in many accidents. Although mandatory safety standards, operation regulations and personnel training are applied by utility companies at worksites, it has been reported that many incidents where power lines hit the equipment occur every year, resulting in fatalities or serious injuries at worksites.

According to the U.S. Bureau of Labor Statistics (BLS), there were 6,000 fatal electrical injuries that happened on workers in the U.S. between 1992 and 2013, and 24,100 non-fatal electrical injuries from 2003 to 2012 [1]. More than 90 percent of these worksite incidents occurred because equipment or workers contacted electrical live circuits when workers were working in the proximity of power lines. While in Canada, according to the data from Alberta Municipal Affairs, a total of 4894 power line contacting accidents were reported during the period of 2006 to 2014 in Alberta, as shown in Figure 1.1 [2]. Among those incidents, 3663 and 1212 contacts were associated with overhead power lines and underground power cables, respectively. As a result, 9 fatal injuries and 81 non-fatal injuries occurred. These tragedies have prompted serious safety concerns at worksites.

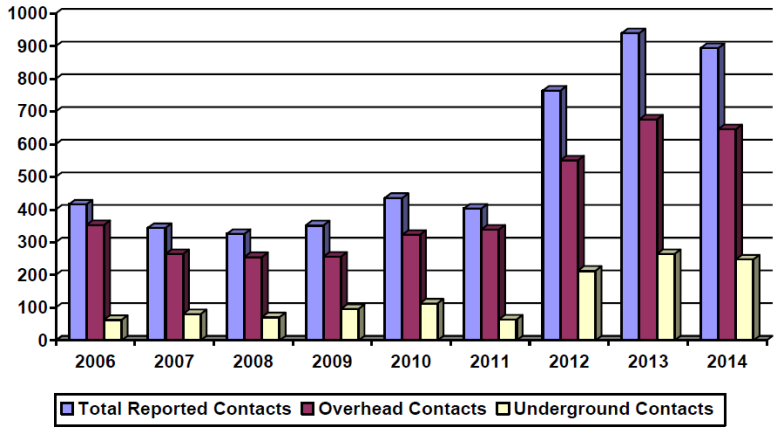

(a) Power line contacts

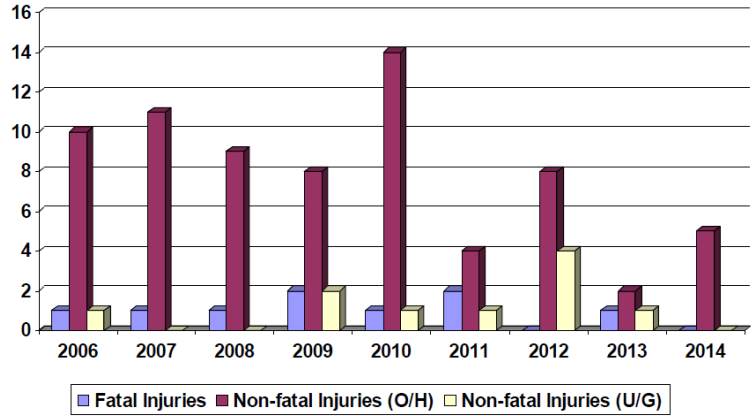

(b) Power line contact caused injuries

Figure 1.1 Reported power line contacts and injury data during 2006 to 2014 [3]

As per statistical data from Alberta Municipal Affairs [2], most of the power line contacting accidents happen at distribution lines which are commonly present at most construction and maintenance worksites. When workers are working in the proximity of energized distribution lines, the equipment (e.g. cranes) that workers operate may come into contact with live lines. This could lead to accidental energization, electric hazards and personnel safety incidents. Therefore, the main safety concern at worksites is that equipment contacts energized distribution lines.

Surprisingly, Figure 1.1(a) shows that the number of incidents due to power line contacting has rapidly increased in the last decade although the mandatory safety standards, operation regulations have been improved and revised over the years. This strongly implies that it is challenging to reduce the contacting incidents only by modifying and improving standards and regulations. It also suggests that technical gaps exist and research should be conducted to improve the technical knowledge and skills to prevent electric hazards resulting from the equipment operation and its contacting with live distribution lines.

1.1 Description of Power Line Involved Electric Hazards

Electric hazards often occur when the equipment contacts a live distribution line since a) overhead lines are typically not insulated; b) underground cables are unnoticed in ground digging practice; c) workplaces are usually crowded and not well organized; d) large and heavy mobile equipment, especially with lifting and extending components, is hard to be precisely controlled.

Table 1.1 shows the number of different power line contacts reported in 2013 and 2014 in Alberta, Canada. Clearly, the power line contacting accidents mainly occur on the large and heavy mobile equipment, such as cranes, excavators, drillers, and dump trucks.

Table 1.1 Electrical power line contacts [3][4]

Overhead systems	**No. of contacts in 2013**	**No. of contacts in 2014**
Vehicle-mounted equipment (booms, hoists, cranes, etc.)	54	57
Trucks with raised boxes and vehicles transporting high loads (dump trucks, aerial lift, concrete pumps, etc.)	112	94

Excavating or earth moving vehicles	136	123
Farm implements (irrigators, croppers, etc.)	101	121
Relocating structures (grain bins, material handling and storage, etc.)	18	4
Vehicles out of control	168	168
Aircraft, parachutes, kites, etc.	7	2
Failing, brushing or trimming trees	46	44
Drilling and seismic equipment	4	11
Others (ladders, scaffolds, etc.)	30	22
Total	**676**	**646**

Underground systems	**No. of contacts in 2013**	**No. of contacts in 2014**
Excavating equipment	189	175
Vehicle hitting transformers, pedestals, etc.	67	56
Others	8	17
Total	**264**	**248**

Figure 1.2 shows the situation of accidental energization of equipment, which is a scenario of trip grounding case in a power system. The equipment is generally grounded at worksites. This equipment grounding is implemented by connecting the equipment to a temporary grounding rod. The rod is primarily applied to form an electric circuit loop with substation grounding. When the equipment is energized, a protection relay at an upstream breaker is used to detect signals and trip the fault overcurrent. If this fault can be detected and removed immediately,

the electric hazard can be avoided. Unfortunately, the trip grounding detection at the breaker is not always as effective as expected in practice. Since grounding resistance can be very large and worksite can be anywhere along power lines, conventional protection relay may not be able to distinguish between a normal load current or a fault current and trip the circuit.

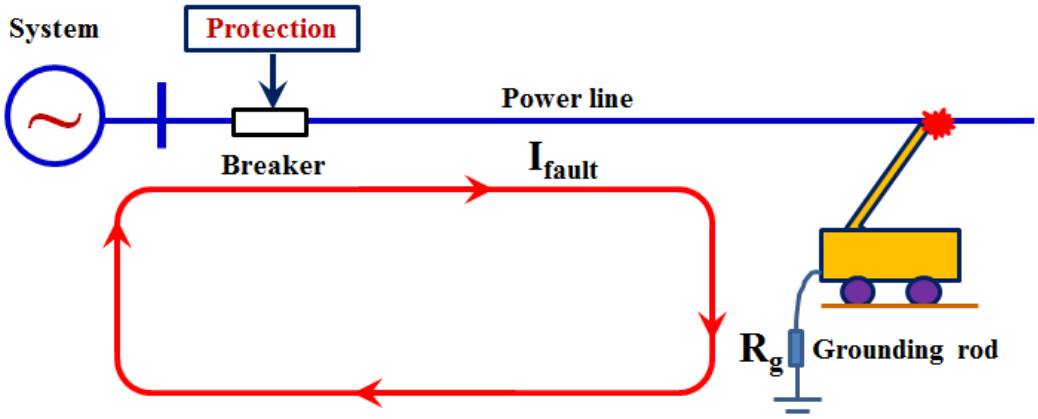

Figure 1.2 Situation of accidental energization of equipment

Consequently, the energized equipment may not be detected and continue to work as being a part of the grounding fault loop and live circuit. This part of the live circuit could produce electric hazards to the public and workers in the proximity. Furthermore, non-utility equipment may not even be grounded, which makes the electric hazard potential even more serious.

1.2 Existing Protection Methods and Issues

To date, four main technical methods including insulation, isolation, equipotential bonding and grounding have been used as protection methods. They can be used on its own or in combination with others to provide personal protection for the public and workers standing or working near the energized facilities. These four protection methods are described as follows:

Insulation

Insulation for workers can be provided by personal protective equipment (PPE) such as insulated gloves, footwear, mats, platforms, and booms. These tools

produce non-conductive separation between workers and energized equipment. However, insulation equipment is not always available in practice. For example, most boom trucks have no insulated boom section, utility workers are not always equipped with proper insulated gloves and footwear, and non-utility workers, such as construction builders and farm keepers, may not be well trained or equipped with electrical protective equipment. It should be emphasized that even if those insulations are available, insulation alone is not sufficient to provide an effective protection against electrical hazards.

Isolation

Isolation is achieved by setting up physical and visual obstructions, such as barricades and barriers, to alert the public and workers to potential danger. However, isolation methods require a large area around the equipment, and although it is an effective method for the public, it is impractical for workers who need to work inside the barricade or operate the equipment.

Equipotential Bonding

Equipotential bonding is a method by which conductive parts are physically interconnected to maintain a common potential. The objective of bonding is to avoid harmful shock currents by minimizing any potential difference across worker's body. Equipotential bonding alone is applicable for hot-line works. However, it is difficult and costly to create an equipotential zone to cover the whole area of the worksite.

Grounding

Grounding is the most common practice at worksites. It is a method by which worksite equipment is connected to a permanent or temporary grounding rod. Once the equipment is energized, a protection relay at a substation should trip the circuit as quickly as possible and minimize ground voltage rise. A permanent grounding can be the tower grounding with a resistance around 0.1 to 2 ohms. A temporary grounding typically uses a two-meter single grounding rod with a

resistance of 10 ~ 100 ohms or even higher value. Based on the large variations of soil resistivity and weather condition in Alberta, the possible grounding resistance ranges widely between 10 and 1000 ohms. Consequently, in most cases, the resistance of the temporary grounding rod is much higher than system impedance and a significant fraction of line voltage appears on the grounding rod and the equipment.

In the case of trip grounding shown in Figure 1.2, an equivalent electric circuit is depicted in Figure 1.3(a). In order to provide a verified trip grounding practice, the grounding resistance should be small enough to cause a low impedance path. As a result, ground fault current can be able to flow back to the source, and ensure a fast ground fault tripping to interrupt accidental worksite energization. In the wide range of grounding resistance values, take values of 10 to 1,000 ohms for example, the higher the grounding resistance, the smaller the fault current will be, and in turn the longer trip time. This inverse relationship of time and current is described in Figure 1.3(b). A long tripping time is not acceptable since longer tripping time could lead to more exposure to dangerous voltage which results in greater accident severity or a fatal electric shock. Furthermore, in some extreme cases where very high grounding resistance exists, because the small fault current is too small, the relay may not be able to effectively detect the fault and fails to interrupt worksite energization.

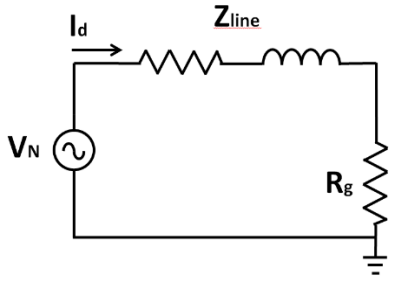

(a) Equivalent electric circuit in trip grounding situations

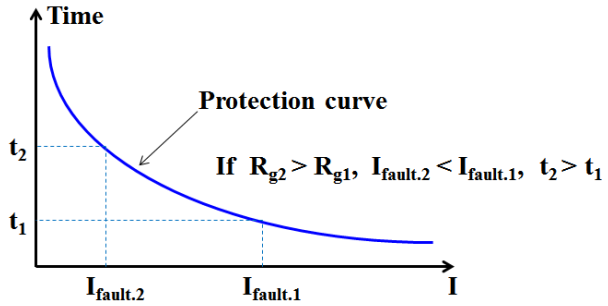

(b) Sensitivity of the protection device

Figure 1.3 Impact of grounding resistance on the trip time

Even if the permanent grounding with low grounding resistance is available, the time of trip grounding may not satisfy safety requirement. This is because the tripping time of protection devices is also dependent on worksite fault locations. The farther the worksite is away from the source, the higher the line impedance becomes. Hence, the farther worksite or higher grounding resistance can reduce the fault current, leading to a longer response time or non-response of protection relays.

To summarize, grounding method is not able to produce safety with full confidence. Instead, it may even produce a false and misleading signal of safety.

In this thesis, a new active protection method for distribution system is proposed to ensure a reliable and fast clearing of worksite energization. This method utilizes an active signaling approach to monitor electric hazard potential at worksites. Once worksite equipment gets contacted with a live power line, a signal generator will immediately send a signal from the worksite to the nearest power line recloser. A proper control of the recloser will automatically trip the corresponding live line in 0.1 s ~ 0.15 s, as long as the equipment grounding resistance is below 1000 ohms. Therefore, personnel can be better protected from electrical hazards.

1.3 Thesis Objectives and Scope

This thesis aims to address the challenges of prompt monitoring for accidental energization and improve its effectiveness and reliability in clearing the induced electric hazards at worksites by using power electronics and modern signal processing technologies. It should be noted that the signaling process in this study only uses the existing power lines as communication media.

The specific research objectives are summarized as follows:

- Review the essential causes of worksite electric hazards and corresponding traditional methods used at worksites to prevent electric hazards;
- Develop a new method for worksite energization protection. Signal generating devices are implemented to send signals from accidental contacting incidents, and signal detecting devices are used to quickly detect the signal with a distinctive pattern and trip the upstream recloser permanently to remove the electric hazard concern;
- Propose two signal generating schemes, develop their design procedures with corresponding algorithms for effectively generating safety alert signal from the signal generator, and promptly and effectively detecting the signal in signal detectors; Verify the developed schemes through extensive simulations and experimental tests.

In order to protect safety in a reliable way, two types of active signaling schemes are proposed in this thesis. A simple diode-based signaling scheme is proposed first with a simple configuration but restricted application range. Subsequently, the scheme is further refined by a more complicated thyristor-based technology. This scheme is of great advantage in wide range of worksite conditions, such as longer distance and higher grounding resistance applications.

Chapter 2 of this thesis presents the essential causes of worksite electric hazards and the practical voltage limits for safety concerns. It also describes the proposed electronic based active protection method as well as working procedure. Then, this chapter further illustrates the design considerations and challenges considering field environment and practical issues.

Chapter 3 and Chapter 4 demonstrate the design methods for diode-based and thyristor-based signal generators and detectors, respectively. This includes the parameter determination methods of signal generators; the signal detection criteria of signal detectors; and the applicable ranges of corresponding active devices. Sensitivity study results are also provided to verify the effectiveness of the proposed methods.

Chapter 5 compares the proposed active protection method for worksite safety with traditional relay protection. It also explores the impact of fault arc on the proposed schemes.

Finally, the main conclusions of this thesis and future works for this field are summarized in Chapter 6.

Chapter 2
Proposed Method for Worksite Energization Protection

As reviewed in Chapter 1, the current technology for worksite energization protection is not sufficiently effective to protect workers from injuries due to the equipment accidental energization. A reliable protection method with fast response to clear the accidental energization is highly expected to be implemented at worksites. In this chapter, a new protection method with two signal generating schemes used to prevent the injuries from the worksite accidental energization is proposed, verified, and discussed in a practical manner.

The response time of conventional relay protection depends on the proper relay pickup setting corresponding to a specific fault level. This may induce missing or delayed relay pickups, which could cause a dangerous voltage exposure and injuries to workers. Unlike conventional relay protection methods, this study proposes a new method that involves actively sending a current signal from worksite and detecting the signal by a signal detector on the other side. Once the signal with unique characteristics is detected, an upstream recloser at the place where the signal was detected will immediately trip and interrupt worksite energization. This active protection method has been proven to be extremely reliable and efficient because it has a fast response time upon receiving signals to help worksite maintain a safe condition and thus avoid a worksite accidental energization and corresponding injuries.

In this chapter, major reasons of electric hazards at worksites and accidental energization accidents are firstly reviewed and analyzed in Section 2.1. Subsequently, voltage limits for keeping personal safety are presented in Section 2.2. Then the proposed active protection method and two signal generating schemes are demonstrated in Section 2.3, followed by design considerations and challenge description in Section 2.4 and summary and conclusions are shown in Section 2.5.

2.1 Essential Causes of Electric Hazards

The electric shock resulting in injury or death is essentially caused by the current conducting in human body. When two parts of human body are connected into a circuit with electric potential difference, current will form and conduct through the human body. This current flow in human body may exceed the tolerable human body current limit [5] and produce injury or even death. Figure 2.1 shows the relation between tolerable current and time, given by both Dalziel's equations [6]– [8] and Biegelmeier's curve [9]. The higher current value tolerable to human body, the shorter time human body can tolerate. In addition, it is reported that it is more likely that heart ventricular fibrillation occurs with increasing magnitude and duration of the current conducted through a human body at 60 Hz [10].

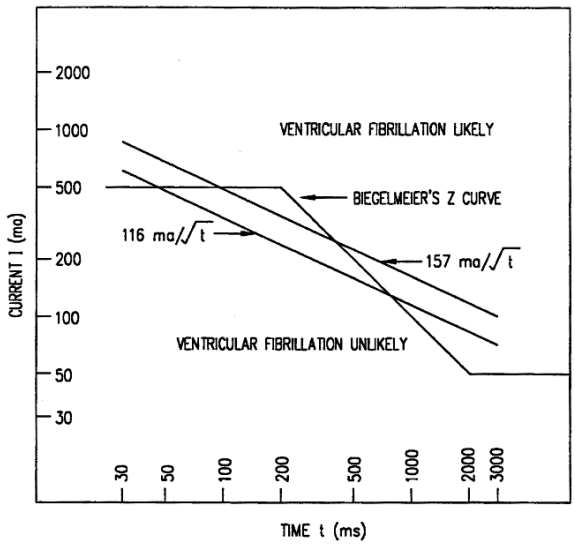

Figure 2.1 Body tolerable current and time [10]

As shown in Figure 1.2 at Section 1.1, the most possible cause of power line contacting to workers is introduced by heavy and large mobile equipment. When equipment accidently contacts a live power line, an excessive Ground Potential Rise will form at the equipment and the grounding area close to the equipment and thus may introduce high Touch Voltage when a worker touches the

equipment and Step Voltage when electric potential difference forms between two feet when a worker is standing at the surrounding worksite as shown in Figure 2.2 (a).

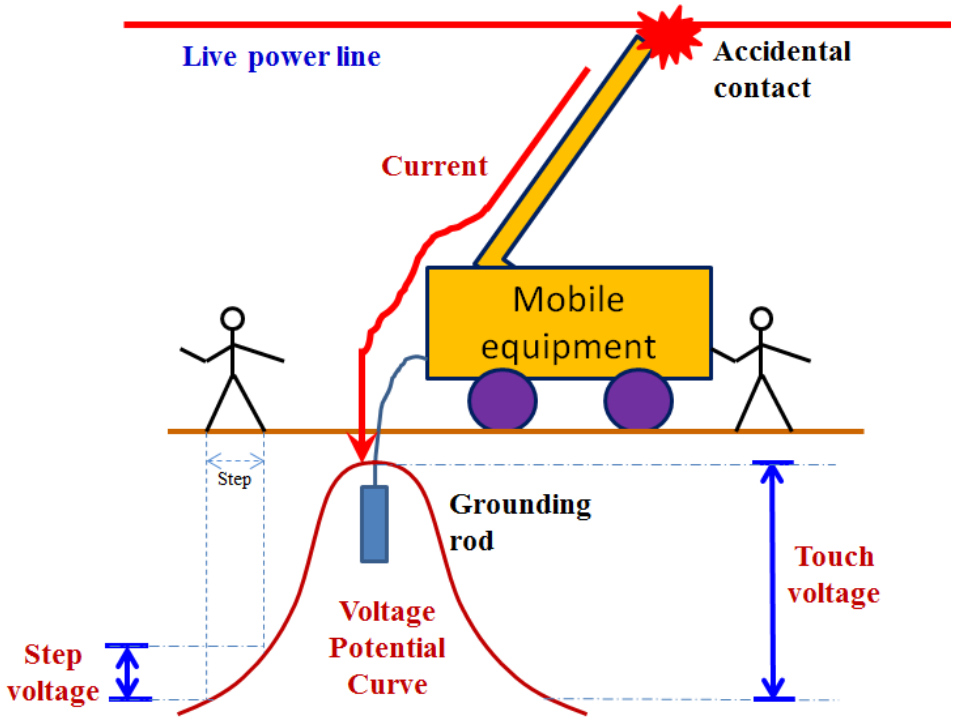

(a) Step Voltage and Touch Voltage

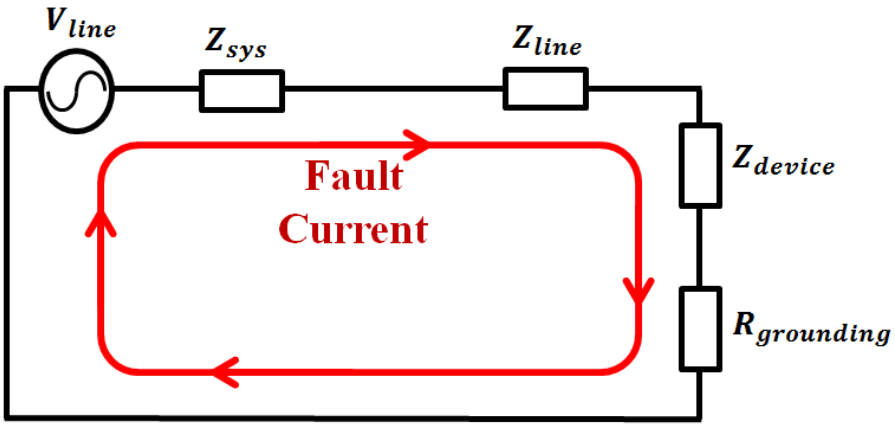

(b) Fault current loop

Figure 2.2 Main causes of worksite electric hazard

To clearly show the essential causes of electric hazards, the mechanism of Ground Potential Rise, Touch Voltage and Step Voltage are explained as follows:

Ground Potential Rise is the maximum electrical potential difference caused due to accidental contacting that may occur and subsequent fault current passing through the circuit.

Under normal conditions, the mobile equipment connects a grounding rod in the earth and near zero ground potential is caused on the ground if the equipment is properly operated. However, for an incident of a grounding fault when the mobile equipment contacts live power line, the portion of fault current, which is conducted by the grounding rod into the earth, causes a significant rise of the grounding potential with respect to remote earth. This Ground Potential Rise produces an amount of voltage, equal to the maximum grounding current times the resistance of grounding rod, as presented in Equation 2.1.

$$V_{GPR} = I_{max} \cdot R_g \tag{2.1}$$

where

V_{GPR} is the grounding voltage due to Ground Potential Rise,

I_{max} is the maximum grounding current,

R_g is the grounding resistance.

Since the impedance of upstream distribution system and power line in the fault circuit is usually much smaller than the grounding resistance, the voltage developed on the grounding is much larger than that on others. Consequently, a great Grounding Potential Rise can be induced.

Touch Voltage is the voltage between an energized object and a person when he or she touches the object.

Once mobile equipment accidentally contacts the energized power line, current path is conducted to the surface of equipment through the media of metal or other conducting parts. The voltage of the equipment is almost equal to the live line-to-ground voltage.

When the equipment contacts a live power line, workers at worksites touching the vehicle or equipment operators attempting to get out of the vehicle may be exposed to the full line-to-ground voltage. The touch is smaller than Ground Potential Rise:

$$V_T \leq V_{GPR} = I_{max} \cdot R_g \tag{2.2}$$

where

V_T is the touch voltage on worker contacting the equipment.

Step Voltage is the voltage between the two feet of a person standing near an energized grounding object.

When a fault occurs at a tower or substation, the current will conduct into the earth. As the resistivity of the soil at the different location is different, a corresponding voltage distribution will occur. The voltage difference in the soil surrounding the grounding system can present hazards for personnel standing in the vicinity of grounding system. Any person "stepping" in the direction of the voltage gradient could be subjected to hazardous voltages. The step voltage can be obtained by [10]:

$$E_s = \frac{\rho \cdot K_s \cdot K_i \cdot I_G}{L_s} \tag{2.3}$$

where

ρ is the soil resistivity,

K_s is the geometrical factor,

K_i is the corrective factor,

I_G is the maximum grid current that conducts between grounding rod and surrounding earth (including *dc* offset) in Ampere (A),

L_s is effective length in m,

I_G/L_s is the average current per unit of buried length of grounding system conductor.

If there is a ground grid present, the maximum step voltage is assumed to occur over a distance of 1 m, beginning at and extending outside of the perimeter conductor at the angle bisecting the most extreme corner of the grid. For the usual burial depth of 0.25 m < h < 2.5 m [11], K_s is

$$K_S = \frac{1}{\pi}\left[\frac{1}{2 \cdot h} + \frac{1}{D+h} + \frac{1}{D}(1 - 0.5^{n-2})\right] \tag{2.4}$$

where

D is the spacing between parallel conductors in m,

h is the depth of ground grid conductors in m,

n is geometric factor composed of factors n_a, n_b, n_c, and n_d.

For a significant distance away from any given site, hazardous step voltage can still be produced, and the voltage increases with the current that conducts into the ground. Soil resistivity and layering are major factors influencing the severity of the hazard at a specific worksite. As shown in [12], high soil resistivity tends to increase the step voltage.

Hazards from external transferred voltages are usually avoided by applying the existing methods as mentioned in Chapter 1, and these dangerous points should be labeled as that same to live lines. To ensure safety, the actual Touch Voltage or Step Voltage should be less than the respective maximum allowable voltage limits.

2.2 Voltage Limits for Safety Concern

To ensure the safety of a worker, the amount of shock energy that the person absorbs should be less than a limit. As to the maximum voltage in an accidental

circuit, it should not exceed the limits defined in Equation 2.5 [10]. For touch voltage, the limit is

$$E_{touch} = (R_B + \frac{R_f}{2}) \cdot I_B \tag{2.5}$$

where

E_{touch} is the touch voltage limit in V,

R_B is the resistance of a human body in Ω,

R_f is the ground resistance of one foot in Ω,

I_B is the RMS magnitude of the current through the body in A.

For body weight of 50 kg

$$E_{touch50} = (1000 + 1.5C_s \cdot \rho_s) \frac{0.116}{\sqrt{t_s}} \tag{2.6}$$

For body weight of 70 kg

$$E_{touch70} = (1000 + 1.5C_s \cdot \rho_s) \frac{0.157}{\sqrt{t_s}} \tag{2.7}$$

where

C_s is a corrective factor to compute the effective foot resistance in the presence of a finite thickness of surface material,

ρ_s is the resistivity of the surface material in Ω·m,

t_s is the duration of shock current in seconds.

Similarly, the step voltage limit is

$$E_{step} = (R_B + 2R_f) \cdot I_B \tag{2.8}$$

For body weight of 50 kg

$$E_{step50} = (1000 + 6C_s \cdot \rho_s) \frac{0.116}{\sqrt{t_s}} \tag{2.9}$$

For body weight of 70 kg

$$E_{step70} = (1000 + 6C_s \cdot \rho_s)\frac{0.157}{\sqrt{t_s}} \quad (2.10)$$

where

E_{step} is the step voltage in V,

C_s is a corrective factor to compute the effective foot resistance in the presence of a finite thickness of surface material,

ρ_s is the resistivity of the surface material in Ω·m,

t_s is the duration of shock current in seconds.

Based on the above equations, for a general dry sandy or gravel soil ground with surface layer resistivity of 1200 Ohm • m, a granite layer with a corrective factor of 3.2687 [13], and a fault clearing time of 0.100 s, the safety limits of touch voltage and step voltage for 50 kg person are calculated as around 2500 V and around 9000 V, respectively. In reality, the value of grounding resistance varies with its moisture content, soil characteristics, temperature and other environmental condition. This makes it difficult to reach voltage limits on worksite. A practical permanent grounding may have grounding resistance of around 0.1 ~ 2 ohms, but a temporary one typically have grounding resistance of around 10 ~ 100 ohms. If no other protection methods are used, once the equipment is energized, such temporary grounding with high grounding resistance can likely cause injury or death in the proximity. To prevent this tragedy, an alternative method to eliminate electric hazards can be implemented. This method involves an action to shut down the energization source, i.e., trip the corresponding power line.

2.3 Proposed Active Protection Method

Resulting from worksite energization, the signal transmitted can be in the form of a significantly modified power frequency disturbance. This disturbance with signaling power supplied by contacted live line voltage, named as inbound signal, is generated at worksite and transmitted upstream through the existing

power line. To perform this inbound signal transmitting, the devices including a signal generator (SG) and signal detectors (SD) are installed.

As shown in Figure 2.3, the SDs are permanently installed at each recloser and a portable SG is installed at the worksite between the equipment and grounding rod, behaving as a guard watching the worksite at all times. Under a normal condition, no signal will be generated. However, when the accidental contacting on the power line occurs, the equipment is energized immediately by the power source from the live power line, and the SG will be triggered immediately as well. As a result, an emergency signal with a special pattern will be generated by SG and sent out through the contacted power line to the upstream recloser. The SD at the recloser closest to the signal transmitting direction is able to detect and recognize the special signal to trigger a trip action on the recloser within several cycles (about 0.1 s ~ 0.15 s). Therefore, dangerous voltage exposure time can be significantly reduced and the worksite can be maintained at a safe condition.

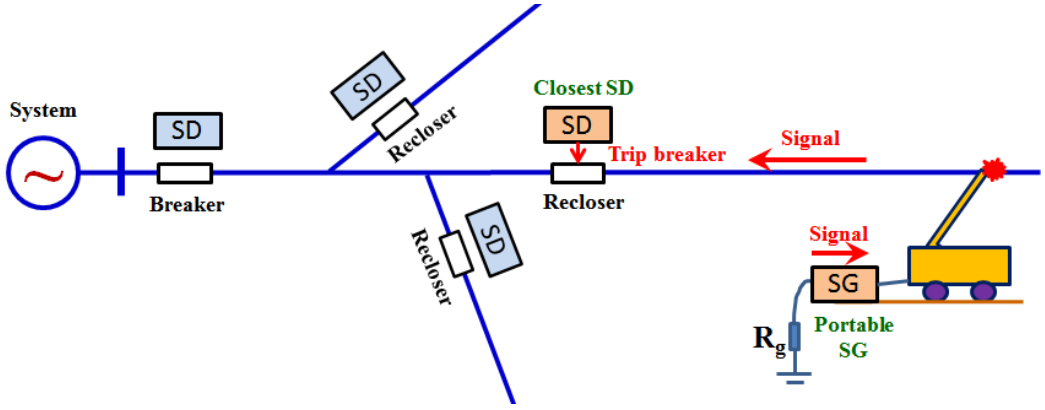

Figure 2.3 Schematic diagram of the proposed method

This method is essentially an active grounding fault protection method without time delay. To fit various worksite conditions, two signal generating schemes using different semiconductor devices are proposed in this study. They are diodes-based active protection scheme and thyristor-based active protection scheme.

2.3.1 Diodes-Based Active Protection Scheme

This scheme involves a simple configuration of signal generator (SG) sending current disturbance through diodes.

Under normal circumstance, when the equipment is free of contacting to the power line, no voltage is built between the anode and cathode of the diode, and the diode is off and no signal will be sent out. As shown in Figure 2.4, if the equipment accidentally contacts the power line and becomes energized, the power line voltage will be instantly applied on the diode. The voltage between SG anode and ground can be assumed as same to the phase to ground voltage of power line, considering the tires of the mobile equipment are usually insulated. When SG voltage direction is switched from anode to cathode, the diode will be turned on and automatically turned off when the voltage direction is changed again. In this way, the current distortion is created as a signal transmits to the upstream of the power line.

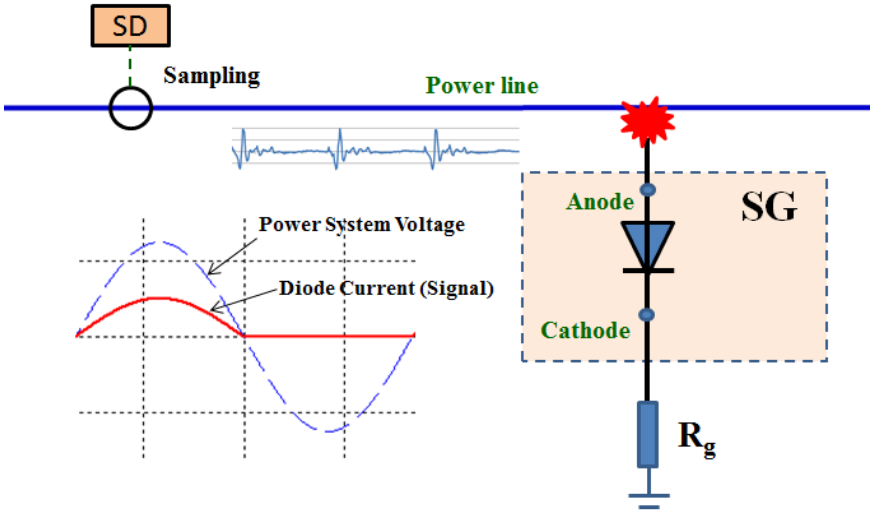

Figure 2.4 Description of the proposed diode based method

According to the direction of line voltage, the diodes are in a status of being on or off which generate signals in a half sinusoidal waveform.

The signal detector (SD) is a microprocessor-based device that can be mounted on the existing recloser. The trip command signal from SG can be easily

obtained and implemented to trip the recloser permanently. The SD has been embedded with a highly efficiency algorithm based on the half sinusoidal pattern of the generated signals. Consequently, quick signal extraction and identification can be ensured. The communication route is temporarily built by an existing power line between worksite and the upstream recloser closest to the SD.

2.3.2 Thyristor-Based Active Protection Scheme

In the worksite environment with high soil resistivity, the strength of the generating signal may be too low for SD to detect the signal. In order to solve this challenging situation, an improved thyristor-based active protection scheme is proposed with distinctive signal characteristics to ensure detection sensitivity and accuracy for a wide application range.

The SG in this scheme is mainly composed of thyristor devices. Similar to diode-based scheme, if the equipment is free of contacting to the power line, no voltage potential is built between the anode and cathode of the thyristor, and the thyristor is off and no signal will be sent out. As shown in Figure 2.5, if the equipment accidentally contacts the power line and becomes energized, the phase to ground voltage on live line will be instantly applied on the thyristor. Simultaneously, the control gate of the thyristor is triggered and a firing pulse string starts to apply to a specified phase angle during the positive cycle of the power line voltage. The thyristor will be immediately turned on when the firing pulse is applied on the gate and automatically turned off when the voltage decreases down to zero and the current direction is changed again. In this way, the current distortion is created as a specific signal with a certain firing angle transmits to the upstream of the power line.

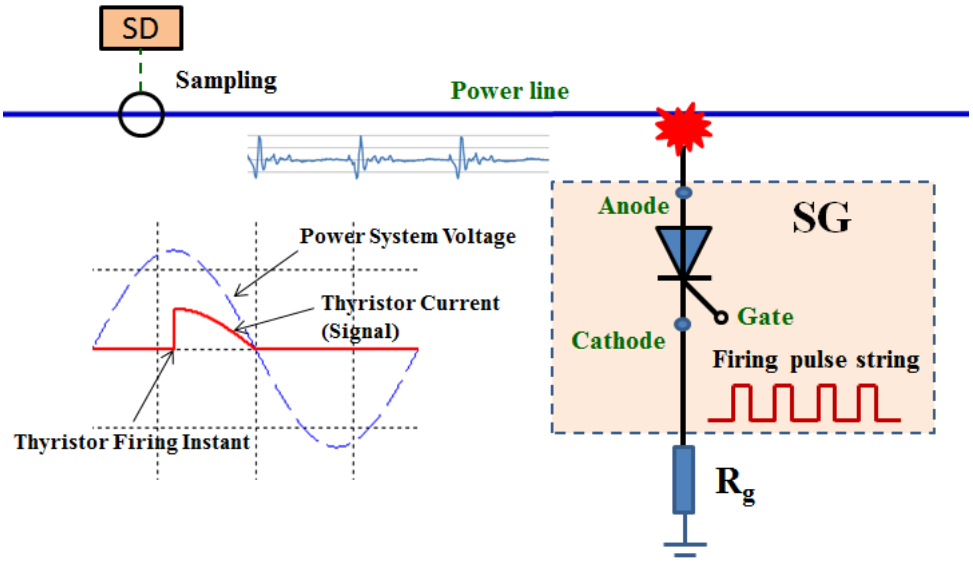

Figure 2.5 Description of the proposed thyristor based method

The main advantage of thyristor-based method is the ability to generate highly distinguishable signals, which effectively differentiates the signal received from other transients and disturbances at upstream reclosers. Furthermore, a new energy-based detection algorithm based on the distinctive signal pattern can overcome the difficulties arising from the low signal strength in an unfavorable worksite condition. Thus, this scheme can be applicable to a wide range of worksite conditions.

In this active protection scheme proposed in this study, the signal strength is ensured by the SG parameter design, and the grounding tripping time is determined by the signal detection device. There are no other devices required to fulfill the scheme. Since the worksite location and grounding resistance do not have significant effects on the sensitivity and speed of trip grounding, the method can be practical and effective.

2.4 Design Consideration and Challenges

To ensure that the signal can be detected with high accuracy, the generating signals should have strong strength and distinctive patterns. However, for generating this kind of signal, it requires both an ideal worksite condition, especially in ground resistance, and a large current-carrying capability in the

signal generator which requires a large physical device size. Moreover, detecting the distinctive characteristics of signals normally requires complicated control and sophisticated arrangement, which increases the chance of device malfunction. Therefore, the following questions relevant to the above challenges are expected to be answered in the proposed two schemes:

- What is the maximum current that a portable power electronic device is capable to carry? Is this generated current strong enough for a detection purpose? If not, is there any alternative method in signal extraction or detection?

- Is the proposed scheme applicable to a wide variety of field conditions considering the influence of factors such as soil resistivity, humidity, and temperature? If not, what is the applicable range and limitations of the scheme? And what is the performance in the most unfavorable worksite condition in terms of detection accuracy and responding time?

- How should a unique signal with distinctive pattern be generated to distinguish worksite signals from natural disturbance or other power line based signals? Meanwhile, is it possible that a simple gate triggering and control scheme are implemented to decrease device malfunction probabilities?

- How to effectively detect and response to the disturbance signals in a fast and accurate manner? For a safe and reliable protective device, it is important to response immediately with certainty, so that worksite safety can be assured as well as power reliability. Meanwhile, absence of falsely tripping a circuit is equally important for utilities.

- In a distribution system with large disturbance due to load transient or capacitor switching, will the device send out false alarm or trip command when worksite is in a safe condition? Will the supply of power still be reliable in normal operation and not affected by the implemented SG and SD devices?

In the design process of proposed schemes in Chapter 3 and 4, above questions are answered and relevant issues are addressed accordingly. The results and conclusions are summarized in Section 2.5.

2.5 Summary and Conclusions

Regarding the comparison between diode and thyristor based protection schemes, the thyristor-based protection scheme has an advantage of unique and distinctive signal patterns developed by pre-set gate controls and advanced detection algorithm. Thus signals indicating worksite energization condition shall be distinguished from natural current variation and other waveform transient, leading to a more accurate detection and reliable power supply.

On the other hand, diode-based scheme provides a reliable device performance with a rapid response. Developed with a simple configuration, the reliability of SG in this scheme only depends on the performance of diodes, the technology of which has been dependable and well established.

The proposed two schemes provide proactive and firm protection for worksite safety. The main characteristics of proposed active protection schemes can be summarized as follows:

- Relatively inexpensive devices are employed without impairing the reliability of the communication route. No other communication devices are required to be built along the power line, which decreases equipment costs and labor expenses.

- Harmonics have little impact on their performances as harmonics produce consistent, periodic distortions or zero-crossing-shifts in the waveform, which can be eliminated by signal extraction process.

- No appreciable signal attenuation is introduced by shunt capacitors or transformers; therefore, no significant modification of the distribution network is required.

- Fast response action without time delay ensures personal safety at worksites.

- The proposed method with two signal generating schemes is applicable to a wide range of worksite conditions, leading to a reliable protection of worksite safety.

Based on the results from theoretical analysis and simulation verifications, this new active protection method proves to be feasible and reliable, especially suitable for worksites equipped with heavy and large mobile equipment which is operated close to the live power lines.

Chapter 3

Design and Verification of Diodes-Based Active Protection Scheme

In the pursuit of reliable signal generating performance, a simple configuration of active protection scheme based on diodes without gate control is proposed first. In this protection scheme, the Signal Generator (SG) is easily implemented by diodes, and the Signal Detector (SD) is built according to the characteristics of generating signals.

3.1 Signal Generation

3.1.1 Structure of Signal Generator

The line to ground voltage of distribution system normally ranges from 7.2kV to 20kV and even higher. To make the device more economic and reliable, the actual signal generator configuration is composed of several identical signal generating units which are connected in series. The circuit of signal generator is shown in Figure 3.1.

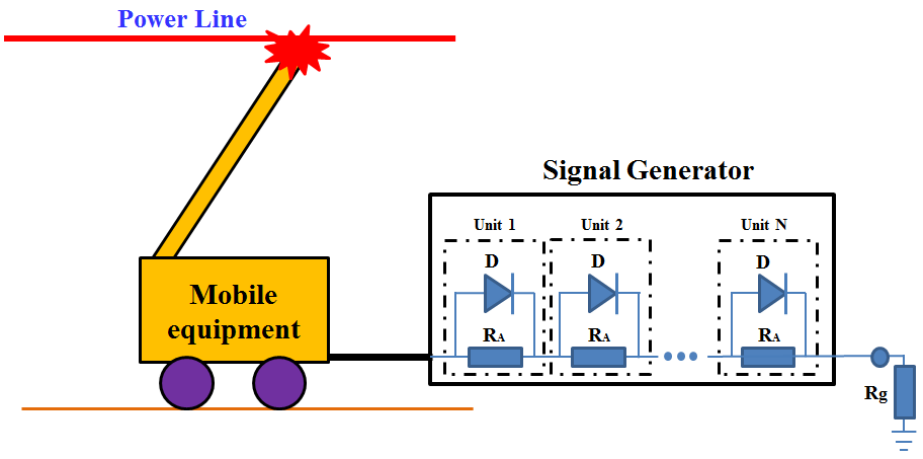

Figure 3.1 Structure of Signal Generator (SG)

Each signal generating unit is assembled by a diode (D) to generate one-way current distortion, a voltage dividing resistor (R_A) to even off-state voltage to each diode unit. The signal generating units will bypass positive current but block negative current based on the characteristics of one-way diode sets.

Detailed signal generating process is illustrated as follows:

- In the normal safety condition, the mobile equipment is away from live line, keeping SG in an off-state condition without energization.
- Should the mobile equipment touches the power line, a half cycle sinusoidal waveform signal will be generated as the diodes conduct positive current wave from power line to ground until it reverses direction.
- During the reverse-bias condition of diodes, fault current is limited by the voltage dividing resistor (R_A) to an extremely low level (around 0-2 A), which can be assumed as open circuit.

The generated current distortion, i.e., signal, is shown in Figure 3.2(b). This current distortion is superimposed on the load current of power line and reaches the closest upstream SD. Then the SD is able to identify and detect the signal.

The number of signal generating unit is dependent on the power system voltage. During the negative cycle, the maximum off-state voltage of each diode is limited to 2000V, and the typical line-to-ground voltage of the three-phase distribution line is around 10 – 25 kV, so 5 units are used in SG for 13.8 kV line-to-line system while 10 units are used for 25 kV line-to-line system. The value of R_A has little impact on signal generation. High impedance would be preferred to limit fault current magnitude. To keep the device requirement to minimum specifications the value of R_A is selected as 10,000 Ohms.

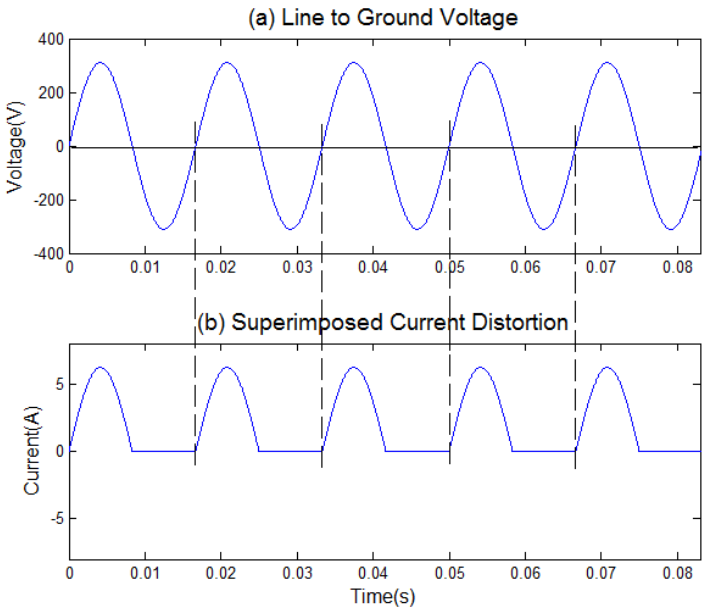

Figure 3.2 Current Distortion (Signal)

In comparison with the conventional electronic signal generator, this signal generating scheme is more reliable because it uses the line voltage as power source to start up immediately once energized due to a fault condition. In addition, the on and off pattern is very simple as well. Since all diode sets will be naturally fired on and off by flowing current, a low chance of breakdown can be expected.

3.1.2 Theoretical Analysis of Main Circuit

Based on the diode structure of signal generator, the main circuit is analyzed to investigate major characteristics of the signal generation process.

The case where SG fires between phase A and ground is shown in Figure 3.3. In this circuit, $\sum R_A$ is the summation of R_A of N units, and $\sum V_D$ is the voltage on N diode sets when there is no conduction. The steady state sinusoidal voltage on each diode $v_D(t)$ can be expressed as

$$v_D(t) = \frac{1}{N}\sqrt{\frac{2}{3}} \cdot V_N \cdot \sin(\omega t) \cdot \frac{\sum R_A}{\sum R_A + R_g} \tag{3.1}$$

where

V_N is the phase-to-phase system voltage at the worksite,

R_g is the grounding resistance of worksite temporary grounding rod.

Using superposition principle, the signaling process is equivalent to injecting a negative voltage source $-v_D$ between the two ends of diode sets. The signaling transient can be calculated with a circuit energized by $-v_D$ as shown in Figure 3.4, where Z_{sys} is the system impedance, Z_{line-1} is the equivalent line impedance of the upstream system and R_g is the grounding resistance. In this circuit, the other two phases and loads are approximated as open circuits.

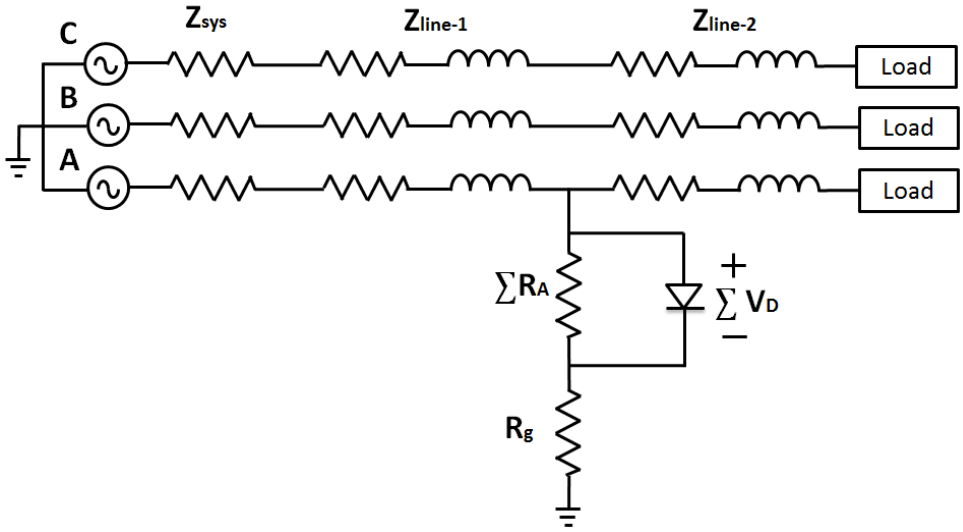

Figure 3.3 The analysis circuit for single phase signaling

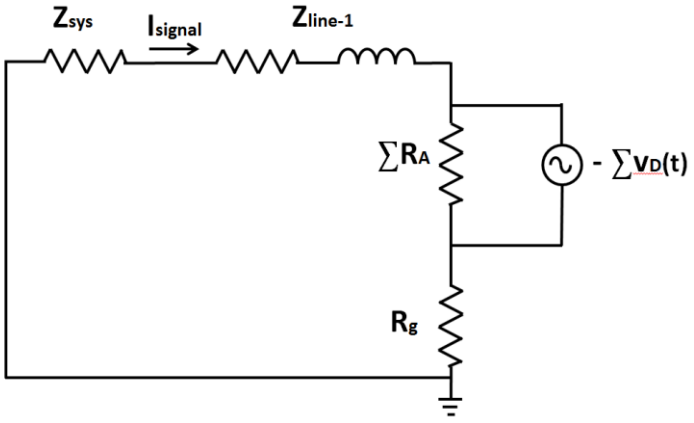

Figure 3.4 Equivalent Signaling Circuit

If the diode is fired on v_{RA}'s zero-crossing point at forward bias, then turned off when current reverses direction, the current distortion, which is the signal, can be determined as:

$$i_{signal}(t) = \sqrt{\frac{2}{3}} \cdot V_N \cdot \sin(\omega t) \cdot \frac{\sum R_A}{\sum R_A + R_g} \cdot \frac{1}{R_g + Z_{line-1} + Z_{sys}}$$

$$\approx \sqrt{\frac{2}{3}} \cdot V_N \cdot \sin(\omega t) \cdot \frac{1}{R_g}, \omega t \in [0, \pi] \quad (3.2)$$

The peak of $i_{signal}(t)$ shows the maximum value of generating signals, which is

$$I_{peak} = -\sqrt{\frac{2}{3}} \cdot V_N \cdot \frac{1}{R_g} \propto \frac{1}{R_g} \quad (3.3)$$

Figure 3.5(a) indicates the original current at upstream recloser during normal operation, which is a standard sinusoidal waveform. When worksite is accidentally energized, positive half cycle sinusoidal waveform signals shown in Figure 3.5(b) are generated and added to original circuit current, resulting in a signaling detected current shown in Figure 3.5(c). A zoom-in figure of a single signaling cycle is drafted in Figure 3.6.

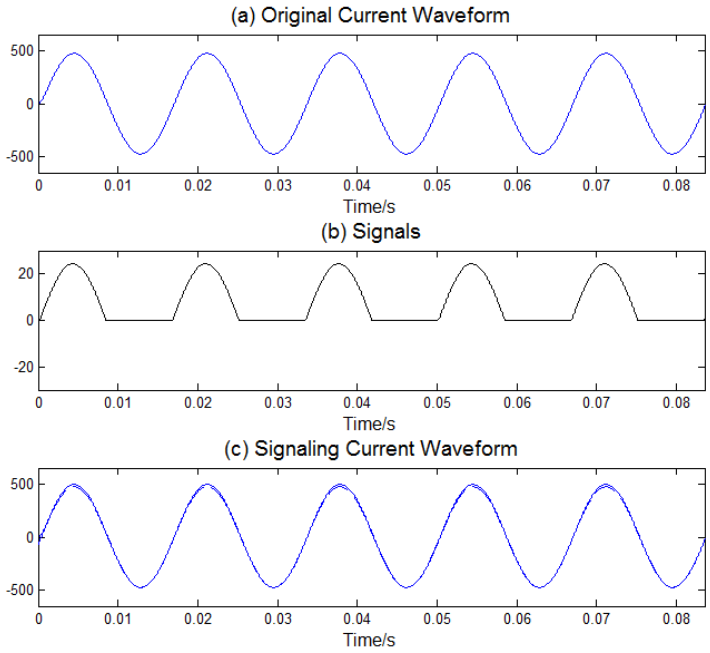

Figure 3.5 Comparison of original current waveform with signaling waveforms

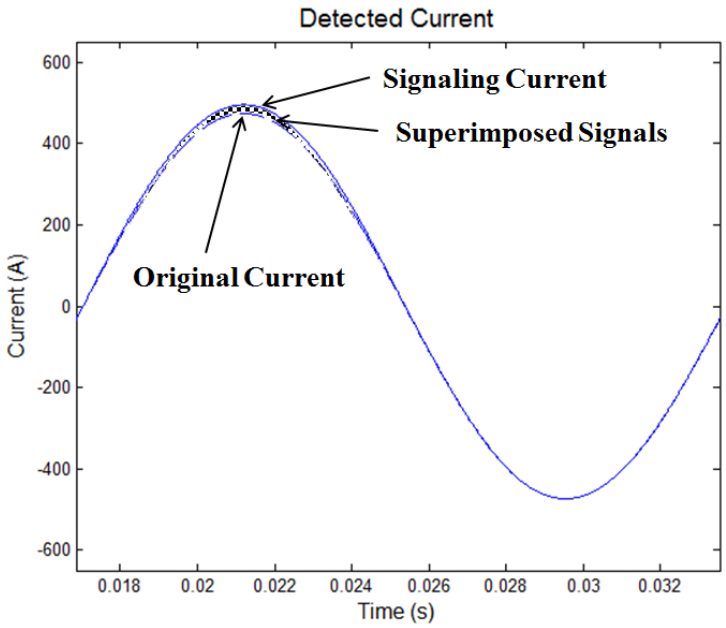

Figure 3.6 Superimposed signal in one cycle

Disturbing signals only exist in positive half cycles in phase with worksite voltage. Assuming the grounding resistance varies between 10 Ohms to 1000

Ohms covering almost all grounding circumstances, the peak value of superimposed signals varies in a wide range as shown in Table 3.1.

Table 3.1 Peak value of superimposed signals

		13.8 kV	25 kV
Grounding Resistance	10 Ω	1126.7 A	2041.2 A
	1000 Ω	11.3 A	20.4 A

Since the SG contains only durable diodes and resistors, no any control circuit involved, and each resistor only need to have a capacity of 2kW with 2A carrying current, it is of reliable performance and small size to satisfy the worksite application.

3.2 Signal Detection

By knowing the waveforms of signaling current, the detection process is built according to the comparative differences of detected current with and without signals. A main characteristic of superimposed signals is magnitude shift in different harmonic orders. As a result, this characteristic is used as detection indicators.

3.2.1 Characteristics of Superimposed Signals

In order to distinguish the differences of current with and without signals, Fourier Transform is applied to superimposed signals to transfer waveforms from time domain to frequency domain.

Assume the half cycle superimposed signal is $f(t)$, which is

$$f(t) = \begin{cases} \mathrm{A} \cdot \sin(wt)\,, 0 < t < \frac{T}{2} \\ 0, \frac{T}{2} < t < T \end{cases} \tag{3.4}$$

where

A is the peak value of superimposed signal.

Then Fourier Transform is performed to analyze the frequency spectrum as below.

$$F(n) = \frac{1}{T}\int_0^{T/2} \mathrm{A}\cdot\sin(wt)\cdot e^{-jnwt}dt = \frac{1}{2\pi}\cdot\left(\frac{1}{1-n}+\frac{1}{1+n}\right), n = 0,2,4,6,\ldots \quad (3.5)$$

Assuming signal amplitude is 18 A as a common case, the magnitudes of different harmonic orders in superimposed signals calculated from Equation (3.5) are shown in Figure 3.7. Clearly, frequency spectrum of superimposed signals indicates strong signal strength in DC component, fundamental frequency and 2nd order harmonics.

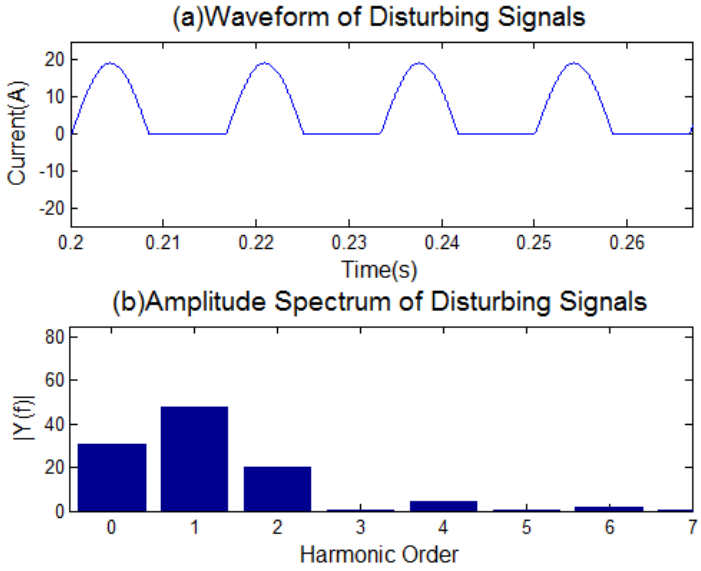

Figure 3.7 Disturbing Signals in both time and frequency domain

In order to distinguish signaling current, a comparison of frequency spectra between field measured detected currents with and without artificially added signals are shown in Figure 3.8, while ratios (A) calculated from Equation (3.6) are indicated above each bar.

$$A = \frac{Magnitude_{with\ Signals}}{Magnitude_{without\ Signals}} \quad (3.6)$$

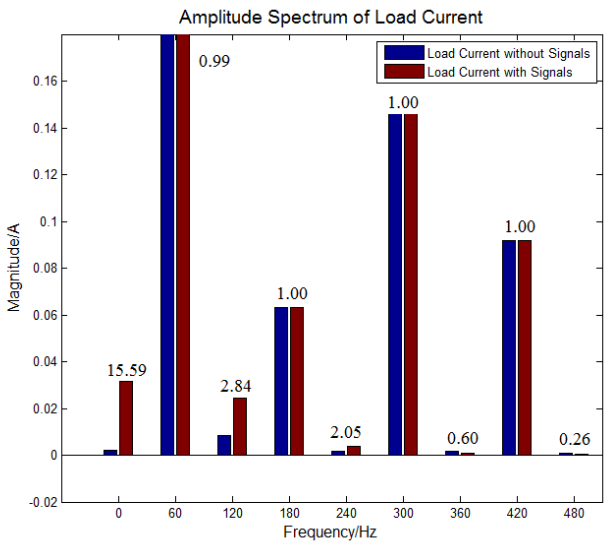

Figure 3.8 Frequency Spectrum of Detected currents with and without signal

Figure 3.8 clearly indicates that the most significant distinction in detected current with and without superimposed signals is the 15.59 times difference in DC component. Therefore, the magnitude of the DC component can be used as a main indicator to distinguish signaling current from non-signaling ones.

For the DC component, we define DC ratios (R) of each cycle as DC magnitude divided by amplitude of detected current including signal in this cycle, and the average DC ratios among consecutive four cycles is utilized as signaling strength. As the definition, DC ratios (R) can be derived as:

$$R = \frac{I_{DC}}{I_P} = \frac{\frac{\sqrt{2}\cdot V_N}{\sqrt{3}\cdot\pi\cdot R_g}}{I_P} = \frac{\sqrt{2}\cdot V_N}{\sqrt{3}\cdot\pi} \cdot \frac{1}{R_g \cdot I_P} \tag{3.7}$$

where

I_{DC}: Magnitude of DC component in detected current (A)

I_P: Amplitude of detected current (A)

V_N: Rated Line-to-line Voltage of Distribution Line (V)

R_g: Grounding resistance (Ohms)

From the equation, DC ratio is inversely proportional to the product of grounding resistance (R_g) and detected current peak (I_P). Since I_P is significantly dependent on load current, thus the most sensitive parameters in signal strength are the grounding resistance and load current amplitude. Figure 3.9 shows their coordinating relations in 13.8 kV system, in which bright and dark colors are used to represent strong and weak signals respectively.

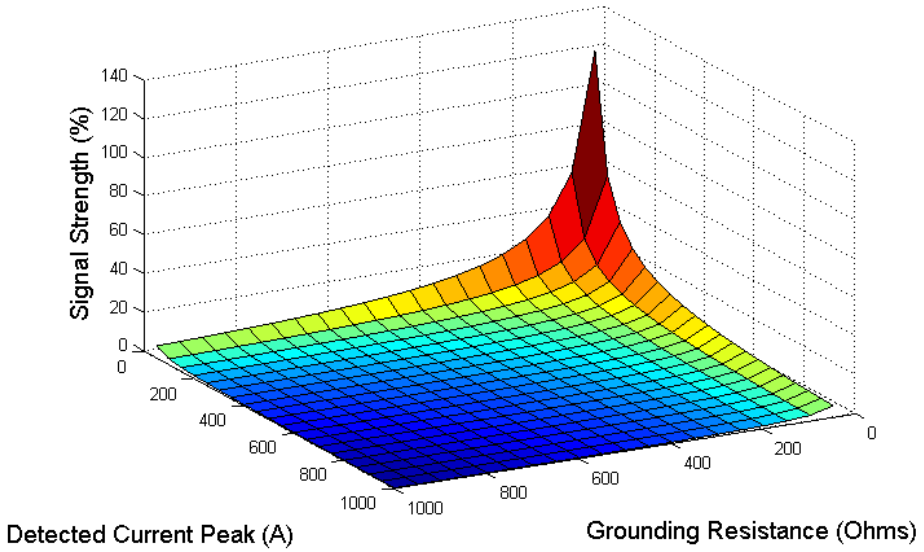

Figure 3.9 Signal strength related to main parameters

Based on the theoretical analysis of DC ratios and signal strength, the detection threshold is set in advance. Current cycles with signal strength higher than the pre-set threshold are detected as signaling cycles.

3.2.2 Detection Process

Based on former theoretical analysis, a DC component threshold should be set as one of detection criterions. The original intuitive idea of detection is: Current cycles with DC magnitude higher than a certain threshold is regarded as signaling cycles while current cycles lower than pre-set threshold are assumed as non-signaling cycles. As a result, for the benefit of detection accuracy, the threshold would be preferred to be set low to assure better detection; however, in order to eliminate false trigger resulted from transient or load variation, a high threshold is

more favorable. Based on abundant actual field measurement data available, in which DC ratio of each cycle is indicated as Figure 3.10, we notice that there is not a clear fixed threshold to distinguish signaling and non-signaling DC ratio. As the colors point out the distinction of DC ratio with and without signals respectively, there are some overlapping red and bule points. Even worse, some DC ratio data points in non-signaling cycles can be higher than most of the signaling cycles in certain cases. However, we notice that these singular points always appear with intermittency but not consistency. So it is reasonable to assume that these singular points stem from some system transients, such as capacitor switching, lighting strikes, etc. Because of the intermit appearance, immense DC ratio fluctuation can be found around these singular points, leading to a high deviation rate in surrounding areas.

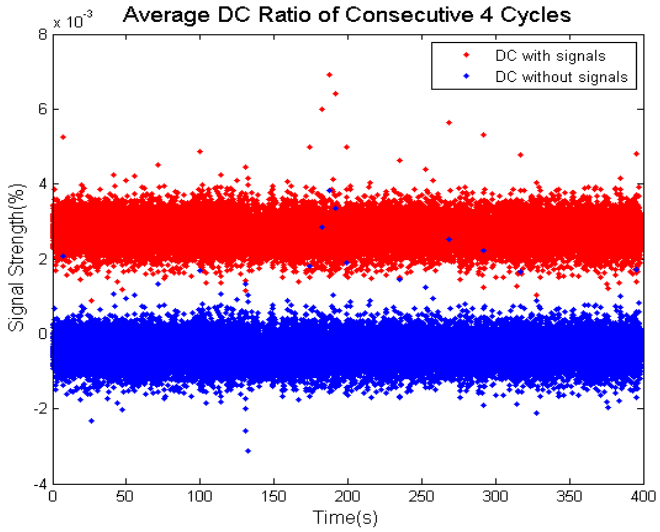

Figure 3.10 DC magnitude of each consecutive 4 cycles with 0.3% signal strength

Due to the non-consistent characteristic of singular points, we develop a standard deviation test to exclude them in front of main criterion estimating DC ratios. Five key terms are defined before detection process.

- Definition 1: Voltage waveform is used as a time reference, and “one current cycle” is defined as current waveforms from the zero-crossing

point of voltage positive cycle to the zero-crossing point at the next positive cycle, as shown in Figure 3.11.

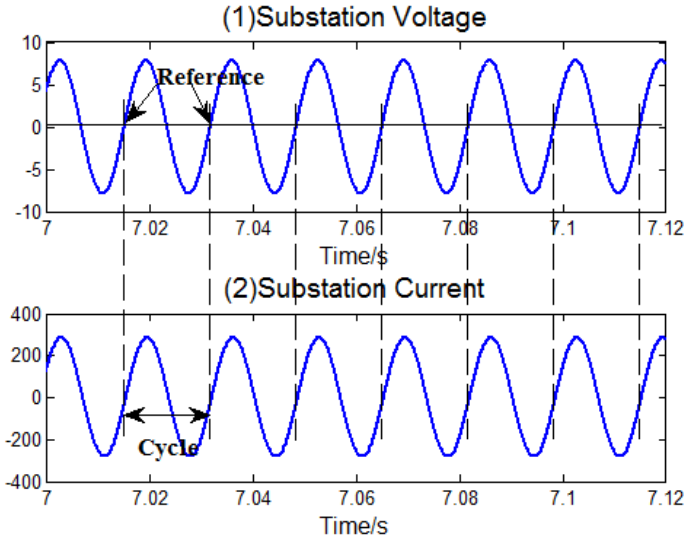

Figure 3.11 Definitions and Reference of a Current Cycle

- Definition 2: In order to eliminate measurement errors and soften natural variation between each cycle, we take the average DC ratios of preceding consecutive 4 cycles as the signanl strength ($S(i)$), which is defined as:

$$S(k) = \frac{\sum_{i=k-3}^{k} R(i)}{4} \tag{3.8}$$

where

$R(i)$ is DC component ratio in each cycle;

$S(i)$ is the signal strength.

- Definition 3: If DC magnitude in consecutive four cycles fluctuates excessively such that the standard deviation among these four cycles exceeds a certain threshold, the whole variation period would be defined as “Zone_0”, in which a system transient normally exists.

- Definition 4: To allow the transient to decay and the fluctuation to stabilize, the same length of time following "Zone_0" is defined as "Zone_1", and then "Zone_2". After a transient, DC magnitude can still be higher than the normal stage even with low standard deviation. In these cases, higher than normal deviation thresholds "Threshold_1" and "Threshold_2" respectively, should be implemented to avoid false alarm.

- Definition 5: Except for the period of "Zone_0", "Zone_1" and "Zone_2", other periods in detected current is defined as "Zone_regular", in which the distribution system is supposed to be in a steady state. And "Threshold_regular " is in effect accordingly.

Figure 3.12 shows a period of detected current without signals collected from field measurement, in which an obvious system transient exists. The definition of "Zone_0", "Zone_1" and "Zone_2" given here is to eliminate the effects of system transient in detection process.

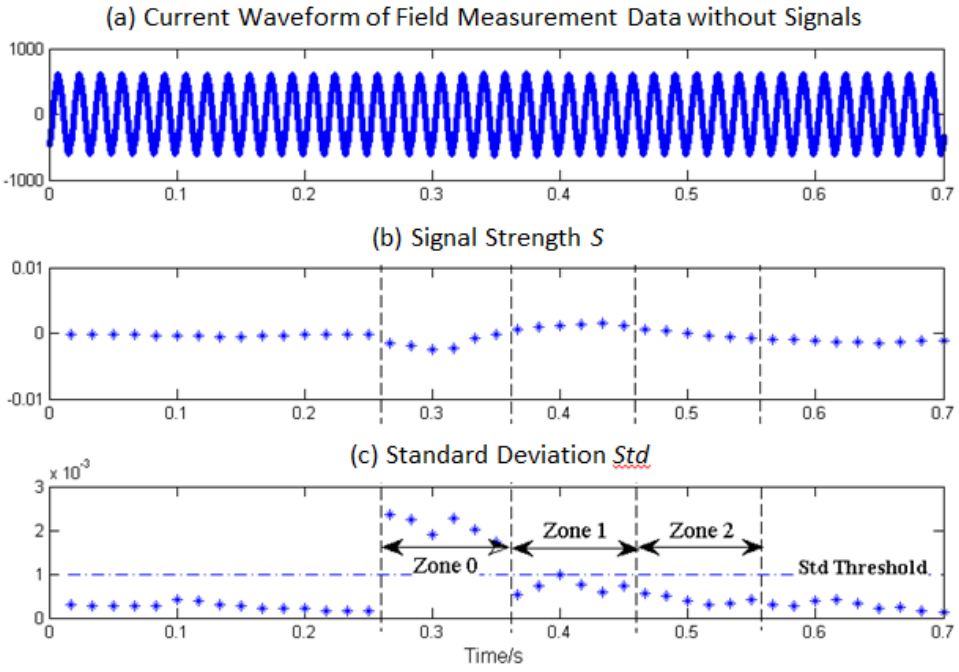

Figure 3.12 Definition of "Zone_0", "Zone_1", and "Zone_2"

Getting all the definition clarified, detection process algorithm works as shown in Figure 3.13:

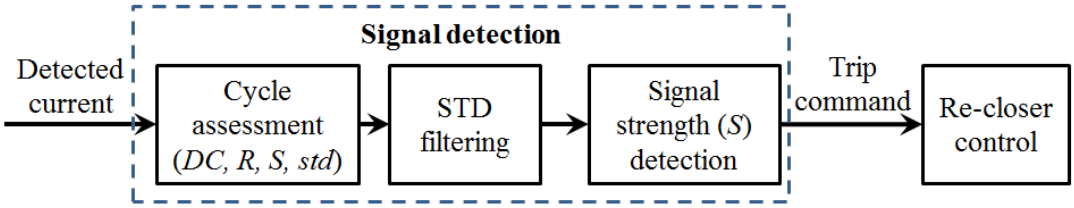

Figure 3.13 Signal Detection Process

- Step 1: Calculate the DC magnitude ($I_{DC}(i)$) and ratios($R(i)$) between DC magnitude and cycle amplitude; Compute the average DC ratio as signal strength ($S(k)$) and standard deviation($std(k)$) of DC ratios ($R(i)$) in every consecutive four cycles;

$$S(k) = \frac{\sum_{i=k-3}^{k} R(i)}{4} \tag{3.9}$$

$$std(k) = \sqrt{\frac{\sum_{i=k-3}^{k} (R(i) - S(k))^2}{4}} \tag{3.10}$$

- Step 2: Set standard deviation threshold (STD) and DC ratio threshold "Threshold_regular", "Threshold_1", "Threshold_2" for "Zone_regular", "Zone_1"and "Zone_2", respectively; Since "Zone 0" is judged as non-signaling zone automatically from STD detection, no ratio threshold is needed.

- Step 3: If std(i) > STD, detect it as non-signaling point (det = 0);

  Else if it is in "Zone_1", use "Threshold_1" as detection criterion;

  Else if it is in "Zone_2", use "Threshold_2" as detection criterion;

  Else, use "Threshold_regular" as detection criterion.

Going through such a filtering detection process by excluding large transient disturbance, a decent threshold can be employed. By this method, the detection procedure can not only assure high detection rate of signaling cycles, but also eliminate false alarm in system transient stage.

3.2.3 Threshold Selection

Four main thresholds are needed to be deciding in the detection procedure: standard deviation threshold (STD), and DC ratio thresholds ("Threshold_regular", "Threshold_1", "Threshold_2"). These thresholds are set according to long time on-site measurement results.

- ***Standard deviation threshold:***

A 5 minutes' section with large system transient in measurement data is selected to measure data distributed probability. The standard deviation ($std(k)$) of consecutive 4 cycles non-signaling current in this section is calculated and shown in Figure 3.14. Figure 3.15 depicts the comparison of signal strength ($S(k)$) (average DC ratios) with and without signals.

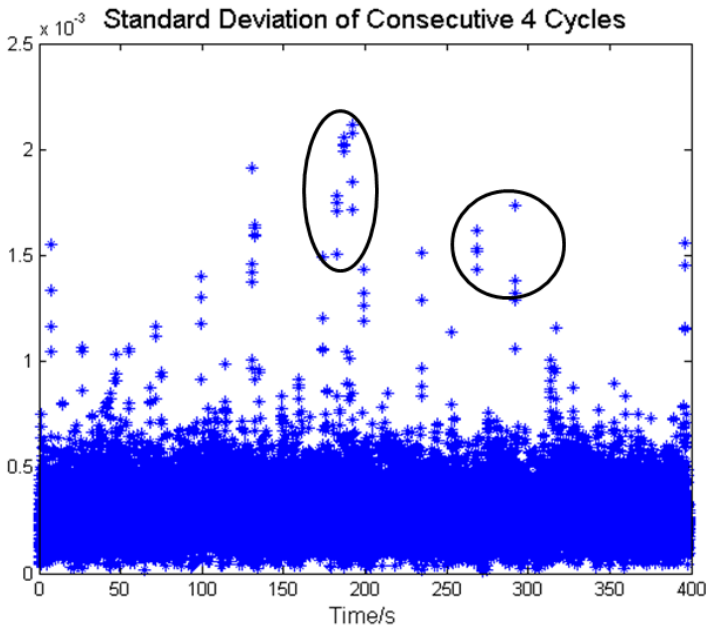

Figure 3.14 Standard Deviation of DC Magnitude in Consecutive 4 Cycles without Signal

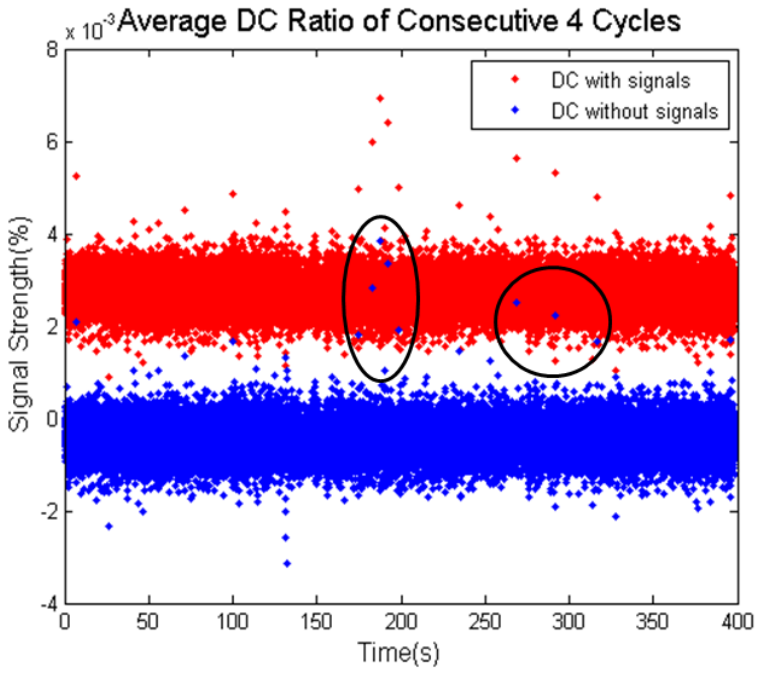

Figure 3.15 Signal Strength (average DC ratios) of current with and without signals in the same period of time

Comparing Figures 3.14 and 3.15, those non-signaling cycles that show a high DC strength in Figure 3.15 also have an extremely high standard deviation in Figure 3.14. This happens at points around 200 second and 300 second. It confirms that a standard deviation threshold methodology is useful in excluding transient state or other current fluctuation cycles.

In order to set a proper standard deviation threshold (STD), probability distribution is measured from around one week of field data including more than 36 million cycles. The probability density curve and cumulative distribution curve are shown in Figure 3.16 and 3.17, respectively. For a confidence interval of 99.5% as commonly practiced in statistics, STD threshold is close to and therefore selected as $1x10^{-3}$. In this case, 99.73% of current cycles with $std(k)$ lower than $1x10^{-3}$are assumed to be in steady state without fluctuation. And the data points with $std(k)$ higher than $1x10^{-3}$ are denoted as transient cycles, in which enormous current disturbance may exist.

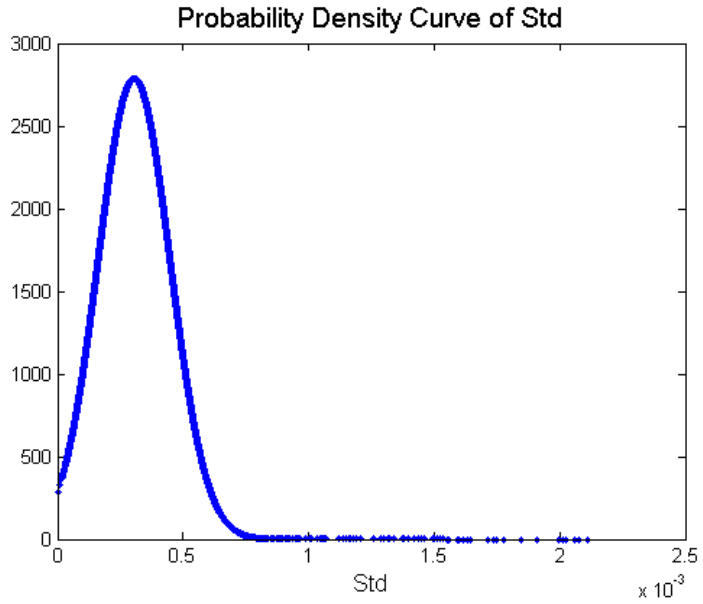

Figure 3.16 Probability Density of std in normal detected current

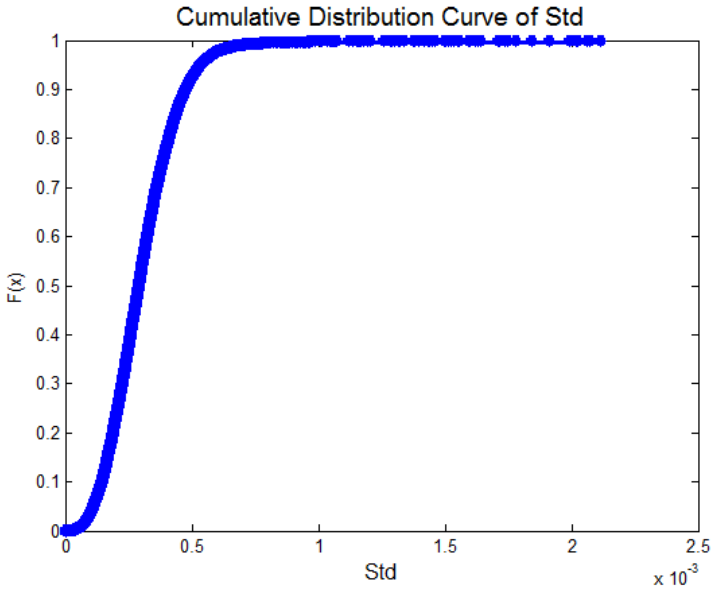

Figure 3.17 Cumulative Distribution of std in normal detected current

By setting STD using Cumulative Distribution method, the singular points implying large current fluctuation can be excluded from natural load current, and the remaining cycles after filtering are shown in Figures 3.18 and 3.19.

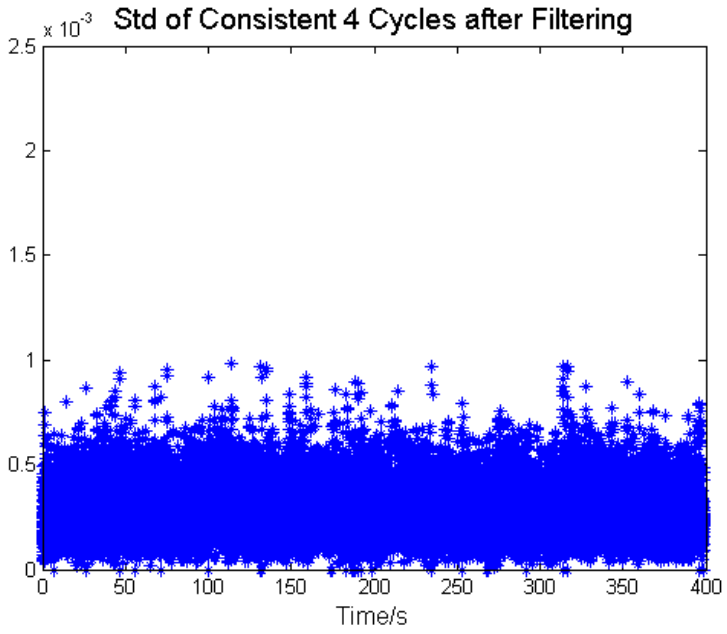

Figure 3.18 Standard Deviation of DC Magnitude in Consecutive 4 Cycles after Filtering

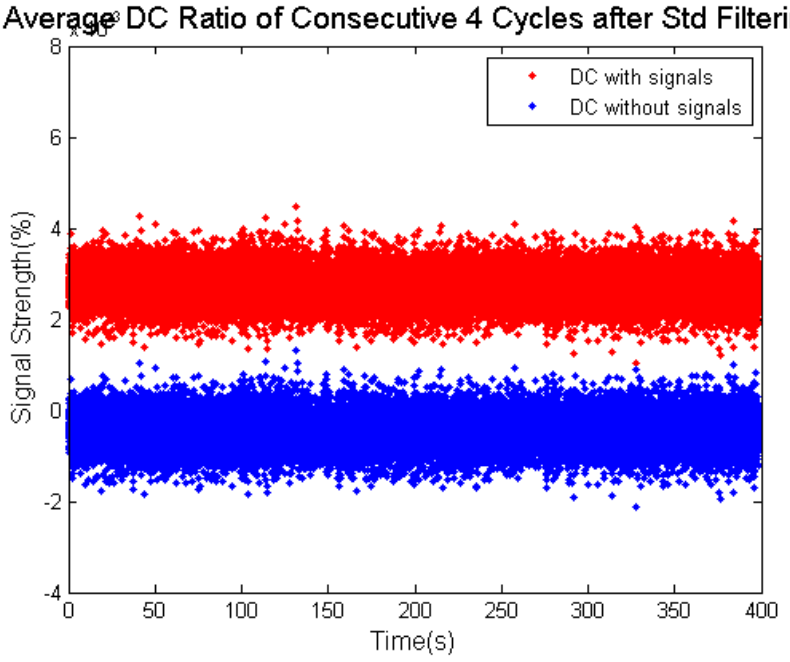

Figure 3.19 DC ratios of current with and without signals after STD filtering

After applying standard deviation threshold for singular points screening, singular points are denoted as non-signaling cycles so as to eliminate false alarm. And a clear distinction of DC ratios with and without signals has been achieved, which simplify and accelerate detection process.

- ***Signal Strength (average DC ratios) threshold:***

For the main detection criterion, signal strength (average DC ratios) is used as detection index. Initially, DC ratio in non-signaling current is investigated. By evaluating various measurement data from various feeders, it is found reasonable to estimate the average DC ratio in steady state current without signals varies from -0.2% ~ 0 to 0 ~ +0.2%, and is found to remain stable within these region for a decent time.

While sensitivity means the accurate detection rates in signaling period, and specificity indicates the correctly undetected rates in non-signaling period, we are seeking for a threshold that has both high sensitivity and high specificity. Considering the two extreme variation ranges being the most unfavorable cases, DC component varying between -0.2% ~ 0 without signals is used to determine the least sensitivity while 0 ~ +0.2% is used for the least specificity. Specificity and sensitivity percentage from measurement data are as following.

Table 3.2 The least specificity

Threshold (%)	Specificity
0.13	79.10%
0.15	90.84%
0.18	98.27%
0.20	99.58%
0.23	99.97%
0.25	100%
0.28	100%
0.30	100%

Table 3.3 The least sensitivity

Signal Strength(%) / Threshold(%)	**0.2**	**0.3**	**0.4**	**0.5**	**0.6**
0.13	21.43%	96.52%	99.99%	100%	100%
0.15	9.46%	90.20%	99.99%	100%	100%
0.18	1.81%	69.55%	99.91%	100%	100%
0.20	0.44%	49.61%	99.53%	100%	100%
0.23	0.04%	21.96%	96.66%	99.99%	100%
0.25	0.00%	9.77%	90.52%	99.99%	100%
0.28	0.00%	1.89%	70.18%	99.91%	100%
0.30	0.00%	0.47%	50.34%	99.55%	100%

Since specificity reveals the non-detected accuracy in non-signaling current, which is determined by natural fluctuations and threshold selection, but irrelevant to signal strength. In order to eliminate false detection, which implies a 100% specificity rate, a signal strength threshold of 0.25% is selected as "Threshold_regular" in Table 3.2, any cycle with signal strength higher than this threshold would be assumed as a signaling cycle and stronger signals are desirable. "Threshold_1" and "Threshold_2" are selected as 0.50% and 0.40% respectively from non-signaling current scanning in "Zone_1" and "Zone_2". Since pre-set the thresholds are standardized by percentage, one set of threshold is applicable to various voltage levels in distribution systems, and independent of operation conditions and fault locations.

Table 3.4 Pre-set Thresholds for signal detection

Term		Threshold (%)
STD		$1x10^{-3}$
DC Ratios	Zone_regular	0.25
	Zone_1	0.50
	Zone_2	0.40

Furthermore, sensitivities are related to both threshold selection and signal strength as shown in Table 3.3, and signal strength is largely depending on grounding resistance (R_g) and detected current peak (I_P). Then, detection specificity and sensitivity are studied through verification tests in Section 3.3.

3.2.4 Implementation of Signal Detector

The schematic of Signal Detector is shown in Figure 3.20. It consists of an A/D converter and a Micro-Control Unit (MCU). The A/D of signal detector collects three phase voltage and current waveforms of the feeder from PT and CT installed for the recloser. The MCU conducts the signal detection process, i.e., cycle assessment, STD filtering and signal strength detection. Once the trip command confirmation is made by MCU, this command will be immediately sent out to the recloser control through serial ports of MCU. Therefore, the recloser control can take action on recloser tripping.

The detailed implementations, including voltage/current data acquisition, trip command sending and SD installation, are as follows.

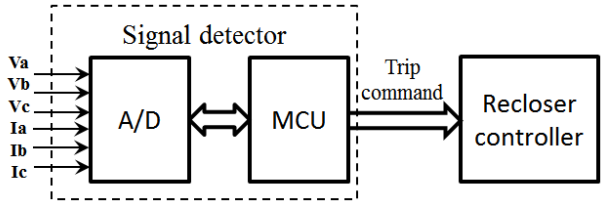

Figure 3.20 Schematic of Signal Detector

- ***Voltage/Current Data Acquisition***

Taking a commonly used local recloser control SEL-651R as an example, the wiring layout of the control is shown in Figure 3.21. Both three-phase voltages at system and load sides of recloser are adopted by the control through PTs. The three-phase feeder currents collected by recloser's CTs and the information of recloser trip/close status are also sent to the control through control cable.

Since all required voltage and current waveform data of the feeder are already collected by the control, the A/D of MCU can obtain them directly from the terminals of control. The front view of control terminals is shown in Figure 3.22.

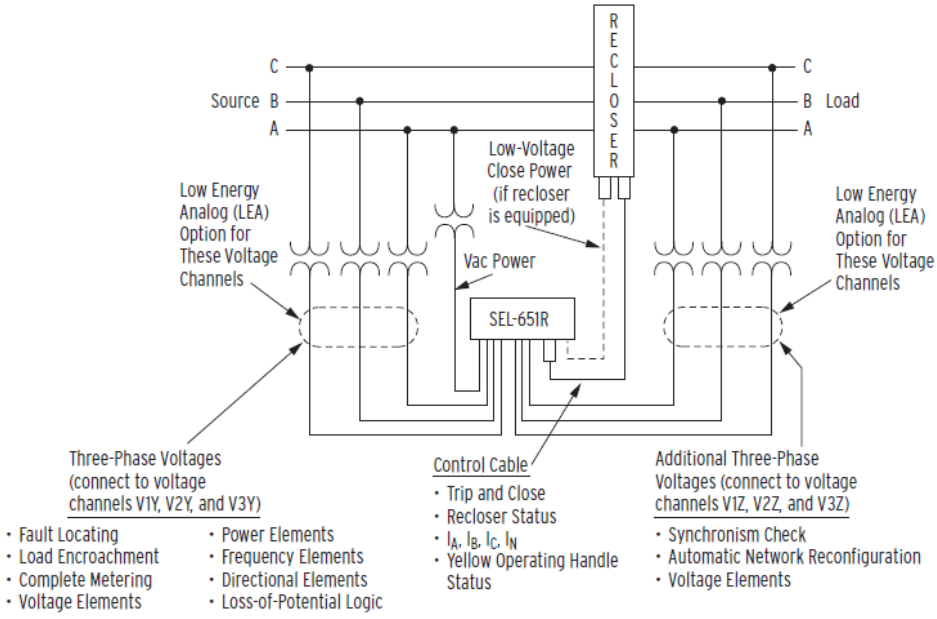

Figure 3.21 Wiring layout of SEL-651R-2 control

- ***Trip Command Sending***

It can be seen from Figure 3.22, there is an EIA-232 serial interface that allows the tripping command from MCU to go through. Thus, the recloser control can receive a trip command through Serial and Telnet binary protocol to trip and lock out the recloser.

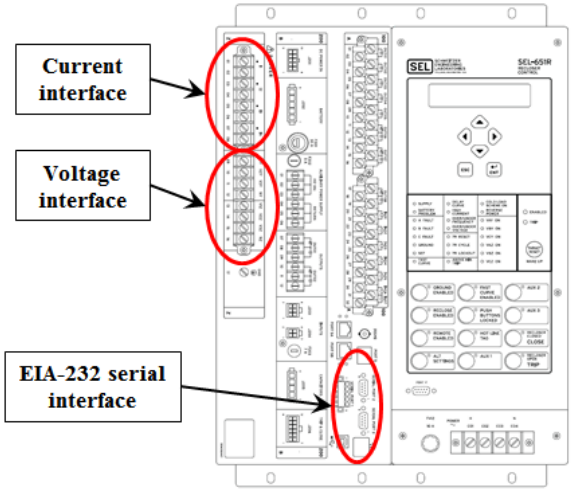

Figure 3.22 Front view of control terminals

- ***SD Installation***

Signal detector (SD) can be made in a small size and allows to be installed in the local control cabinet of recloser by simply connecting to the control terminals as shown in Figure 3.22. The installation location in the cabinet is shown in Figure 3.23.

Figure 3.23 Installation of SD in local control cabinet of recloser

3.3 Verification Studies

Building up from the concept of signal generation and detection, the diode based active protection scheme is presented by simulation studies using utility models with full explanation of detection procedures. This is followed by specificity studies using actual field measurement data and sensitivity studies concerning system parameters and worksite environment.

3.3.1 Simulation Tests

The abnormal conditions simulated can either be attributed to misoperation of recloser or accidental contact of equipment to live power line at the worksite. Thus, the scenario is simulated as a contact of worksite devices to distribution lines.

A typical case will be used as an example to verify the proposed scheme. A grounding resistance of 100 Ohms is used to represent the most probable value of a two meter's grounding rod. In this section, simulations are studied on both 25 kV and 13.8 kV voltage levels.

- ***25 kV Scheme***

Figure 3.24 shows a single-line diagram of the system used to investigate a typical case in 25 kV scheme performances. The system is simplified to a 25 kV distribution system connected to 20 MW resistive load throughout a 20 km line. 'Recloser' represents the closest upstream recloser from worksite, while breaker 'BRK' represents the worksite location where the accidental energization of equipment occurred. The generator is only connecting to one phase of the circuit from 'BRK' on. The worksite is 10 km away from the recloser along the feeder, equipped with proposed device and a temporary grounding rod. The basic system configuration and parameters, as shown in Table 3.5, were extracted from the CYME Power Engineering Software. This software has been commonly used in Canadian utilities for distribution network analysis.

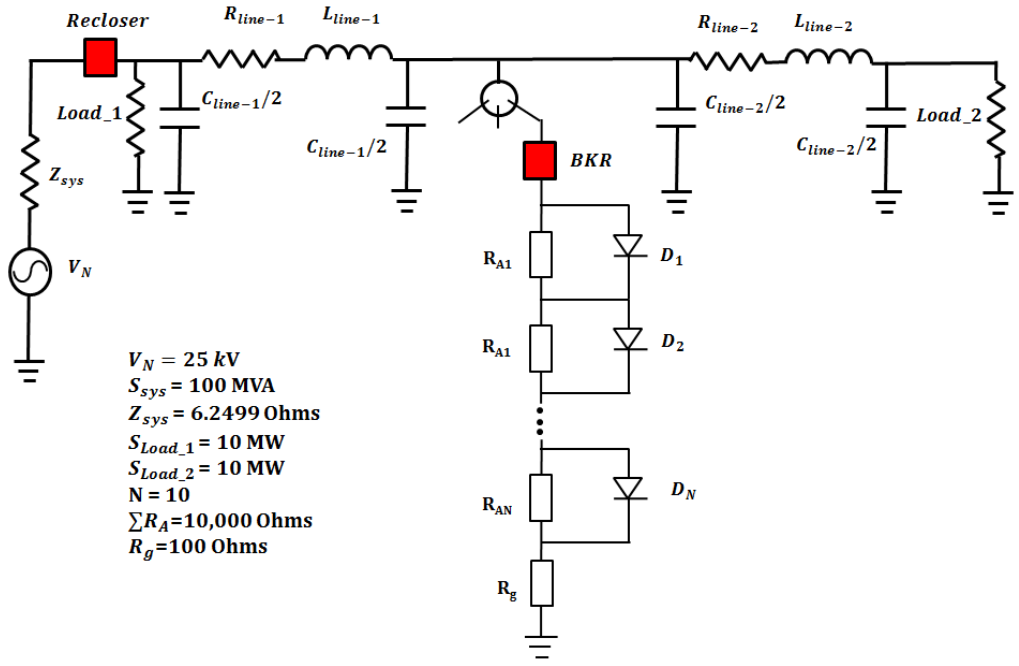

Figure 3.24 Single line diagram of 25 kV simulation circuit

Table 3.5 Line and load sequence impedance parameters in simulations

	Line-1	Line-2

R_1 (Ohm/m) (Positive)	0.2083E-3	0.2083E-3
R_0 (Ohm/m) (Zero)	0.0617E-3	0.0617E-3
L_1 (Ohm/m) (Positive)	0.2083E-3	0.2083E-3
L_0 (Ohm/m) (Zero)	0.1937E-3	0.1937E-3
C_1 (MOhm*m) (Positive)	254.02	254.02
C_0 (MOhm*m) (Zero)	643.23	643.23
Length (km)	10	10

Figure 3.25 illustrates the current waveforms of detected current and distortion waveforms in the scenario of 100 Ohms grounding resistance as the most typical worksite environment. Load current peak in this scenario is 589.7150 A, demonstrating a commonly seen scenario in 25 kV distribution feeder. When worksite device accidentally touches the bare power line, detected current amplitude in the fault phase increases to 748.6074 A.

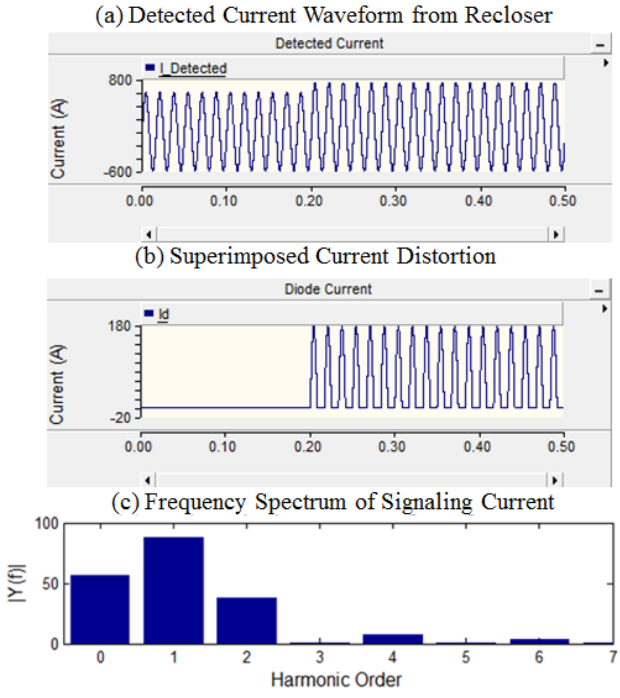

Figure 3.25 Detected current and Implemented Signals

In this simulation, worksite is set to energize at 0.20s. Simulation results indicate that the signal strength of generating signals has a disturbing peak current of 175.9067 A and DC magnitude of 55.9860 A. This is calculated to 7.48% of 748.6074 A detected current amplitude as shown in Figure 3.25.

Standard deviation (*std(i)*) of each consecutive four cycles and pre-set STD threshold of $1x10^{-3}$ is used to exclude singular zones in Figure 3.26 (b). According to pre-set DC ratio thresholds as 0.25% in "Zone_regular", 0.50% in "Zone_1" and 0.40% in "Zone_2", average DC ratios exceeding the threshold are detected as signaling signal as shown in Figure 3.26 (d).

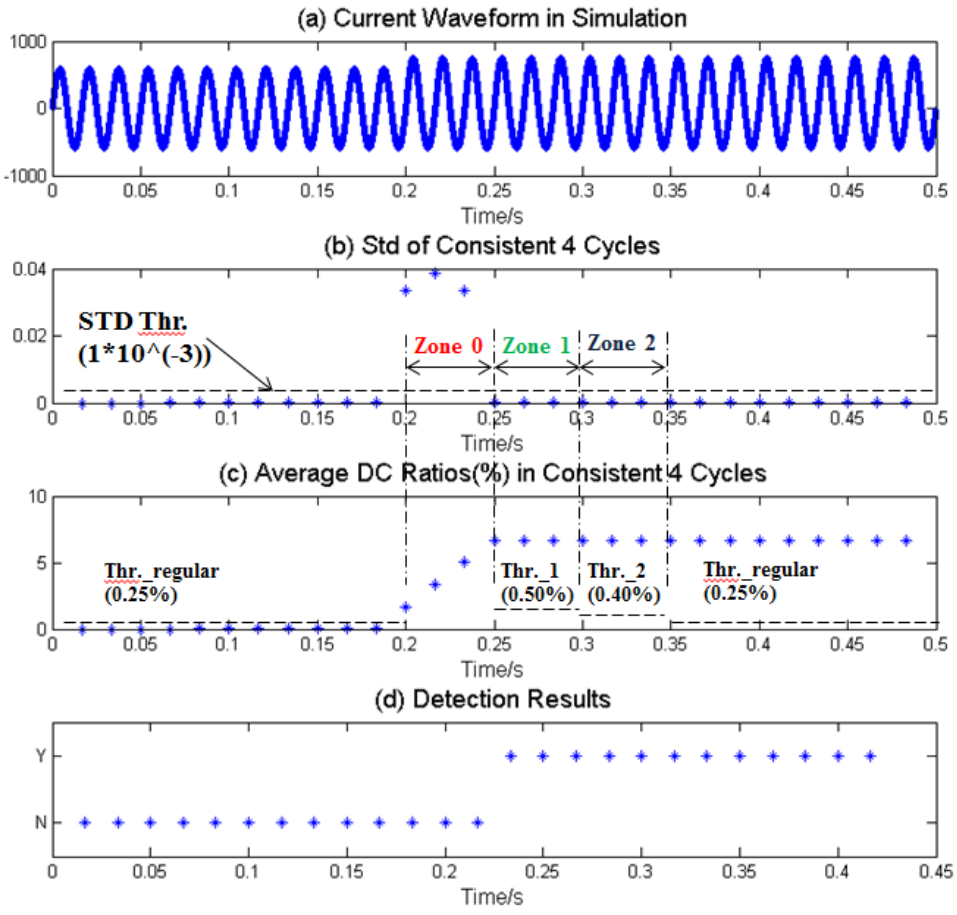

Figure 3.26 Detection results of 25 kV scheme

After worksite energizes at time = 0.20s, a fast response within 0.0667s (4 cycles) to trip the recloser and block its reclosing function is given by the

proposed scheme. This signal recognition and fast response is much efficient than general protection relays.

- ***13.8 kV Scheme***

Compared to 25 kV distribution systems, devices used in 13.8 kV feeders are smaller and lighter, but has a drawback of weak signal due to the inadequate power source from low line to ground voltage. Single line diagram and simulation parameters are shown in Figure 3.27 and Table 3.6.

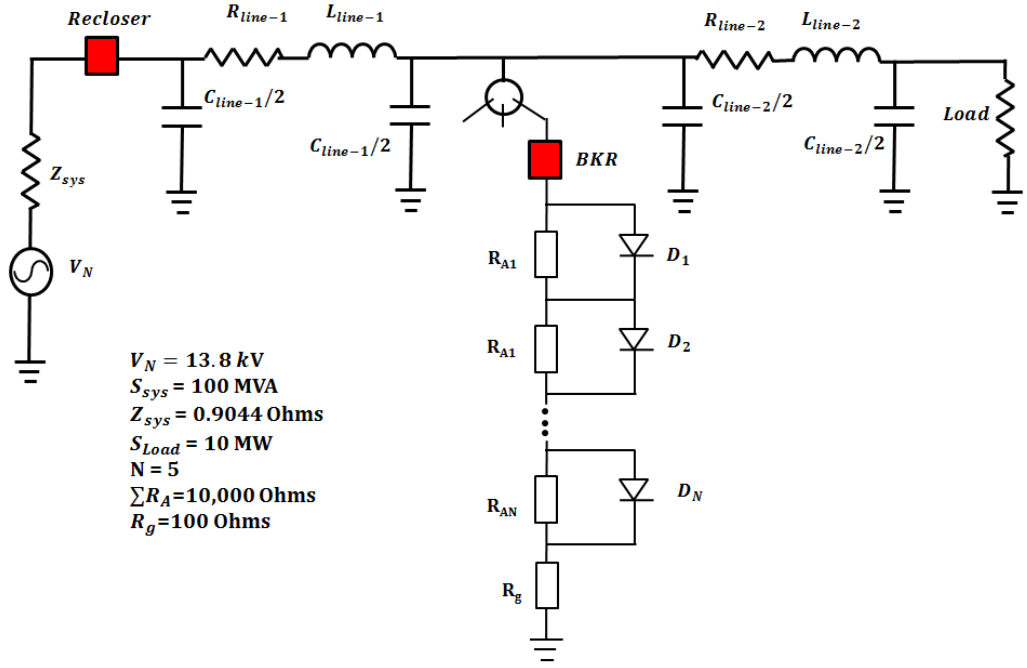

Figure 3.27 Single line diagram of 13.8 kV simulation circuit

Table 3.6 Line and load sequence impedance parameters in simulations

	Line-1	**Line-2**
R_1 (Ohm/m) (Positive)	0.8065E-3	0.8065E-3
R_0 (Ohm/m) (Zero)	0.0617E-3	0.0617E-3
L_1 (Ohm/m) (Positive)	0.2000E-3	0.2000E-3

L_0 (Ohm/m) (Zero)	0.1937E-3	0.1937E-3
C_1 (MOhm*m) (Positive)	254.02	254.02
C_0 (MOhm*m) (Zero)	643.23	643.23
Length (km)	2	2

Similar to the cases in 25 kV scheme, a typical grounding resistance of 100 Ohms is implemented. Current waveforms and current distortions are shown in Figure 3.28. Detected current amplitude before worksite contacting is 479.5435 A, proved to be a common scenario in 13.8 kV distribution feeder. By the time that worksite device touches the power line, detected current amplitude of the faulted phase increases to 571.7610 A.

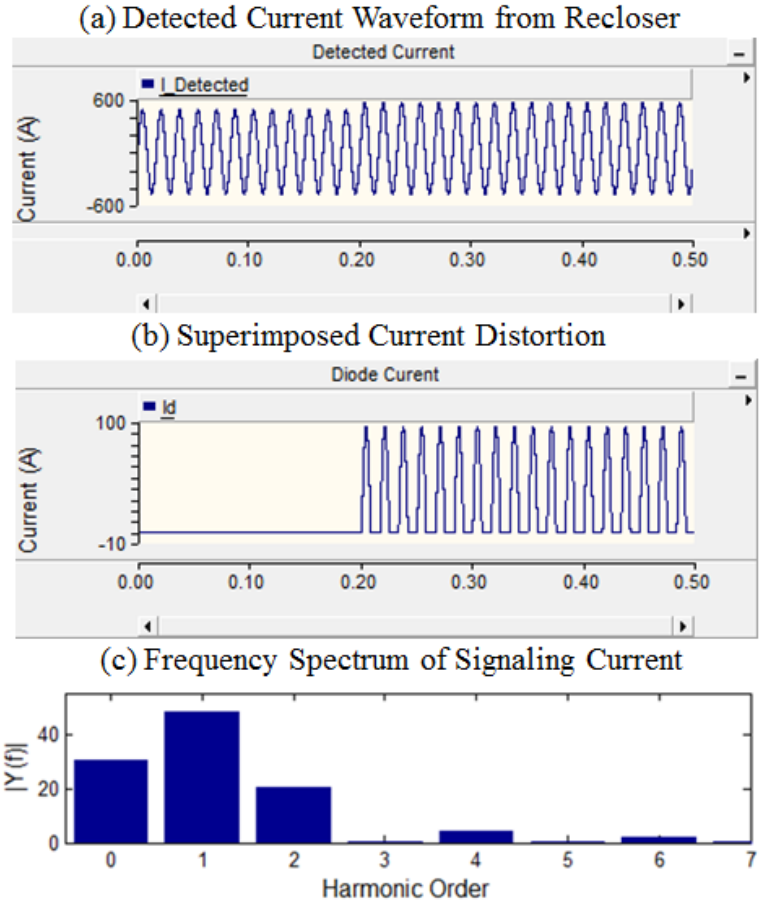

Figure 3.28 Detected Current and Implemented Signals

From the frequency spectrum of signaling current as shown in Figure 3.28 (c), the DC magnitude of signaling current reaches 30.54 A, constituting 5.34% of current amplitude 571.7610 A, and exceeds pre-set threshold 0.25%.

Since detection threshold has been standardized by percentage, no alternative sets of threshold need to be decided in 13.8 kV system. While worksite is energized at time = 0.20s, the detection process is shown in Figure 3.29.

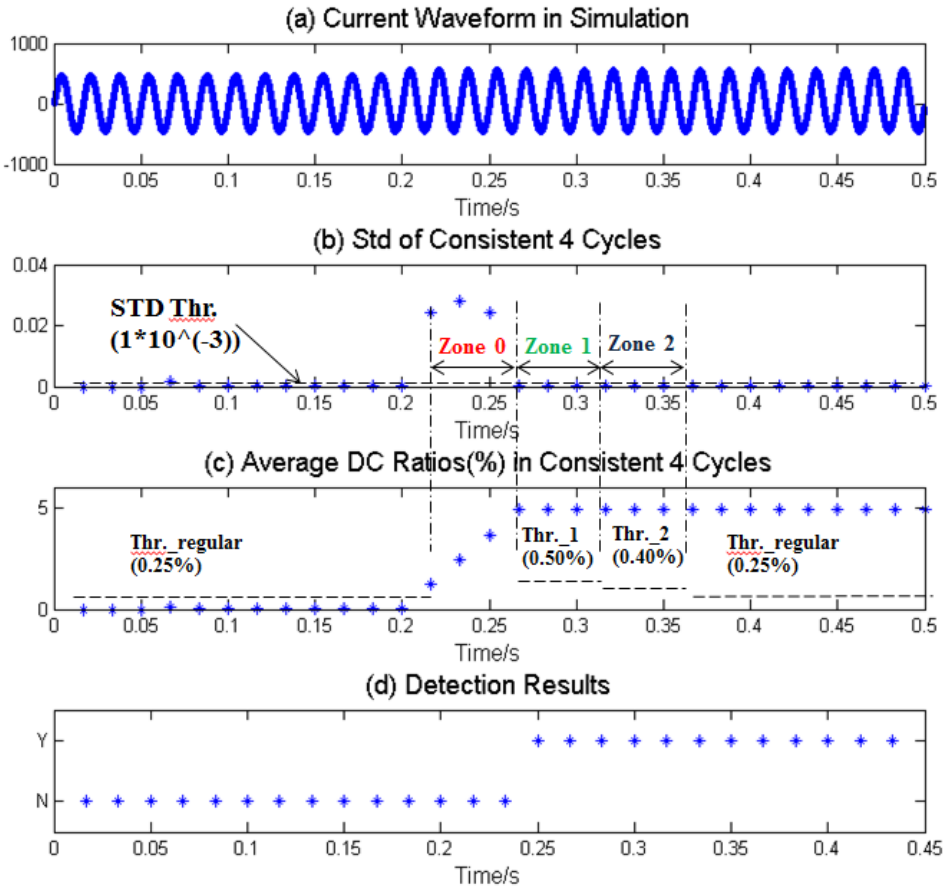

Figure 3.29 Detection results of 13.8 kV scheme

In this typical case with 100 Ohms grounding resistance and 571.7610 A detected current amplitude, the detection device demonstrates a fast response within 0.0667s (4 cycles) and 100% accuracy.

The results show a promising detection accuracy of 100% and a quick reaction within 0.067 s (4 cycles) in both 25 kV and 13.8 kV distribution systems. This

clearly indicates that this power line based trip grounding scheme is capable for providing adequate and essential protection for personnel safety and equipment protection.

3.3.2 Specificity Studies

Natural load variation is another concern for detection accuracy and false alarm. When no signals have been sent, we have to assure no false detection is triggered for power system reliability and stability. To estimate the false alarm rate, two weeks' field measurement data under normal load variation have been scanned through our detection process. Here we extract a 5 minutes' segment shown in Figure 3.30 to demonstrate no false alarm even in massive load variation period.

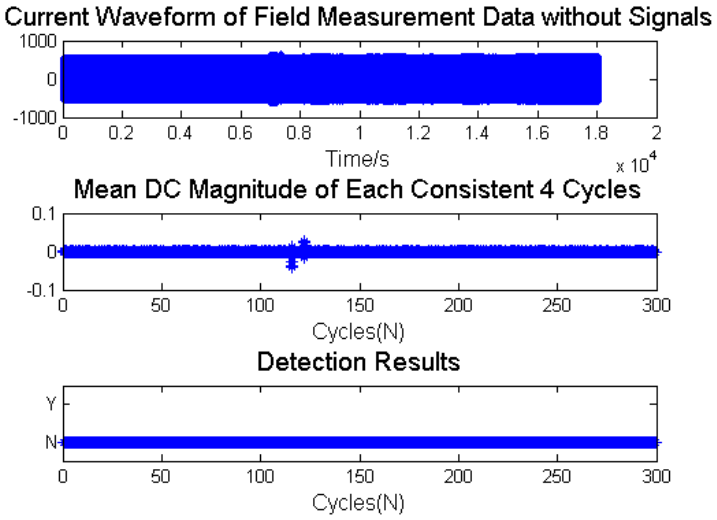

Figure 3.30 Scan of field measurement data under normal circumstance

Analysis of the data shows that the distortion between consecutive cycles caused by natural variation of loads is around 1.5% of RMS current, but no false detection occurred under natural distortion during a two weeks' data scanning.

The long-time span of measurement data indicate that our SD device will not have any interruption on natural load variation, assuring 100% specificity.

3.3.3 Sensitivity Studies

While a promising specificity has been inherently achieved in natural load variation of the measurement data, detection accuracy should be estimated with consideration of the various system parameters to determine the application range. System main parameters, including fault level, load capacity, distance from worksite to recloser, and grounding resistance can vary within a probable range. Signal strength in each circumstance is attained from simulation as a signal indicator. The most sensitive parameters are investigated by their composed impacts on signal strength and application restrictions.

- ***Variation of system parameters***

Extensive simulation tests are conducted in which key parameters involved are varied, including fault level, load capacity, distance from worksite to recloser and grounding resistance. Base case parameters are shown in Table 3.7, and the variations are shown as percentages of the base parameter values. The base case parameters used here are selected in the concern of variation range.

Table 3.7 Parameters in Base Case

	13.8 kV	25 kV
Fault Level (MVA)	100	300
Load capacity (MW)	10	10
Feeder length (km)	4	20
Worksite distance (km)	2	10
Grounding Resistance (Ohms)	300	300

Results of parameter studies of 25 kV and 13.8 kV schemes are shown in Figure 3.31 and Figure 3.32, respectively. The percentage variations of key parameters are included, while assessment of sensitivity is described by the signal strength (average DC ratios) in detected current.

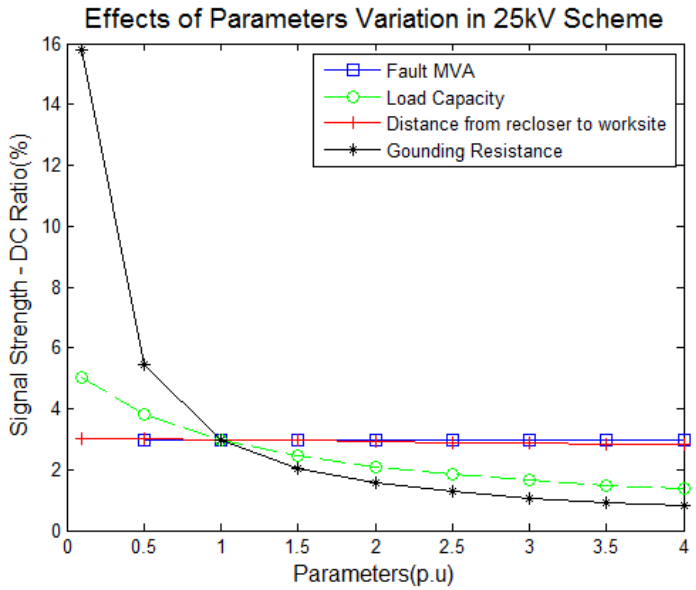

Figure 3.31 Signal strength due to system parameters variation in 25 kV scheme

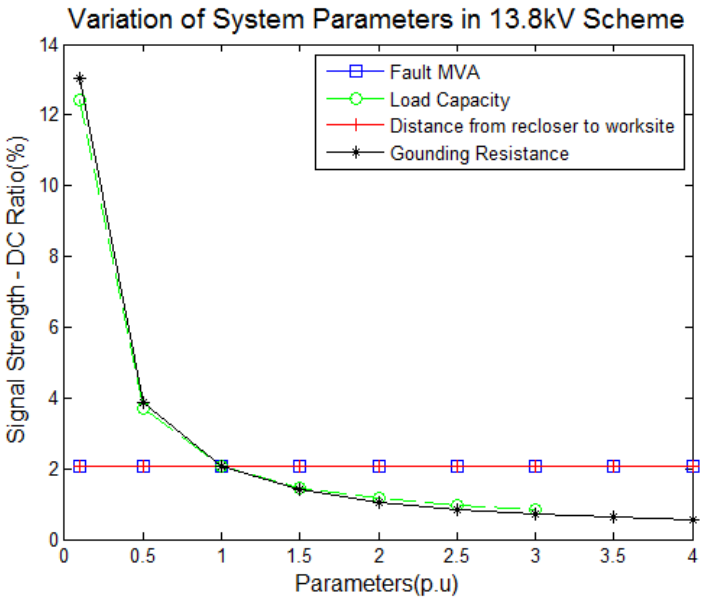

Figure 3.32 Signal strength due to system parameters variation in 13.8 kV scheme

Analysis of the test cases reveals that the generated signals are, in general, insensitive to fault level and fault location. The effect of such parameters can be kept in an insignificant range. However, load capacity and grounding resistance have a significant impact on signal strength. Signal decreases with large grounding resistance and also decreases with a raise in load capacity relating to detected current. These influences may be magnified when both parameters decrease at the same time. Therefore, considering the significant effects due to grounding resistance and detected current, we study these two parameters together to determine the applicable circumstances of proposed scheme.

- ***Grounding Resistance and Load Capacity (Detected Current Amplitude):***

As mentioned in Section 3.2, signal strength as a signal indicator is inversely proportional to the product of grounding resistance (R_g) and detected current amplitude(I_P) . Considering the practical concern of 10% voltage sag and 20% margin, DC strength as signal indicator is calculated as:

$$S_P = \frac{I_{DC}}{I_P} \cdot 90\% \cdot 80\% = \frac{\frac{\sqrt{2} \cdot V_N}{\sqrt{3} \cdot \pi \cdot R_g} \cdot 90\% \cdot 80\%}{I_P} = \frac{\sqrt{2} \cdot V_N}{\sqrt{3} \cdot \pi} \cdot \frac{1}{R_g \cdot I_P} \cdot 90\% \cdot 80\% \quad (3.11)$$

where

I_{DC}: Magnitude of DC component in detected current (A)

I_P: Amplitude of detected current (A)

V_N: Rated line-to-line voltage of distribution line (V)

R_g: Grounding resistance (Ohms)

Detection accuracy is studied based on distribution probability of measurement detected current as analyzed above. In order to assure 100%

detection accuracy, the signal strength has to reach at least 0.6% in the case of 0.25% DC detection ratio as shown in Table 3.3.

- 25 kV scheme:

For 25 kV scheme, the coordination range between grounding resistance and the amplitude of detected current with 0.6% strength signals is shown as region A in Figure 3.33. Signals generated from worksite condition within region A can be 100% detected, while the detection accuracy cannot be promised in region B.

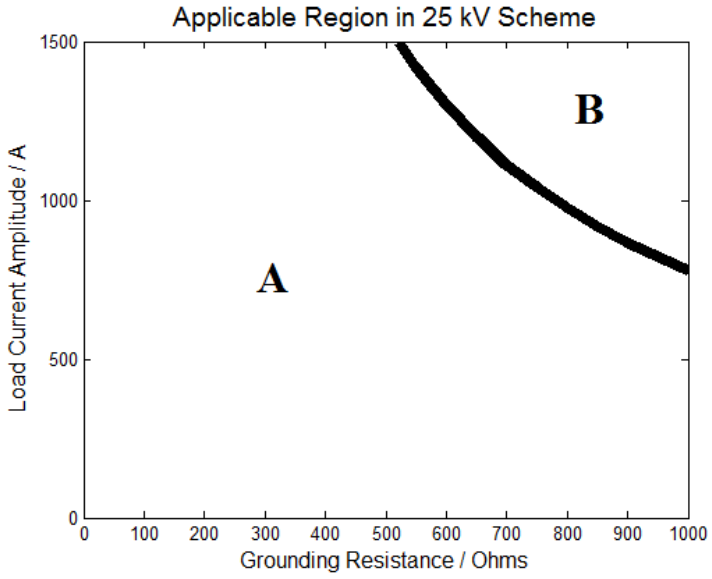

Figure 3.33 Applicable worksite conditions in 25 kV scheme

With a high grounding resistance, signals cannot be set up powerfully, leading to inadequate signal strength. On the other hand, in a feeder with strong load capacity, signals may be covered or mixed with natural disturbance or other line transient. Combining these two factors, worksite conditions in the region of B in Figure 3.33 with high grounding resistance and high detected current may not achieve a 100% detection rate.

- 13.8 kV scheme:

Comparing to 25 kV scheme, the lower line-to-ground voltage in 13.8 kV system has a natural disadvantage in signal generation. This leads to more

restrictions in grounding environment and load capacity. In order to generate at least 0.6% signal strength for 0.25% DC percentage as detection criterion, grounding resistance and detected current amplitude should meet the range within region A in Figure 3.34.

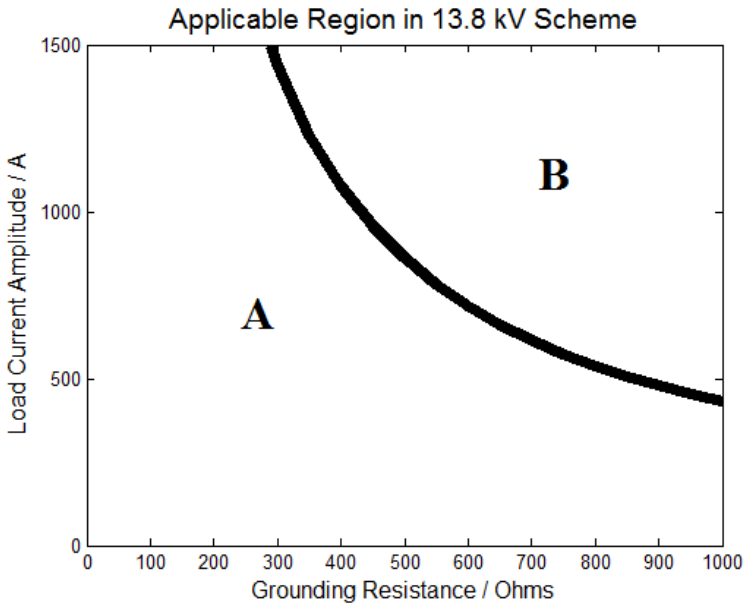

Figure 3.34 Applicable worksite conditions in 13.8 kV scheme

The applicable range of proposed diode-based active protection scheme is limited by worksite conditions, detection accuracy can be assured by acceptable grounding resistance and low to medium load capacity. However, such worksite conditions cannot always be assured in reality. Therefore, in order to extend the applicable worksite circumstances and assure a promising accuracy, an improved protection scheme based on thyristor sets is proposed in Chapter 4.

Chapter 4
Design and Verification of Thyristors-Based Active Protection Scheme

Through implementation of Power Electronics devices, communication signals can be shaped to a unique pattern and particular feature. In this proposed scheme, thyristor sets are implemented to enhance the specific characteristics of signal.

4.1 Signal Generation

The thyristor-based signal generator is designed to generate sufficient signal strength in a wide range of worksite environment and to ensure the recognizable signal pattern.

4.1.1 Structure of Signal Generator

Similar to the diode based signal generator, to make the device more economic and reliable, the actual signal generator configuration in thyristor-based scheme is also composed of several identical signal generating units. These units are connected in series and a common control. The circuit of signal generator is shown in Figure 4.1.

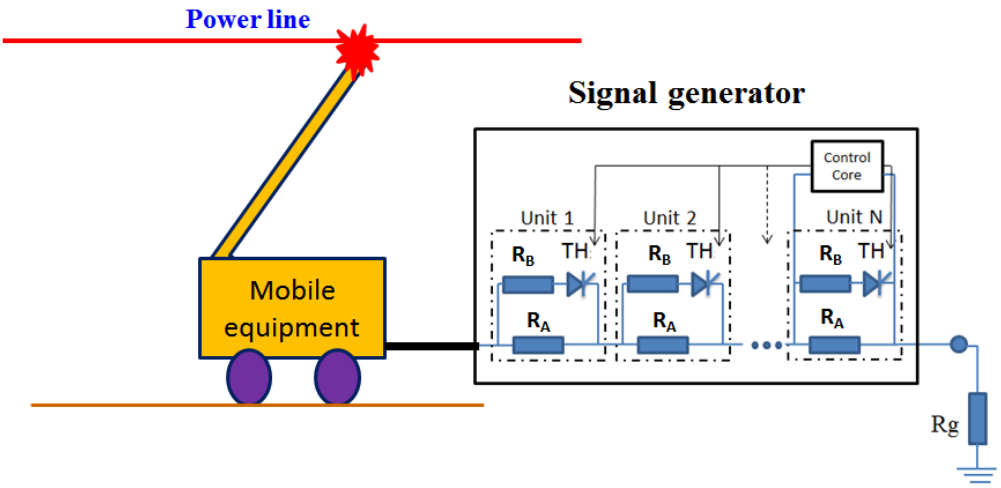

Figure 4.1 Structure of Signal Generator (SG)

Each signal generating unit consists of: (1) a thyristor (TH) to generate a one-way current distortion, (2) a voltage dividing resistor (R_A) to equalize off-state voltage to each thyristor unit, and (3) a current limiting resistor (R_B) to restrict generated signals to a range that satisfy thyristor on-state current. All these signal generating units are controlled by a single controller to achieve the same firing angle and firing patterns.

The detailed signal generation process is illustrated in following:

- In the off-state condition of thyristors, fault current is limited by the voltage dividing resistor (R_A) to an extremely low level (around 0-2 A). This can be regarded for this purpose as open circuit.
- Once a zero crossing point on voltage rising edge is detected by the controller, a turn-on impulse will be sent to each thyristor simultaneously after (π-δ) time delay in every two cycles. Since the current limiting resistor (R_B) is much smaller than voltage dividing resistor (R_A), current commutates rapidly to thyristor path when thyristors are turned on.
- When current waveform goes down to zero and reverse direction, thyristors are turned off automatically.

The generated current distortion, i.e. signal, is shown in Figure 4.2(3). It will be superimposed on the load current of power line and reach the closest upstream signal detector (SD) that is able to extract and identify the signal.

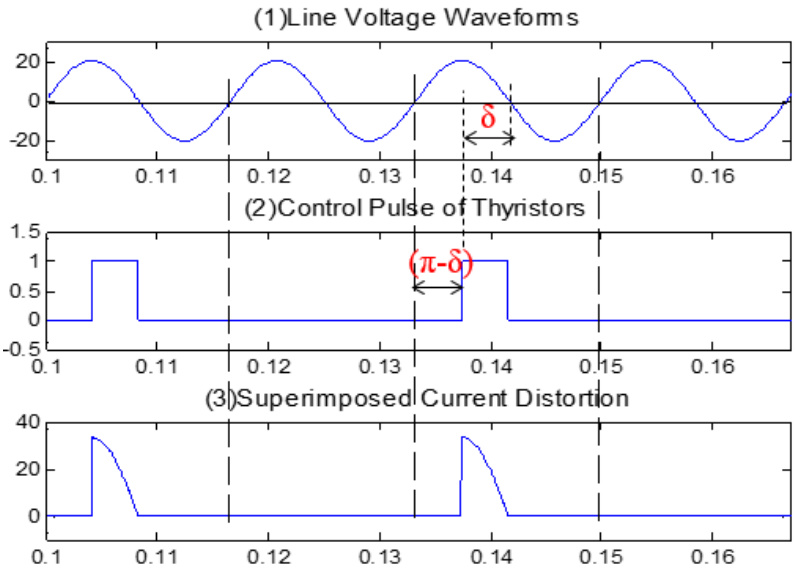

Figure 4.2 Current Distortion (Signal)

Compared to diode based signal generator, this signal generating scheme has a more distinct shape because of the pre-set gate control pulse of thyristors' on and off pattern. Due to this unique feature, signals are easier to be detected and confirmed. Therefore, the chances of false tripping is minimizes.

4.1.2 Parameter Determination of Main Circuit

As can be seen in Figure 4.1, the main circuit of the generator consists of N identical units and each unit has three components, i.e., thyristor (TH), voltage dividing resistor (R_A) and current limiting resistor (R_B). Therefore, the circuit parameters to be determined include: number of units (N), voltage dividing resistance (R_A), current limiting resistance (R_B) and firing angle (δ) of thyristor.

The circuit parameters of signal generator determine the signal pattern and signal strength. Certainly, stronger signal strength would be helpful for distinguishing the signal from natural load current. However, generating a

stronger signal requires larger capacity and current withstand ability of circuit components as well. This results in a larger size of the device. A balance has to be met between strong signal strength and reasonable generator size in parameter determination.

The other hand to be considered is that the signal generator must also be able to work properly at various worksites with different soil conditions. Different soil conditions indicate different grounding impedances which significantly impact signal strength. To ensure sufficient signal strength at various grounding conditions, one solution is to gradually change the firing angle to meet the required signal strength. The drawback is longer time duration. The problem arising is that the trip grounding method also requires critical signal response speed. Therefore, only fixed firing angle can be selected. As a result, the challenge of finding a proper firing angle has to be overcome.

With the above considerations, the circuit parameters must be designed to enable the strongest signal generation under the following conditions.

— Fixed thyristor firing angle to enhance the speed of trip grounding

— Maintain a small size such that the device is portable for use at many different types of worksites

— Suitable for a wide range of grounding resistances

To satisfy the above requirements, the following steps are taken in the parameters determination process.

- Step 1: derive an equation for signal strength estimation.
- Step 2: find the practical limits of component parameters while keeping a portable size.
- Step 3: determine the parameters to enable the circuit to generate the strongest signal within practical limits.

In this process, a two-meter long grounding rod is employed. This reflects the most common field practice. This normally results in a grounding resistance from 10 Ohms to 1000 Ohms for a variety of soil conditions.

- ***Step 1: Theoretical analysis***

The case where SG fires between phase A and ground is shown in Figure 4.3. In this circuit, $\sum R_A$ and $\sum R_B$ are the summation of R_A and R_B resistance of N units, $\sum V_{TH}$ is the voltage on N thyristor sets when there is no signaling. The steady state sinusoidal voltage on each thyristor $v_{TH}(t)$ can be expressed as

$$v_{TH}(t) = \frac{1}{N}\sqrt{\frac{2}{3}} \cdot V_N \cdot \sin(\omega t) \cdot \frac{\sum R_A}{\sum R_A + R_g} \tag{4.1}$$

where

V_N is the rated phase-to-phase voltage at the worksite.

According to superposition principle, the signaling process is equivalent to injecting a negative voltage source $-v_{TH}$ between the two ends of thyristor sets. The signaling transient can be calculated with a circuit energized by $-v_{TH}$ as shown in Figure 4.4, where Z_{line-1} is the equivalent line impedance of the upstream system and R_g is the grounding resistance. In this circuit, the other two phases and loads are approximated as open circuits.

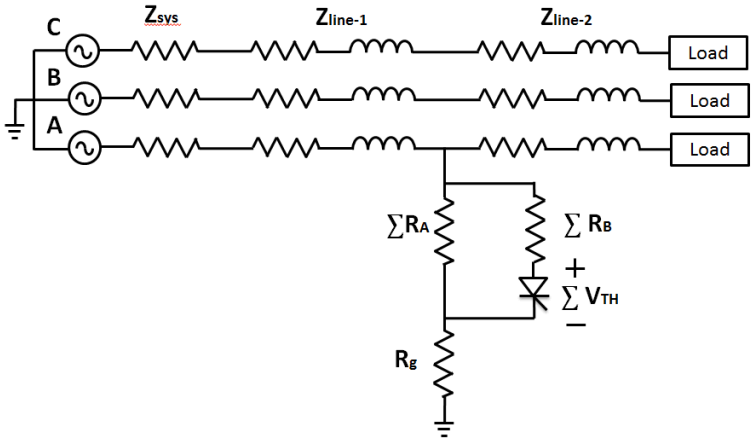

Figure 4.3 The analysis circuit for single phase signaling

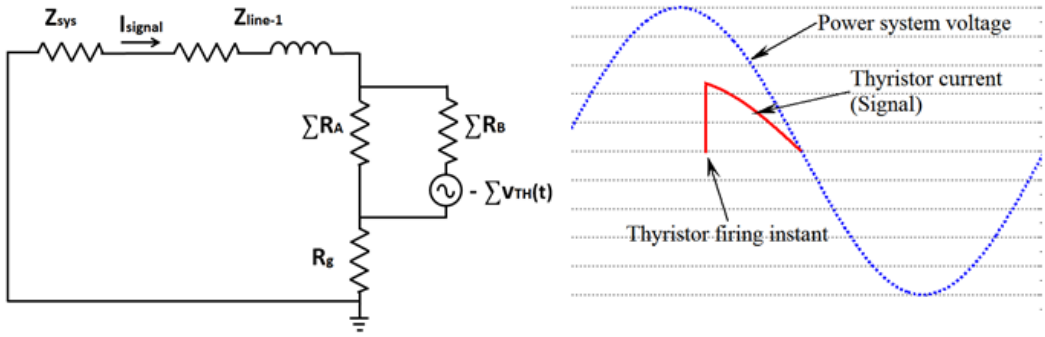

Figure 4.4 Equivalent Signaling Circuit and Generated Signals

If the thyristor is fired ahead of v_{RA}'s zero crossing point by an angle of δ, then turned off when the waveform current switches direction, the current distortion (signal) can be determined as:

$$i_{signal}(t) = \sqrt{\frac{2}{3}} \cdot V_N \cdot \sin(\omega t) \cdot \frac{\sum R_A}{\sum R_A + R_g} \cdot \frac{1}{\sum R_B + R_g + Z_{line-1}}, \omega t \in [-\delta, 0] \quad (4.2)$$

The peak of $i_{signal}(t)$ represents the strength of the active protection signal, which is

$$I_{peak} = -\sqrt{\frac{2}{3}} \cdot V_N \cdot \sin(\delta) \cdot \frac{\sum R_A}{\sum R_A + R_g} \cdot \frac{1}{\sum R_B + R_g + Z_{line-1}} \propto \frac{\sin(\delta)}{\sum R_B + R_g} \quad (4.3)$$

As mentioned above, the grounding resistance Rg can vary in such a large scale between 10 Ohms and 1000 Ohms, and Rg is a very sensitive factor to the signal magnitude according to above equations. As a result, the strongest signal strength is attributed to the lowest grounding resistance, and weakest signal strength to the highest grounding resistance as shown below.

$$I_{peak\_max} = -\sqrt{\frac{2}{3}} \cdot V_N \cdot \frac{\sum R_A}{\sum R_A + 10} \cdot \frac{1}{\sum R_B + 10} = -\sqrt{\frac{2}{3}} \cdot V_N \cdot \frac{1}{\sum R_B + 10} \quad (4.4)$$

$$I_{peak\_min} = -\sqrt{\frac{2}{3}} \cdot V_N \cdot \frac{\sum R_A}{\sum R_A + 1000} \cdot \frac{1}{\sum R_B + 1000} = -\sqrt{\frac{2}{3}} \cdot \frac{10}{11} \cdot V_N \cdot \frac{1}{\sum R_B + 1000} \quad (4.5)$$

where

V_N is the rated phase-to-phase voltage at the worksite.

- ***Step 2: Practical limits for components***

Considering a portable sized device, SG is limited by three practical constraints of the components:

1) The maximum SCR off-state voltage of 1500 V for thyristor TH, $\mathbf{V_{SCR.max}}$

$$V_{SCR} \leq V_{SCR.max} = 1500\ V \tag{4.6}$$

Limit $\mathbf{V_{SCR.max}}$ can be used to determine the number of units *N* with known system voltage.

2) The maximum allowable thyristor current of 100 A for thyristor TH, $\mathbf{I_{SCR.max}}$

$$I_{peak} \leq I_{SCR.max} = 100(A) \tag{4.7}$$

3) The maximum resistor power handling capacity of 5000 W for current limiting resistor R_B, $\mathbf{S_{R_B.max}}$

The resistance capacity of R_B can be calculated by

$$S_{R_B} = \frac{1}{2*2\pi}\int_{\pi-\delta}^{\pi}\left(\frac{I_{peak}}{\sin\delta}\right)^2 (\sin\theta)^2 * R_B\, d\theta \leq S_{R_B.max} = 5000(W) \tag{4.8}$$

where I_{peak} is the peak value of signal; S_{R_B} is the capacity of current limiting resistor R_B.

The upper limits of $\mathbf{I_{SCR.max}}$ **and** $\mathbf{S_{R_B.max}}$ can be used to select a proper R_B with known R_g and firing angle δ.

- ***Step 3: Parameter determination***

Based on the signal strength calculation equation and the practical limits for each component, two sets of parameters are determined for 13.8 kV and 25 kV distribution systems respectively.

1) Numbers of Unit (N)

The number of signal generating units is determined by the maximum SCR off-state voltage V_{SCR} on each thyristor. The criteria are as follow:

$$N \geq \frac{V_N}{\sqrt{3}} / V_{SCR} \tag{4.9}$$

where

N is the numbers of unit;

V_N is rated line-to-line voltage of bus feeder;

V_{SCR} is the maximum cut-off voltage of each thyristor, which is 1500 V.

Based on (4.9), 6 units will be used in SG for 13.8 kV system while 10 units will be used in SG for 25 kV system.

2) Voltage dividing resistance (R_A)

The main function of R_A is to equalize the voltage implemented on each signal generating unit when thyristors are off, and the value of R_A has little impact on signal generation. It is commonly selected, based on experience, to a value of 10,000 Ohms.

3) Firing angle (δ)

From theoretical analysis, current signal strength increases with an increase of sin(δ). Therefore, to generate the strongest signal, we set the firing angle to 90 degrees.

4) Current limiting resistor (R_B)

Signal strength is mainly determined by R_B and R_g as shown in Fig. 4.4. The smaller the R_B and R_g values, the stronger the signal strength will be. The determination of the value of R_B should satisfy both R_B capacity and allowable thyristor current requirements when R_g varies between 10 to 1000 ohms.

For the maximum and minimum R_g, the minimum and maximum thyristor currents can be calculated with respect to various R_B as shown in Table 4.1 and

Table 4.2. Satisfactory results are presented to check the availability of such signal range as shown on the latter two columns in Table 4.1 and Table 4.2 for 11 kV and 25 kV signal generators respectively. The highest signal strength case satisfying these two constrains are selected as R_B sizes highlighted in yellow.

Table 4.1 Parameters for RB in 13.8 kV Scheme

∑RB (Ω) (5 units)	**SCR current I_{peak_min} (A) (R_g=1000Ω)**	**SCR current I_{peak_max} (A) (R_g=10Ω)**	**Satisfy R_B Capacity Requirement (5000W)**	**Satisfy SCR Current Requirement (100A)**
50	9.76	187.61	N	N
100	9.31	102.33	N	N
200	8.54	53.60	N	Y
300	7.88	36.31	Y	Y
400	7.32	27.45	Y	Y
500	6.83	22.07	Y	Y

Table 4.2 Parameters for RB in 25 kV Scheme

∑RB (Ω) (5 units)	**SCR current I_{peak_min} (A) (R_g=1000Ω)**	**SCR current I_{peak_max} (A) (R_g=10Ω)**	**Satisfy R_B Capacity Requirement (5000W)**	**Satisfy SCR Current Requirement (100A)**
100	16.87	185.38	N	N
200	15.46	97.10	N	Y
300	14.27	65.78	N	Y
400	13.25	49.74	N	Y

500	12.37	39.98	Y	Y
600	11.60	33.43	Y	Y
700	10.92	28.72	Y	Y

Tables 4.1 and 4.2 can also be depicted as Figures 4.5 and 4.6.The light and dark blue lines represent the minimum and maximum signal strengths that can be achieved by possible grounding resistance ranging from 1000 Ohms to 10 Ohms. And each size of R_B lead to a specific range of signal strength range as shown by dashed area. The practical constrains are shown in purple and brown lines, and the highest signal strength can be achieved when R_B is equal to 300 Ohms in the 13.8 kV scheme, and 500 Ohms in the 25 kV scheme.

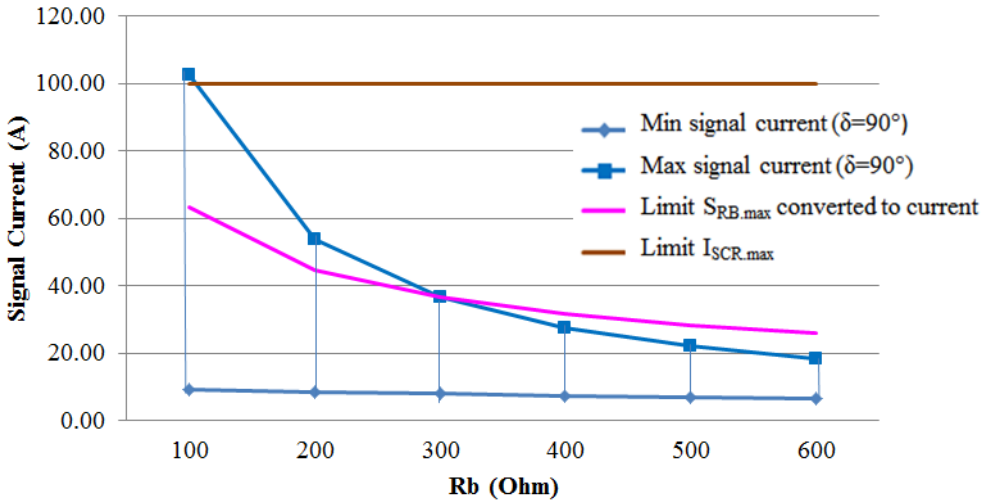

Figure 4.5 Parameter Determination of RB in 13.8 kV Scheme

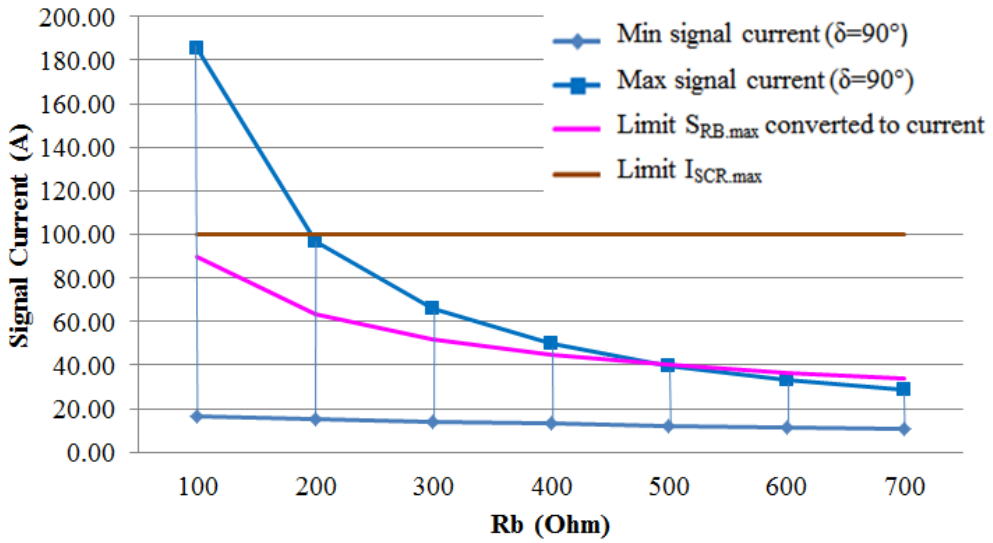

Figure 4.6 Parameter Determination of RB in 25 kV Scheme

Device parameters for the 13.8 kV and 25 kV are summarized in Table 4.3. The parameters for any other voltage level can be obtained in the same manner.

Table 4.3 Parameters of signal generator for 13.8 kV and 25 kV systems

System Voltage	**13.8 kV**	**25 kV**
Number of Units	6	10
Voltage dividing resistance R_A (Ohms)	10000	10000
Current limiting resistance R_B (Ohms)	300	500
Firing angle δ	90°	90°

Base on the above analysis and parameters, when the grounding resistance varies from 10 Ohm to 1000 Ohm, the extreme generated signal strengths calculated by theoretical analysis are shown in Table 4.4.

Table 4.4 Extreme generated signal strength (A) for 13.8 kV and 25 kV systems

System voltage	13.8 kV	25 kV
Best case (R_g = 10 Ohms)	36.31	39.98
Worst case (R_g = 1000 Ohms)	7.88	12.37

4.1.3 Signal Pattern

After the determination of the circuit parameters, the rest of the work regarding signal generation is to figure out the signal pattern.

To obtain the strongest signal, the firing angle is determined as 90 degrees. Hence as shown in Figure 4.7, this signal can be located from 90 degree ahead of zero crossing point to zero crossing point of the falling edge in shift with the voltage waveform. Such a fixed angle firing method not only shortens detection time, but also largely simplifies the signal detection process.

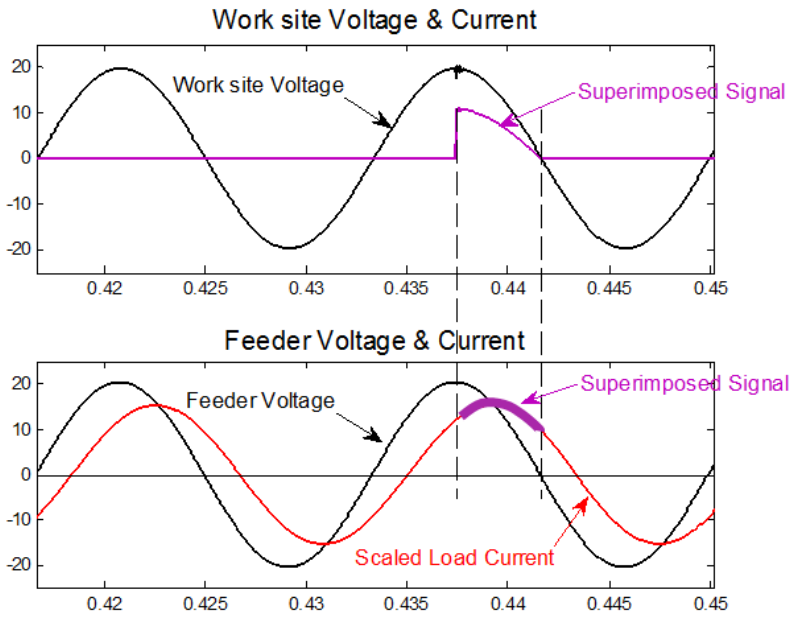

Figure 4.7 Superimposed current signals

An effective yet simple signal extraction methodology at upstream SD is to subtract two consecutive cycles. In these two cycles, one is free of the signal, and the other one contains the signal. Therefore, the current distortion (signal) will be generated once in every two consecutive cycles as shown in Figure 4.7.

It is worth mentioning that the signal strengths shown in Table 4.4 do not mean the signal strength is assuredly sufficient to be recognized by the upstream signal detector. The accomplishment of signal extraction and recognition are also dependent on the background signal (load current), since the signal is superimposed on the load current and sent upstream. Larger load current requires stronger signal so that the signal can be extracted correctly.

The next section will deal with the signal extraction problem.

4.2 Signal Detection

The proposed trip grounding method relies on the powerline as its communication route. Hence it is a fast, reliable, simple and economical method of sending and receiving trip signals. The signal detection devices are installed at various recloser locations. The signal sent from SG, combined with load current, propagates from the worksite location to upstream recloser through various power line paths. Thus, there are two challenges that the signal detection device encounters. One is how to effectively extract the signal from signal carrying detected current, and the other one is how to distinguish signal from other noises. It is necessary for an effective signal extraction algorithm to reliably recognize the signal from detected current.

In response to this requirement, there are three stages leading to tripping the recloser: signal extraction, signal identification and command confirmation. As shown in Figure 4.8, all these process should be completed by the signal detection device.

In signal extraction stage, the generated signal, coming in combined with load current, will be extracted to the greatest extent.

In the signal identification stage, the resulting waveform after extraction stage will be tested using two criterions for identifying the signal existence.

In command confirmation stage, the signal existence will be further confirmed by observing the repetition of the signal.

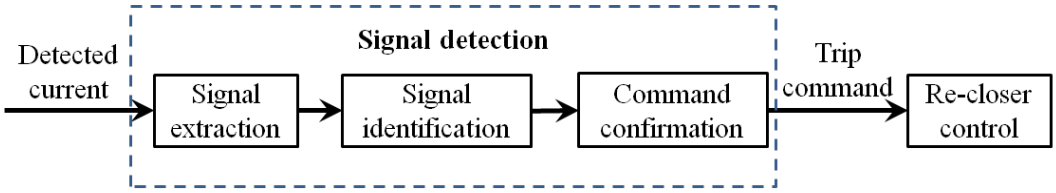

Figure 4.8 Three stages of signal detection

4.2.1 Signal Extraction

The detected current, including the signal picked up from the upstream reclosers can be depicted as Figure 4.9(a). Since the thyristor fires in a fashion such that the signal exists in only one of two consecutive cycles (i.e. cyc1, cyc3, cyc5, etc.), the difference between two consecutive cycles is ideally the expected signal sent from SG at worksite. However, limited by the system voltage and possibly due to the high grounding resistance at worksite, the signal delivered to the upstream recloser may not be strong enough to be distinguished by the simple subtraction method, as encountered on the experiments. To overcome these difficulties, a new signal extraction algorithm named as "two-step signal extraction method" is proposed. This algorithm works through two stages of integral cycle subtraction. As a result, the signal strength can be doubled.

This algorithm is presented in following details.

- Step 1

A feeder current containing a signal with strength of about 3 A is shown in Figure 4.9(a). This current was made of an actual load current taken from field measurements and a simulated signal. The Step 1 signal subtraction yields **S1** as obtained from the function shown in (4.10).

S1= [(cyc2-cyc1), (cyc3-cyc2), (cyc4-cyc3), …, (cyc (*i*) – cyc (*i*-1)), …](4.10)

where 'cyc' indicates the cycle of detected current waveform.

The numerals that follow indicate the sequence number of the detected current cycle.

Following the sequence, N detected current cycles can produce N-1 consecutive signals. These siganls are alternating in positive and negative direction, as shown in Figure 4.9 (b).

Since the load current varies with time, the consecutive cycle subtraction cannot cancel out the load current completely. A small load current variation can be expected to exist in the result. If this load variation magnitude becomes comparable with the signal strength, it may lead to the false identification of the signal. This situation will most likely happen when the load current is large, as the larger load current contains relatively larger load variation.

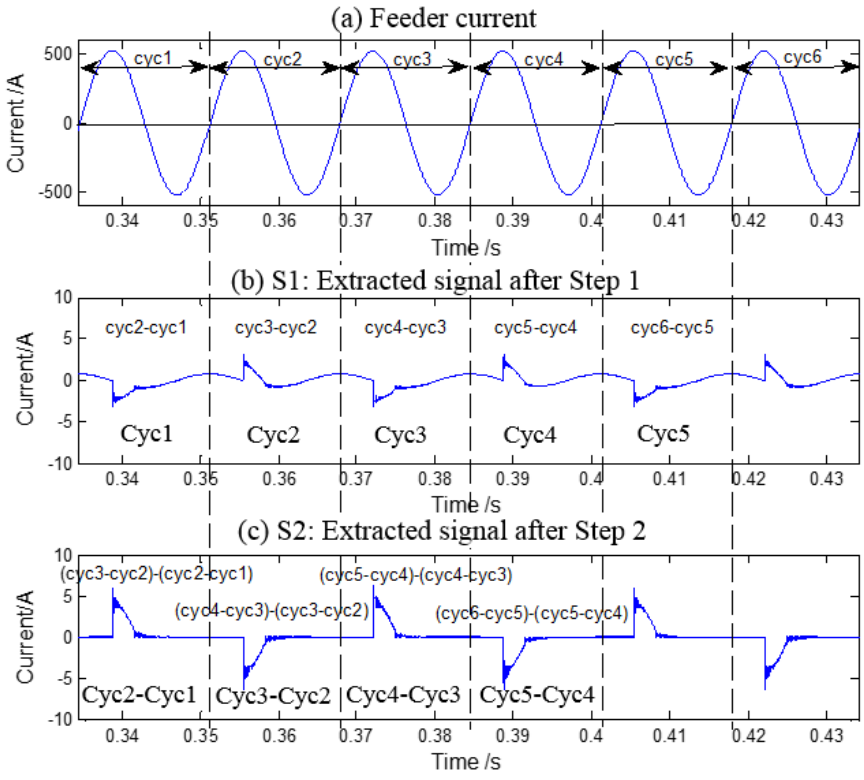

Figure 4.9 Methods of Signal Extraction

- Step 2

The idea behind Step 2 is to eliminate the natural load variation, and enhance the signal strength. The method is to repeat the above subtraction process on the output of signal sequence **S1** in Step 1. The final signal sequence **S2** as shown in Figure 4.9(c) can be expressed in (4.11).

S2= [(Cyc2-Cyc1), (Cyc3-Cyc2), (Cyc4-Cyc3), …, (Cyc (*i*) – Cyc (*i*-1)), …](4.11)

where 'Cyc' indicates cycle of **S1**, and the numerals that follow indicates the sequence number of **S1** cycle.

The Step 2 subtraction doubles the signal strength as shown in the bottom figure of Figure 4.9, since the two nearby opposite signals are superimposed. Meanwhile, the load variation can be canceled out to some extent.

Obviously, N **S1** signals produce N-1 **S2** signals. Therefore, N detected current cycles result in N-2 **S2** signal cycles.

The final signal **S2** can also be formulated by detected current cycle as (4.12) to simplify the algorithm process.

$$\mathbf{S2} = [\ \text{cyc}\ (i+2) - \text{cyc}\ (i+1)\ ] - [\ \text{cyc}\ (i+1) - \text{cyc}\ (i)\ ] \qquad (4.12)$$

The algorithm of "two-step signal extraction method" is demonstrated to be very simple. It is significantly helpful in practical implementations, especially when signal strength is limited by practical conditions.

4.2.2 Signal Identification

After the signal extraction process is completed, criteria have to be set to identify the real signal existence in each S2 signal cycle. To ensure the correctness of the signal identification, two criteria are proposed, i.e., signal energy criterion and signal strength criterion.

The signal energy criterion is used to identify real signal existence from signal energy aspect. Since the signal is generated in fixed 90 degree firing angle, the

signal location in each cycle can be predicted. The 90 degree firing angle means the signal starts from 90 degree after the zero crossing point of voltage rising edge. Then, the signal existence can be determined by signal energy criterion.

The signal strength criterion is used to identify real signal existence from signal strength aspect. After the signal extraction process, the signal has been doubled. Since the generated signal strength range is also known as presented in Section 4, the extracted signal strength range of real signal can be estimated. With the known signal strength range, the real signal existence can be determined by signal strength criterion.

The satisfaction of two criteria indicates the identified signal shape.

- ***Signal energy criteria***

In the entire signal detection process, the voltage is always taken as the reference as shown in Figure 4.10(a). In this figure, the signal cycle is defined as 'Period' with duration from one positive peak of the voltage to the next positive peak of voltage. The 'Period' starting point is also the real signal starting point if there is a real signal. The real signal will automatically end at the zero crossing point of the voltage falling edge. 'seg 1' is the segment from the positive peak of voltage to its declining waveform zero cross point. This is the portion where trip signal may appear. 'seg 2' is the remainder of the 'Period' from zero crossing point of the waveform falling edge to the positive peak.

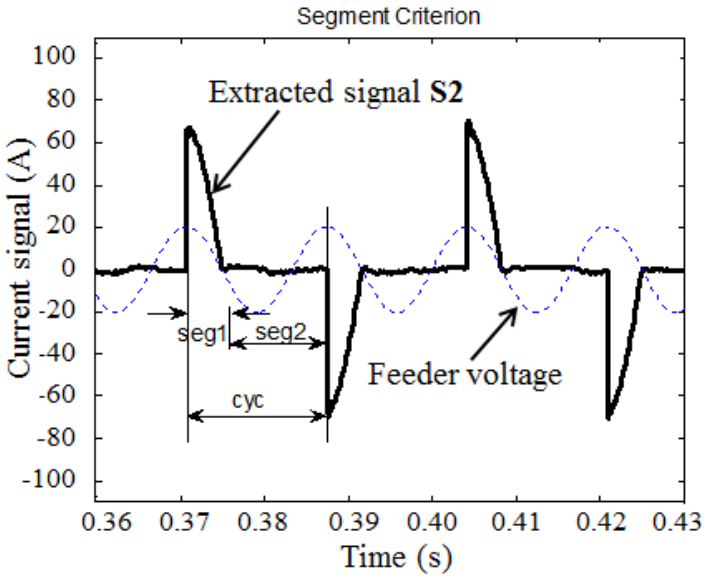

(a) Signal energy criteria

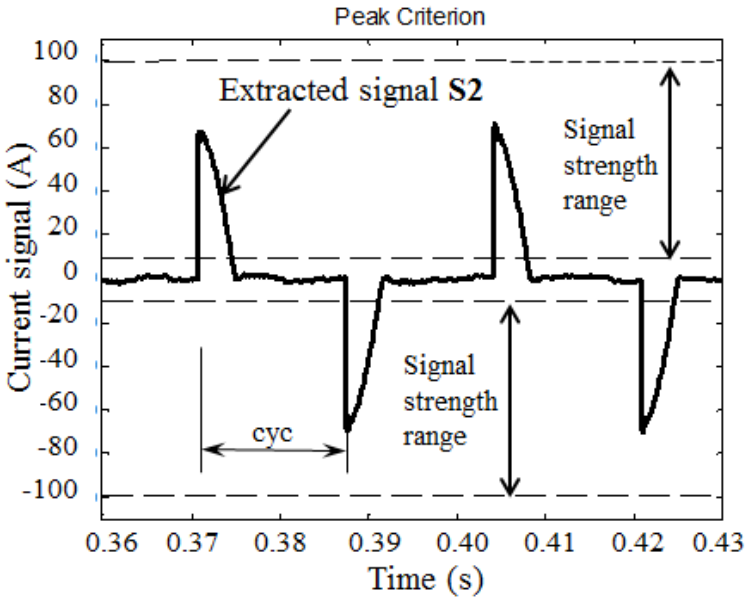

(b) Signal strength criteria

Figure 4.10 Signal identification criterion

A real signal coming from worksite fault will strengthen ‘seg 1’, but not ‘seg 2’. The RMS value of ‘seg 1’ and ‘seg 2’ are quantified and evaluated to determine the existence of real signal. The RMS value is actually the

representation of signal energy. The thresholds of the signal energy criterion are a combined. Identification for segments with real signal and without real signal, and are given by

$$\begin{cases} \text{RMS(seg 1)} > 1.2 \bullet \text{RMS(Period)} \\ \text{RMS(seg 2)} < 1.0 \bullet \text{RMS(Period)} \end{cases} \tag{4.13}$$

where RMS(seg1), RMS(seg2) and RMS(Period) indicate the RMS values of extracted signal **S2** in 'seg 1', 'seg 2' and 'Period' respectively.

The idea of the above threshold setting is that, if 'seg 1' has no real signal, the energy of this segment is very hard to exceed the energy of whole 'Period'. This is because 'seg 1' has only one-fourth of 'Period' and only contains small load current variation in normal condition. If enough energy can be quantified in 'seg 1', it is likely that there is a real signal. To further confirm that the signal is indeed from downstream SG other than significant load variation, the energy of 'seg 2' is also calculated to compare with energy of 'Period' which is the second threshold. If the two inequalities in (4.13) hold true simultaneously, it means that the real signal exists in 'seg 1'.

- ***Signal strength criteria***

The signal strength referred here is the signal peak value. Since the signal strength is mainly determined by system voltage level and grounding resistance, it can be expected to be between the range of 3.5 A and 50 A. This allows a reasonable margin from theoretical analysis in Section 4.1. After being doubled by subtraction algorithms, the real signal strength should fall in the range of 7 A to 100 A as shown in Figure 4.10(b).

Thus, if a real signal exists in a 'Period', it must satisfy

$$7 \text{ A} < I_{\text{signal\_peak}} < 100 \text{ A} \tag{4.14}$$

The lower limit is set to ensure that the natural load current variation will not lead to a false signal identification. Moreover, the upper limit is set to avoid a

false signal identification from current transient that is always much larger than 100A.

Both the signal energy and signal strength calculations are easy to be implemented in digital electronics. This signal identification process avoids complicated mathematical calculations such as FFT or a long memory buffer for storing the past history of the waveforms. Thus, it requires minimal computing time to accomplish the detection of the grounding signals.

The subsequent section discusses the concerns regarding the factors affecting signal identification.

- ***Factors affecting signal identification***

The processed signal will neither result in false signal shape to form when there is no real signal, nor disregard a signal shape when real signal exists. Generally, two factors may affect the signal identification: signal strength and signal strength ratio as defined in Equation (4.15).

$$Ratio_{signal} = I_{signal.peak}/I_{load} = 2I_{peak}/I_{load} \quad (4.15)$$

where

I_{load} is the RMS of load current;

I_{peak} is the generated signal peak;

$I_{signal,peak}$ is the extracted signal peak which is almost the double of I_{peak}.

From interference aspect, the load current variation is the main factor to cause falsely identified signal. Too weak signal strength or too small signal strength ratio may lead to signal missing, and too strong load current variation may lead to falsely identified signal. Even though two criteria consider both signal strength and load interference aspects, the signal identification is still not 100% correct. The further task to figure out the correct trip command is then transferred to the command confirmation part.

4.2.3 Command Confirmation

In order to verify the correctness of the thresholds proposed in Equations (4.13) and (4.14), the investigation was conducted through the load current (around 400A) measurements taken from distribution feeders. 400A is a typical load current level for distribution feeder circuits.

- ***Measurements without signal***

In this investigation, the measurements are free of trip grounding signal. It was expected that no signal would be identified. However, the results, as shown in Figure 4.11, reveal that with the proposed thresholds, trip signal might be falsely identified from the normal load current waveform, although the false signals did not appear frequently. Further analysis shows that generally, the extracted signal (S2) strengths from detected current are around 5.02 A, i.e., 1.25% signal strength ratio (5 A/400 A). But sometimes it can reach up to 21 A (5.25% signal strength ratio), which is equal to a 10 A signal sent from worksite. If the detected current variation is caused by small transient disturbance and happens to form at 'seg 1', the 'two-step signal extraction method' cannot remove the disturbance. Then this disturbance will be falsely recognized as an intentional signal from worksite.

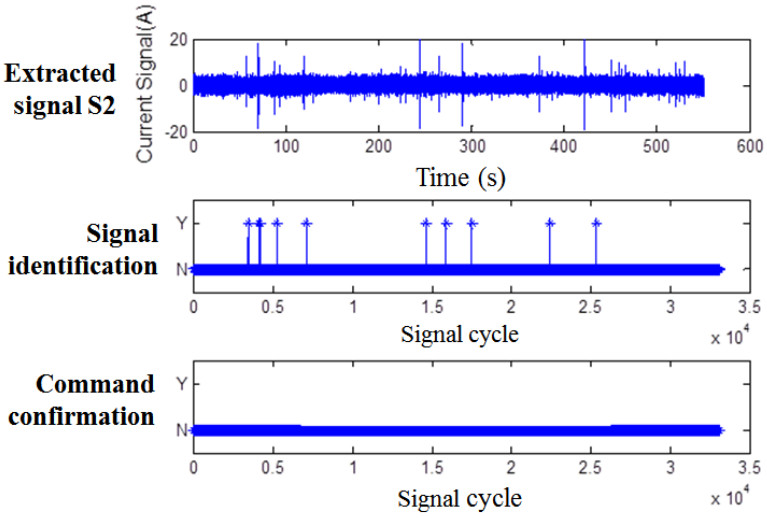

Figure 4.11 Field measurements under normal circumstance

- ***Measurements with superimposed signal***

Figure 4.12 shows the signal identification results for measurements superimposed with 6 A signals. This signal strength is lower than the minimal theoretical signal strength (7.88 A). In this case, the signal strength ratio is only about 3% (12 A/400 A) which is still higher than 1.25% signal strength ratio for most normal load current cases. However, it can be observed that there are some missing signals in Figure 4.12. The reason is that the load current variation or small transient disturbance partially canceled the real signal.

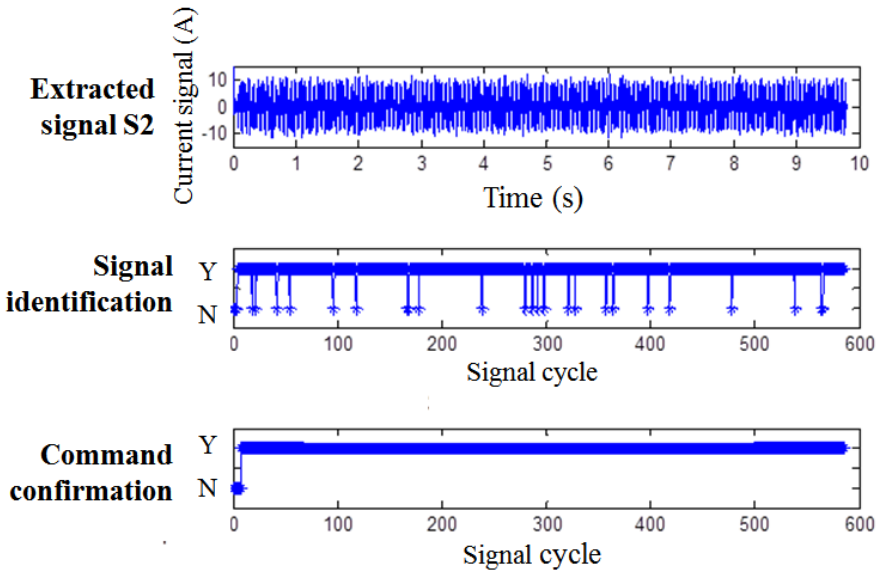

Figure 4.12 Field measurements with superimposed trip grounding signal

Comparison of Figure 4.11 and Figure 4.12 suggests that the load current variation amount overlaps with the generated signal strength. In this case, the identification of only one signal existence is not enough to make a decision on trip command. Fortunately, the signal missing and false identification do not very frequently appear, and the signal will be consecutively sent by SG once the worksite is energized. All these suggest that the identified signal number within a certain period may be used to make final decision to confirm the trip command.

In this report, considering both the condition of short fault clearing time and eliminating rare false tripping from a large amount of measurement data, it is

recommended that four/seven command confirmation scheme is used. It means that once four signals within seven consecutive signal **S2** cycles are positively identified, worksite energization will be confirmed and a command will be sent to trip the recloser. This number can be adjusted in SD for various worksite conditions or systems. An overly conservative command confirmation may result in the delay of trip grounding, while an undiscerning one may result in the false trip action of recloser. Therefore, a balance has to be met.

Figure 4.11 and Figure 4.12 also demonstrates that no false trip command would be sent with four/seven scheme. The long period screening of measurement data confirms that the proposed SD device never had any false decision during normal load conditions.

As mentioned in Section 4.2, N-2 **S2** signal cycles can be extracted from N detected current cycles. Seven **S2** cycles for making command decision need nine detected current cycles and at least six detected current cycles are required if four signals can be successively identified. It implies that the fastest trip grounding time will be 0.1 second and the slowest trip grounding time will be 0.15 second based on the proposed four/seven scheme.

Numerous simulations using different signal strength and measured load currents indicate that the 12 A extracted signal strength $I_{signal.peak}$ and 3% signal strength $Ratio_{signal}$ are basic requirements to ensure correct signal detection in a time span of 0.15 s. The whole process of signal generation and detection are verified through a considerable number of simulations and experiments presented in Section 4.3.

The implementation of signal detector, including voltage/current data acquisition, trip command sending and SD installation is the same as diode-based scheme in Chapter 3. With an advanced Micro-Control Unit (MCU) performing the signal extraction, signal identification, and command confirmation process, the signal detector is able to recognize signals with specific patterns and send out trip command to trip the recloser in a short time.

4.3 Verification Studies

In this section, simulation and experiment results using distribution system models are presented, as well as sensitivity studies.

4.3.1 Simulation Tests

A typical case is used as an example to verify the proposed scheme. A grounding resistance of 100 Ohms is used to represent the most probably resistance value of a two-meter grounding rod. Because of the different voltage levels in distribution system, the parameters of the signal generator are different for different voltage levels. As presented in Section 4.1, the parameters are determined for 25 kV and 13.8 kV system voltages. In this section, all the simulations are based on these two voltage levels.

- ***25 kV Scheme***

Figure 4.13 shows a single-line diagram of the system used to investigate a typical 25 kV scheme. The system is simplified to a 25 kV distribution system connected to a 10 MW resistance load through a 20 km distribution line. The worksite is 10 km away from the recloser along the feeder and a temporary grounding rod on one phase power line. The basic system configuration and parameters, as shown in Table 4.5, were extracted from the CYME Power Engineering Software. This software has been widely used in Canadian utilities for distribution network analysis. Simulation results of detected current from recloser and disturbance current from thyristor are shown in Figure 4.14.

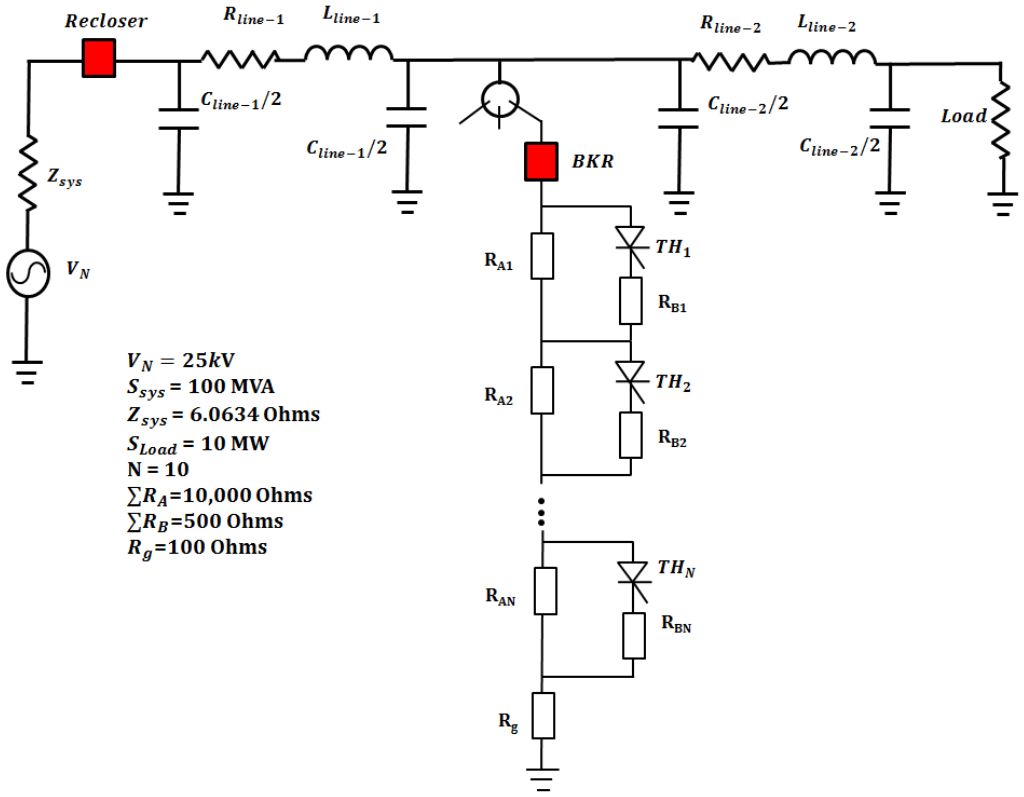

Figure 4.13 Single line diagram of 25 kV proposed scheme

Table 4.5 Line and load impedance parameters in simulations

	Line-1	**Line-2**
R_1 (Ohm/m) (Positive)	0.2083E-3	0.2083E-3
R_0 (Ohm/m) (Zero)	0.0617E-3	0.0617E-3
L_1 (Ohm/m) (Positive)	0.2083E-3	0.2083E-3
L_0 (Ohm/m) (Zero)	0.1937E-3	0.1937E-3
C_1 (MOhm*m) (Positive)	254.02	254.02
C_0 (MOhm*m) (Zero)	643.23	643.23
Length (km)	10	10

(a) Detected Current Waveform from Recloser

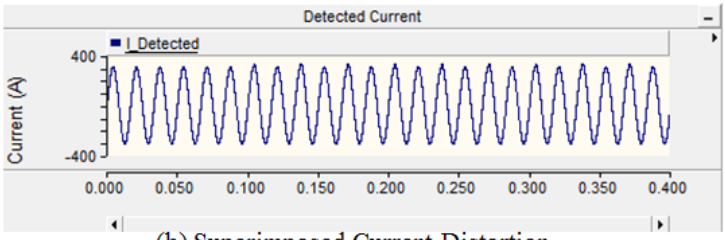

(b) Superimposed Current Distortion

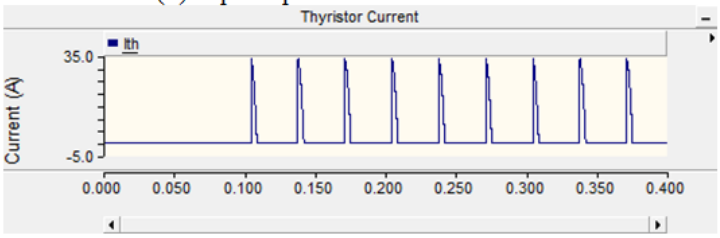

Figure 4.14 Simulation Results of 25 kV Scheme

Figure 4.15 illustrates the results from signal extraction, signal identification and command confirmation when using 100 Ohms grounding resistance, which is a most common case.

In the Figure 4.15, the signal extraction S2 shows the extracted signal through the proposed “two–step subtraction method”. The fault (worksite energization) instant is assumed at 0.033 s. The first S2 signal appears at about 0.067 s after two detected current cycle delays. The signal identification result shows that all the signals can be correctly identified by the proposed signal identification criteria. As the command confirmation is made up of four positively identified signals within seven successive signal cycles, the command in this case is obtained after only 4 successive signal cycles. As a result, the fault can be cleared within 0.1 s timeframe.

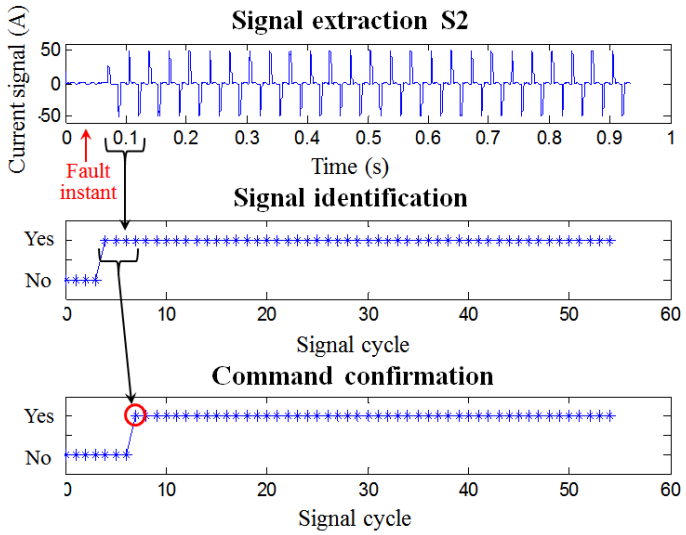

Figure 4.15 Simulation results for ideal load current case (25 kV)

In above simulated case, the current waveform is constant and purely sinusoidal. But in reality, the current can be distorted and time-shifted. In order to imitate a more realistic instance, field measured current waveform under normal condition has been employed as the load current of feeder. By adding the simulated signal on the load current, the composite current waveform appearing at the detector can be obtained. Figure 4.16 shows the signal detection results. The proposed method is also effective in this case.

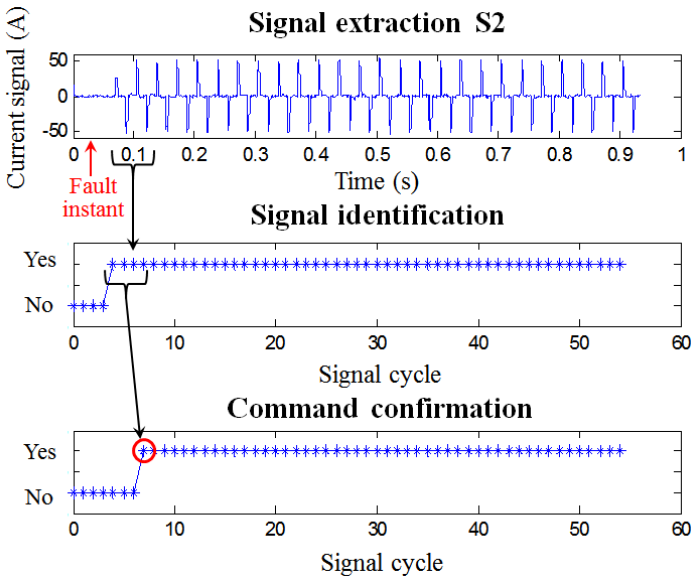

Figure 4.16 Simulation results for the real load current case (25 kV)

Simulation results in above cases indicate that the peak magnitude of signals reached 53.77 A. This signal strength is strong enough to be distinguished from common load current. Moreover, the results clearly indicate a promising detection accuracy of 100% in 25 kV line and a quick reaction within 0.1 s. As a result, this power line based trip grounding scheme is capable of providing dependable protection for personal safety.

- ***13.8 kV Scheme***

Single line diagram and simulation parameters are shown in Figure 4.17 and Table 4.6.

Compared to the 25 kV distribution system, signal generation devices used in 13.8 kV feeder are smaller and lighter due to fewer thyristors, but has a disadvantage of weaker signal strength due to the low voltage level.

Similar to the cases previously used, a grounding resistance of 100 Ohms is analyzed below as the most typical case. Simulation results are shown in Figure 4.18. The detection results of signal extraction, identification and command confirmation are shown in Figure 4.19. In order to simulate the real worksite condition with load variation, scaled field measurement data in normal condition are added and results are presented in Figure 4.20.

With regard to these results, a signal strength of 25.61 A can be achieved in a typical 13.8 kV scheme. In comparison to the 25 kV cases, the lower voltage level weakened the signal strength by about 6.4% signal to load current ratio. However, the “two-step signal extraction method” effectively maintained the signal strength. Moreover, the signal is still strong enough to provide 100% accurate signal identification and 0.1s clearing time for worksite incidental energization.

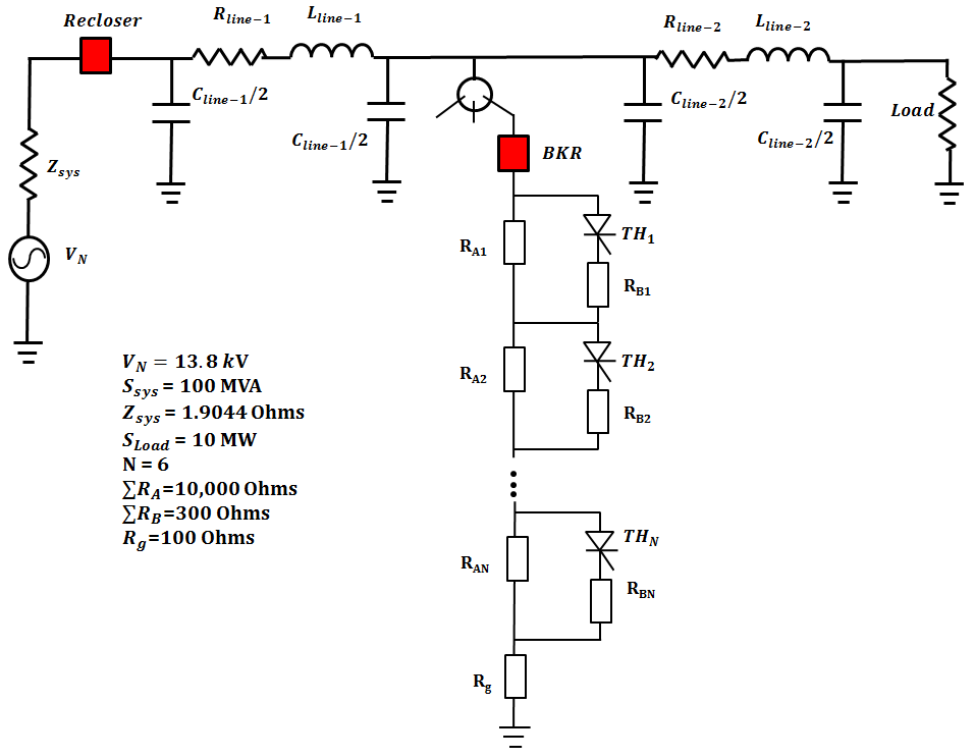

Figure 4.17 Single line diagram of 13.8 kV proposed scheme

Table 4.6 Line and load impedance parameters in simulations

	Line-1	**Line-2**
R_1 (Ohm/m) (Positive)	0.8065E-3	0.8065E-3
R_0 (Ohm/m) (Zero)	0.0617E-3	0.0617E-3
L_1 (Ohm/m) (Positive)	0.2000E-3	0.2000E-3
L_0 (Ohm/m) (Zero)	0.1937E-3	0.1937E-3
C_1 (MOhm*m) (Positive)	254.02	254.02
C_0 (MOhm*m) (Zero)	643.23	643.23
Length (km)	5	5

(a) Detected Current Waveform from Recloser

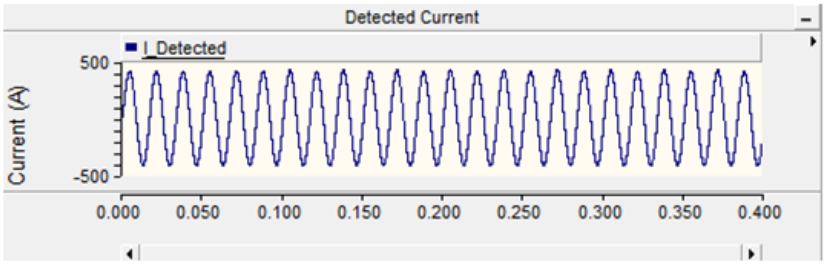

(b) Superimposed Current Distortion

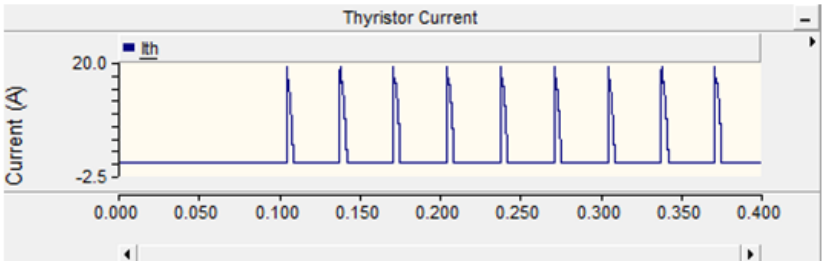

Figure 4.18 Simulation Results of 13.8 kV Scheme

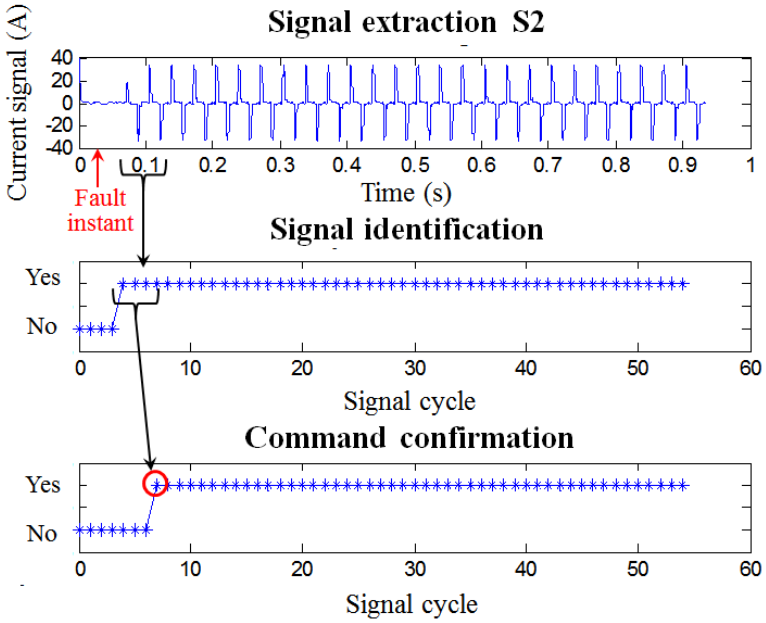

Figure 4.19 Simulation results for ideal load current case (13.8 kV)

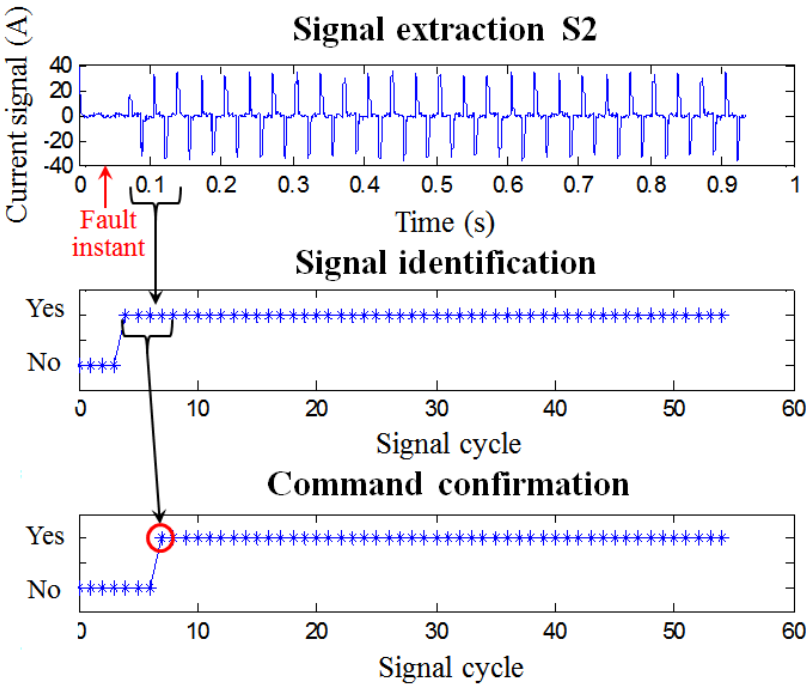

Figure 4.20 Simulation results for the real load current case (13.8 kV)

4.3.2 Sensitivity Studies

While a promising accuracy has been achieved by typical cases in simulation tests, detection accuracy should be further tested to a wide variation of both loads and system parameters.

Extensive simulation tests were conducted in which the key parameters involved were varied, including fault level, load capacity, distance from recloser to worksite, and grounding resistance. Base case parameters are shown in Table 4.7, and the variations are shown as percentages of the base parameter values.

Table 4.7 Parameters in Base Case

	13.8 kV	**25 kV**
Fault Level (MVA)	100	100
Load capacity (MW)	10	10

Feeder length (km)	10	20
Worksite distance (km)	5	10
Grounding Resistance (Ohms)	300	300

Results of each parameter studies are shown in Figure 4.21 and Figure 4.22 for the 13.8 kV and 25 kV schemes, respectively. The percentage variations of key parameters are included, while assessment of sensitivity is described by the peak value of generated signals.

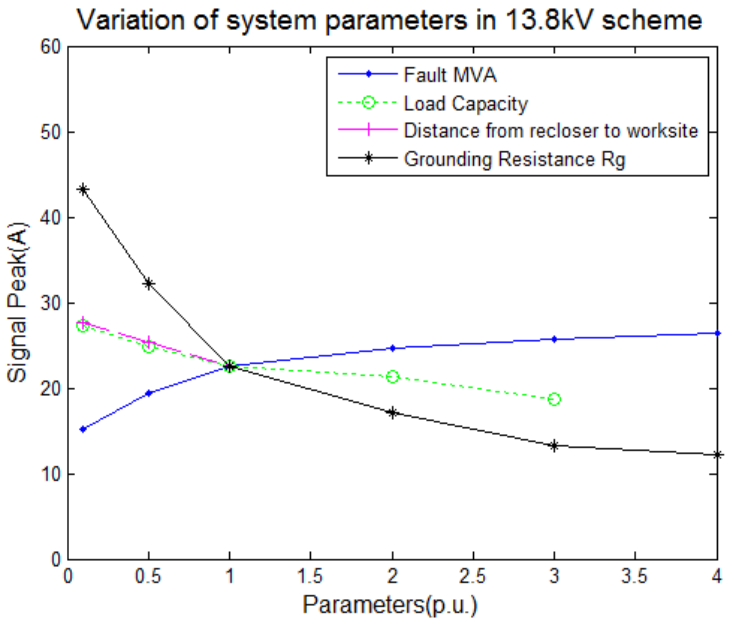

Figure 4.21 Extracted signal strength Isignal.peak due to system parameters variation in 13.8 kV scheme

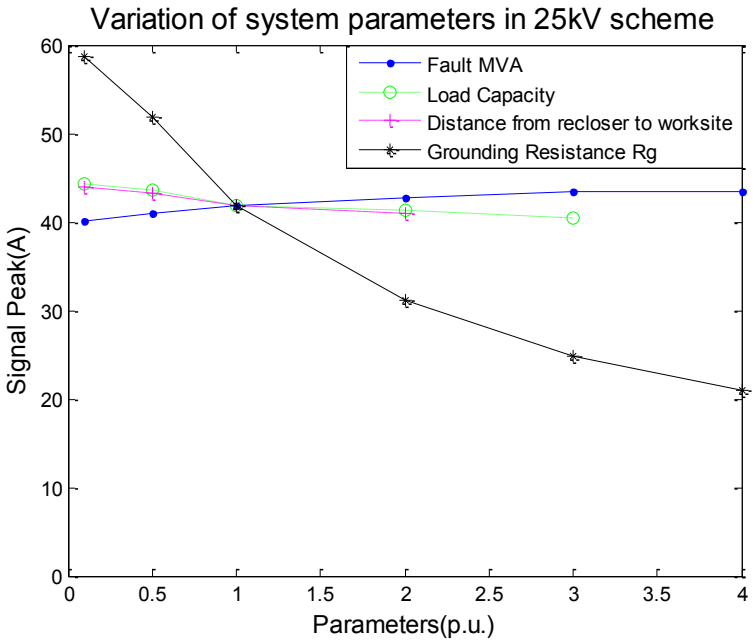

Figure 4.22 Extracted signal strength Isignal.peak due to system parameters variation in 25 kV scheme

Analysis of the complete set of test cases revealed that the generated signals were, in general, less sensitive to load capacity and fault level than grounding resistance and fault location. Signal boosts with larger fault level, but decreases when the load capacity increases. Likewise, longer fault distance and higher grounding resistance have inverse effect on magnitude of the signal. In all cases, grounding resistance proves to have the most influence on signal strength and detection accuracy. This is consistent with the theoretical analysis.

Considerable number of simulations using different signal strength and measured load currents indicate that the 12 A extracted signal strength $I_{signal.peak}$ and 3% signal strength $Ratio_{signal}$ are basic requirements to ensure correct signal detection within 0.15 s. Therefore, the required minimal signal sent from signal generator is 6 A.

In other words, for the 25 kV distribution feeders, the theoretical minimal signal that can be generated is 12.37 A. Therefore, as long as the load current is lower than 800 A, which covers almost all 25 kV feeder loading cases, the trip ground can be guaranteed to be within 0.15 s. However, for the 13.8 kV

distribution feeders, the theoretical minimal signal can be generated is only 7.88 A. The load current has to be limited to 525 A to ensure 0.15 s grounding trip time.

If the signal strength and/or signal strength ratio do not satisfy above requirements, the signal detection processing will take longer.

4.3.3 Experimental Tests

A scaled single line diagram of Figure 4.23 was constructed for experimental verification. In this experimental system, the utility grid, represented by a stiff 120 V AC source, was connected through a small line impedance feeding a constant load. The proposed signal generator was implemented using a one-way thyristor being driven by a 90° impulse control.

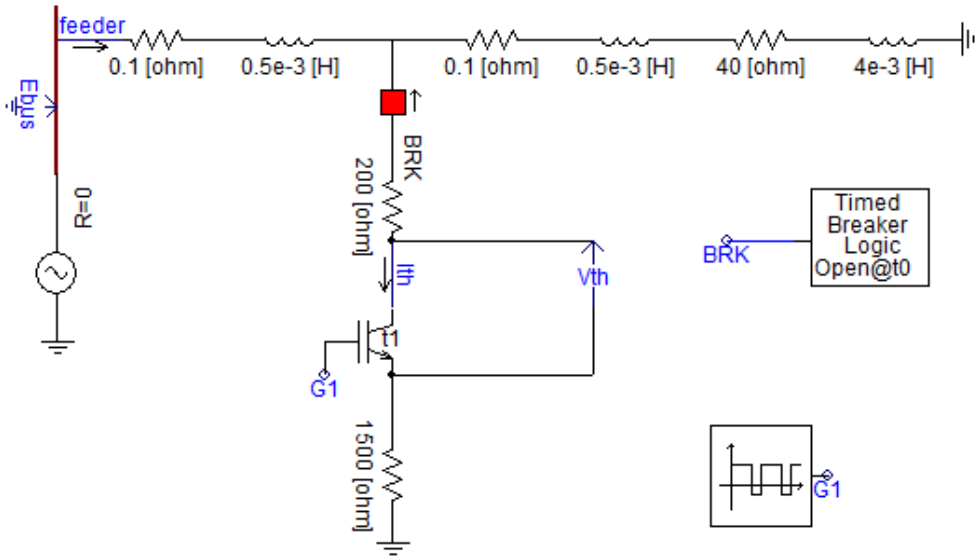

Figure 4.23 Diagram of Experimental Verification

Focusing on the concern of detection accuracy and time delay in a weak signal, the grounding resistance is varied from typical case to the worst case of 1000 Ohms.

The magnitude of the generating signal was adjusted to match the theoretical ratio between signal peak and feeder load current. Assuming that the feeder load

current is 400 A for a real power line, the simulation results of a typical case and a weakest signal case are I_{peak} = 20 A and I_{peak} = 6 A. The corresponding signal strength ratios are 2*20A/400A = 10% and 2*6A/400A = 3%, respectively. In experiment, the normal line current is 3.356 A. So the generated signal peaks were adjusted to 0.188 A which corresponds to 11%, and 0.050 A which corresponds to 2.8% ratio.

- ***Typical case with normal signal strength***

Figure 4.24 and Figure 4.25 present the signal detection results for 11% signal strength ratio with and without 1.0% noise present. The 1.0% noise is added to mimic the total measurement errors although they are normally below this value. The worksite energization instant is assumed at 6.13 s. In these figures, the current signals are the extracted S2 signals scaled to 400 A load current level and 20 A generated signal strength.

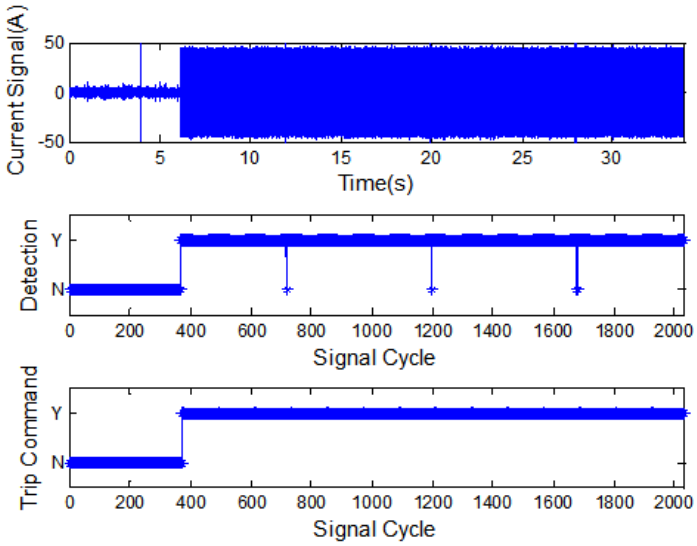

Figure 4.24 Experimental results for 11% signal strength rate

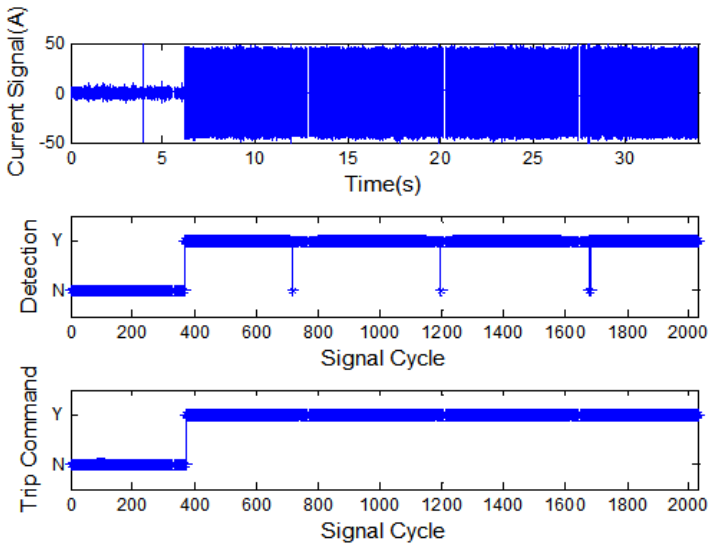

Figure 4.25 Experimental results for 11% signal strength ratio and 1.0 % measurement noise

Table 4.8 Detection results from the strongest signal strength

	Experiment Data		Experiment Data + Measurement Noise	
	Signal identification Accuracy	Command confirmation Accuracy	Signal identification Accuracy	Command confirmation Accuracy
Signaling Period	99.58%	100%	99.76%	100%
Non-Signaling Period	100%	100%	100%	100%

As anticipated, the figures and results shown in Table 4.8 indicate that the signal generation system operates according to the desired signal pattern. A 99% signal identification accuracy and 100% trip command confirmation accuracy are attained, which enables this scheme as a promising new approach to protect worksite safety.

- ***Worst case with weakest signal strength***

Figure 4.26 and Figure 4.27 present the signal detection results for 2.8% signal strength ratio, with and without 1.0% measurement noise. The worksite energization instant is assumed at the 2.35 s mark.

In Figure 4.26 and Figure 4.27, the current signals indicate the extracted signals S2 scaled to 400 A load current level and 6 A generated signal strength.

It can be noticed that, signal identification accuracy decreases with weaker signal strengths. The real signals are more difficult to be detected from background distortion because of the cancellation between the real signal and background distortion. However, despite the difficulty, the summarized signal identification and command confirmation results, as shown in Table 4.9, still verified the effectiveness of the proposed trip ground method with 98.9% signal identification accuracy and 100% trip command confirmation accuracy.

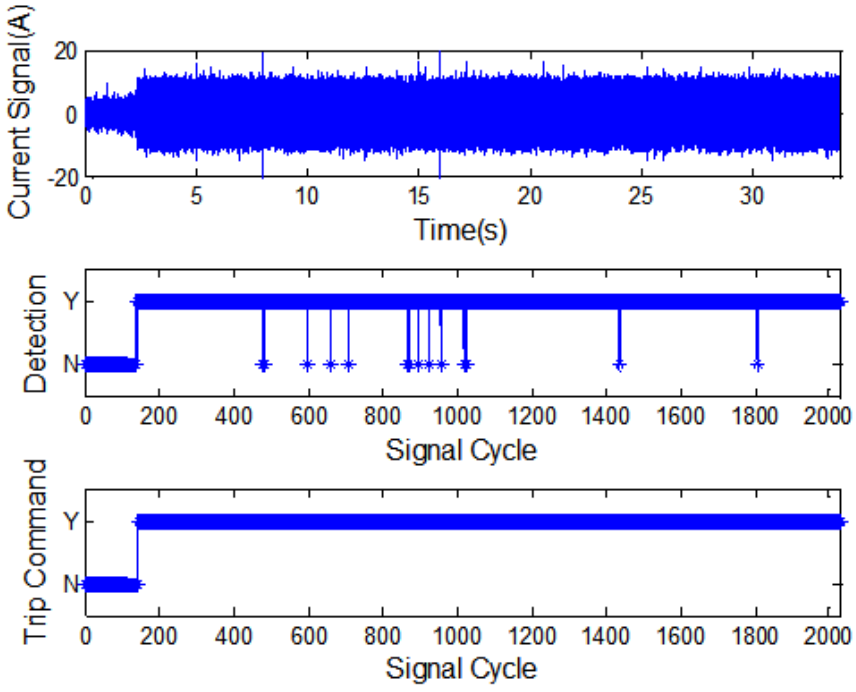

Figure 4.26 Experimental results for 2.8% signal strength ratio

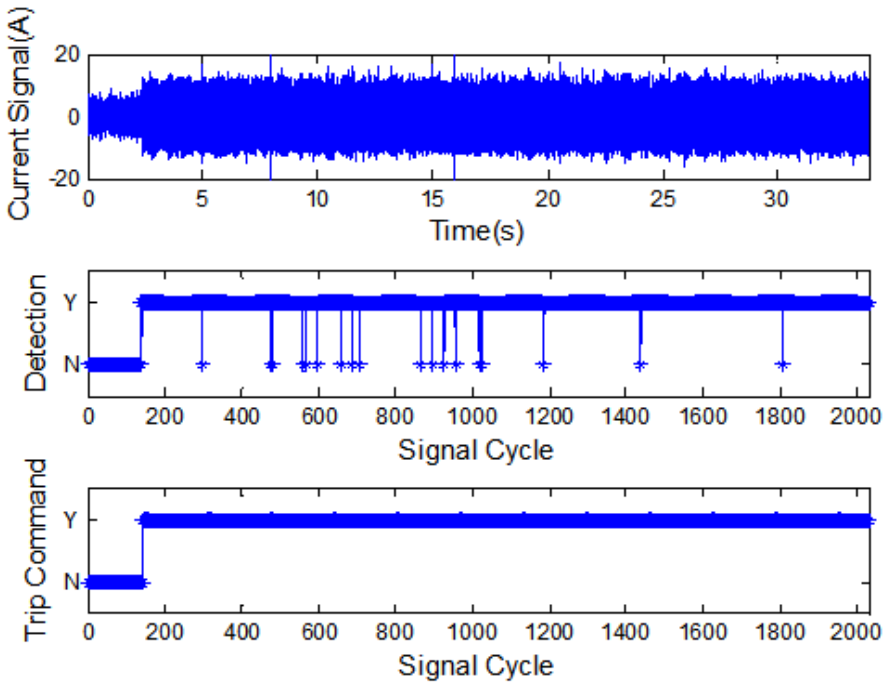

Figure 4.27 Experimental test of 2.8% signal strength rate and 1.0 % measurement noise

Table 4.9 Detection results in the cast of weakest signal strength

	Experiment Data		Experiment Data + Measurement Noise	
	Signal identification Accuracy	Command confirmation Accuracy	Signal identification Accuracy	Command confirmation Accuracy
Signaling Period	99.0%	100%	98.9%	100%
Non-Signaling Period	100%	100%	100%	100%

Chapter 5

Comparison of Relay Protection and Proposed Methods

The conventional method to trip accidental energization of equipment at worksite is realized by overcurrent protective relays. These relays are either electromagnetic devices or microprocessor-based digital devices. The time delay of tripping is dependent on the relay setting and impedance of the fault circuit. Due to the unpredictable grounding resistance and the variation of the worksite location, the trip time can vary in a large range. In contrast, the proposed active trip grounding method is able to trip grounding consistently in several cycles without the influence of grounding resistance and worksite location.

In order to understand the superiority of the new method, the worksite trip grounding performance of the new method is compared with that of the conventional relay protection.

5.1 Performance of the Conventional Relay Protection

The reclosers are normally equipped with overcurrent relays for phase-to-phase fault protection and ground relay for phase-to-ground fault protection as shown in Figure 5.1(a).

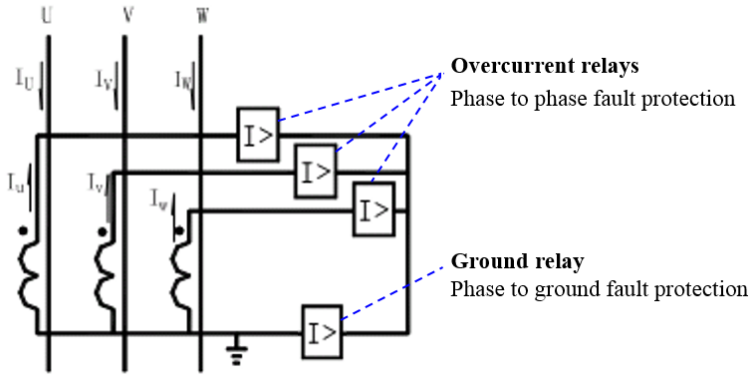

(a) Arrangement of overcurrent relays and ground relay

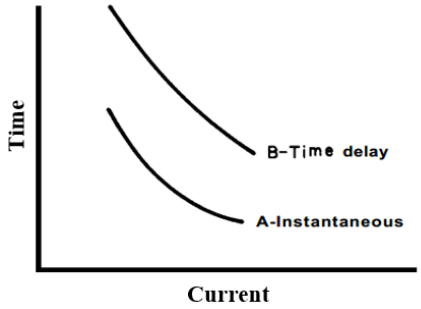

(b) Tripping characteristics

Figure 5.1 Relay protections

The phase-to-phase fault protection for distribution feeders mainly rely on the instantaneous and time-delay overcurrent relays. The tripping characteristic or time-current-curve for conventional automatic circuit recloser is shown in Figure 5.1(b).

The instantaneous overcurrent relay picks up without intentional time delay (normally around 0.08 ~ 0.1s) once a fault occurs. However, this does not cover the entire protective zone of the recloser because of the pickup setting principle. For the phase-to-ground fault, the "reach", or the extent of the instantaneous overcurrent relay circuit length protected zone is dependent on the magnitude of fault current. And this fault current is determined by the impedance of the fault circuit, i.e., the summation of equivalent upstream impedance of the fault point and the grounding resistance. If the grounding resistance is large, the covered length of the instantaneous overcurrent relay will be very short, making it ineffective. At this time, the worksite trip grounding request has to be detected by the defined-time/inverse-time overcurrent relay, which is designed to cover the entire protective zone with time delay. The time delay is determined by the protection coordination requirement, usually between 0.3 ~ 1 second. If the grounding resistance is very large, the time delay before tripping could take a significant amount of time.

The ground relay trips the grounding fault by detecting the zero sequence current. The pickup value must be over maximum unbalanced load current which

is normally selected as 30% to 50% of load current. To avoid the effect of some transients that could lead to false-tripping, the grounding protection always picks up with time delay, e.g. 0.2 or 0.5 seconds and even longer.

To show the performance of the conventional relay protection, a case study is described as follows. Figure 5.2 shows a 13.8 kV distribution feeder connected to a 10 MW load by 15 km power line. The protection zone of recloser A is between A and B with 10 km power line. The worksite is located at 6 km away from the recloser A.

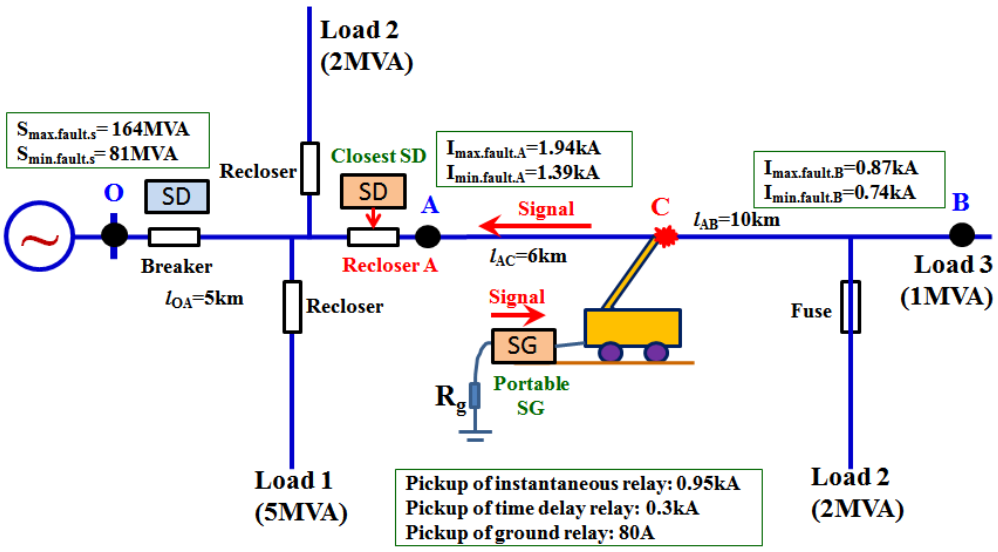

Figure 5.2 System of the studied case

The calculated pickup settings are shown in Figue 5.2. Since the grounding resistance of worksite grounding rod ranges from 10 ohms to 1000 ohms, the fault current due to accidental worksite energization will be in the range of 6.32 A to 405 A. It is obvious that the instantaneous relay cannot definitely detect the fault for all conditions, while the time delay relay may pick up and trip when the grounding resistance is small. The ground relay could detect the fault in most of worksite energization cases, but the trip time is long. Figue 5.3 shows a extremely inverse characterestic of conventional relay which is coordinated with a fuse. The fuse provides protection for a load tap. From Figure 5.3, it can be seen that, even though Rg=10 ohms, i.e., fault current is 405A, which is 1.35 times the time delay

relay pickup value (0.3 kA), the time delay of inverse-time-delay overcurrent relay will be about 10 s. Moreover, 405 A is five times larger the ground relay pickup value (80 A), hence the time delay of ground relay will still be more than 1 s, even though a low time dial setting is used.

Figure 5.4 shows the grounding fault current and tripping time variations when the worksite is energized at locations between A and B. In this figure, only the cases with grounding resistance lower than 30 ohms are presented. The trip time may be shorter than 1 s only when worksite is closer to the source side of the feeder and the grounding resistance is 10 ohm.

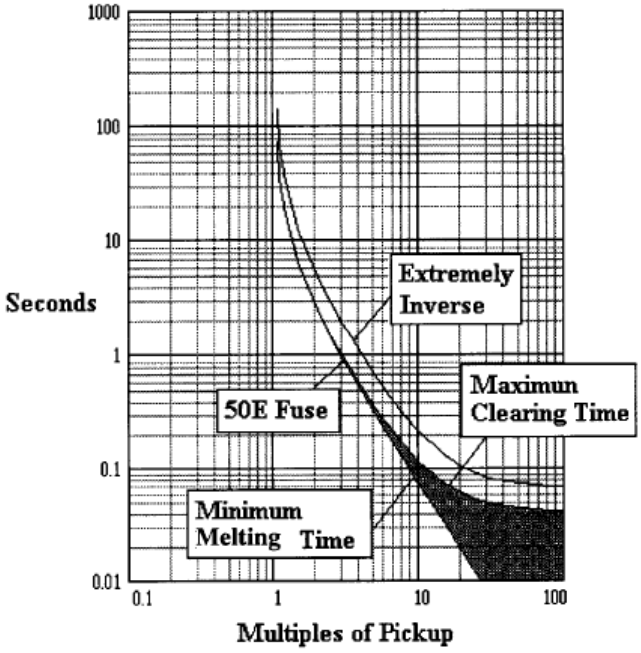

Figure 5.3 Coordination of an extremely inverse time relay and a 50E fuse [15]

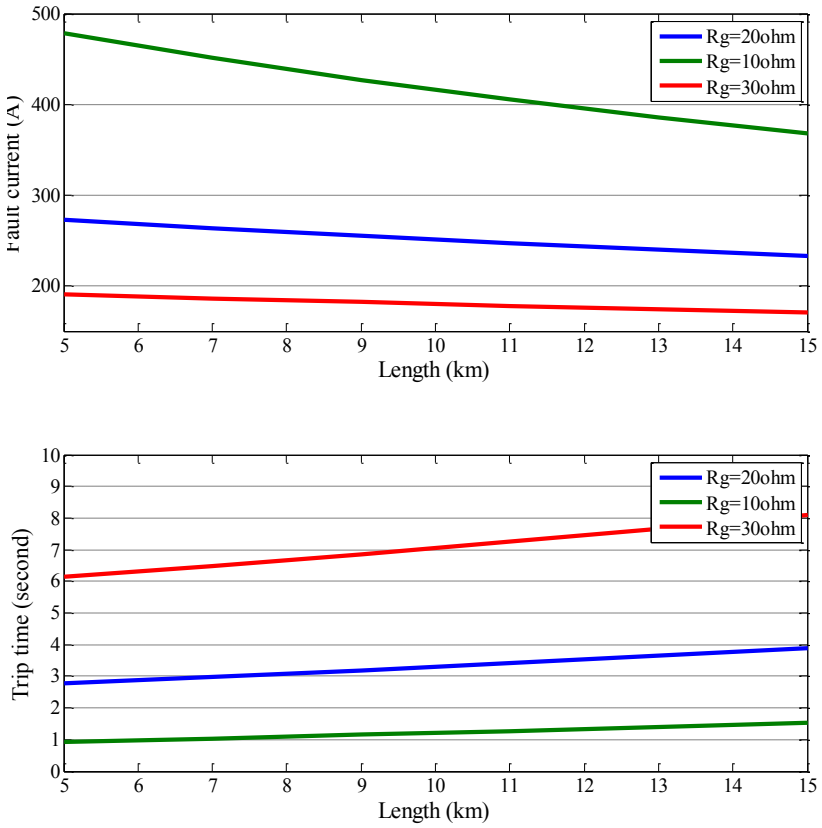

Figure 5.4 Grounding fault current and tripping time

Factoring the large load current and the coordination with downstream recloser, if the recloser is located at the beginning of the feeder, the worksite grounding trip will become ineffective.

5.2 Performance of The Proposed Diode-based Active Protection

The same case has been studied through diode-based active protection scheme with simulation diagram shown in Figure 5.5.

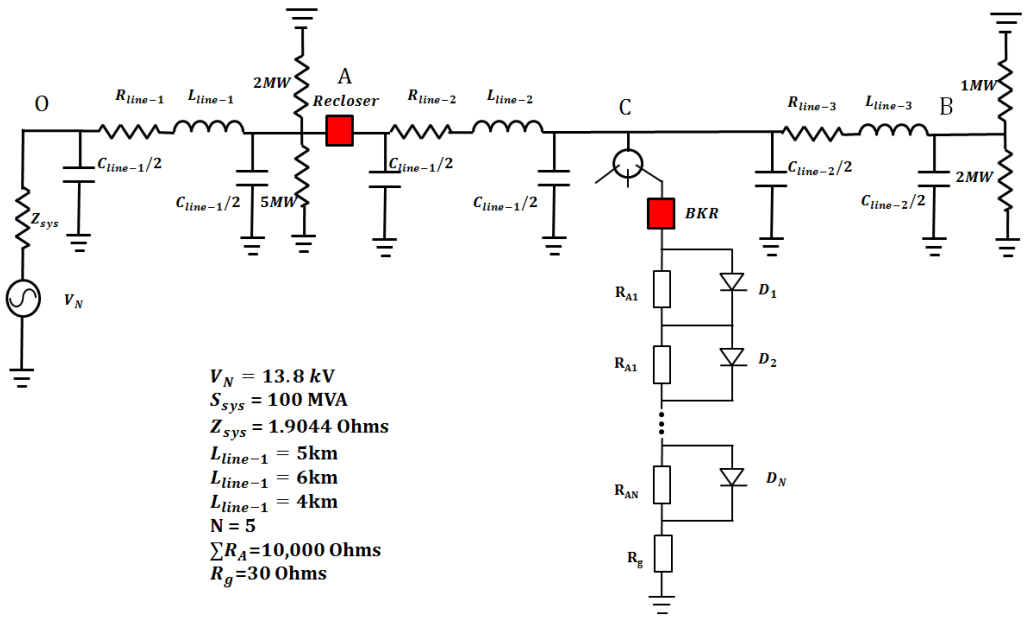

Figure 5.5 Simulation Configuration of Diode-Based Scheme in Studied Case

With a grounding resistance of 30 ohms and detected current amplitude of around 300 A, the signal strength reaches more than 20%, leading to a fast and accurate detection in 4 cycles (0.0667 s) as shown in Figure 5.6.

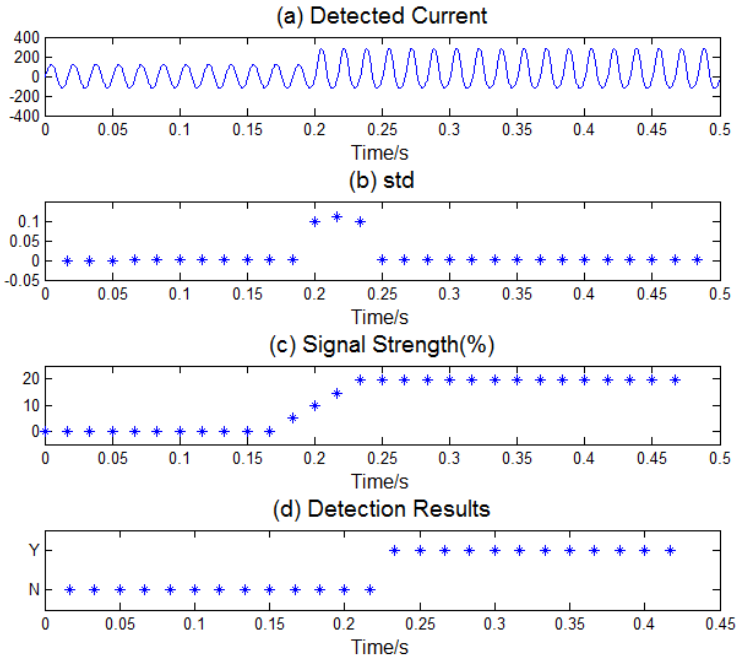

Figure 5.6 Detection Results of Diode-Based Scheme in Studied Case

As indicated in Chapter 3, the most sensitive factors affecting detection results are grounding resistance (R_g) and load current. In most worksite situations with a decent grounding resistance and load current, the signals can be detected in 4 cycles (0.0667 s) as well as a trip command being sent. However in the extreme cases, i.e. rock ground with high grounding resistance or heavily loaded feeder, this signal strength is not high enough for fault detection and other methods may be necessary to cover these conditions.

Compared to traditional overcurrent protection using relays, the diode-based active protection scheme provides a milestone improvement. This scheme shortens the fault clearing time from a couple seconds to 0.067 second, and is immune to the restriction of fault location and most grounding resistances.

5.3 Performance of The Proposed Thyristor-based Active Protection

The typical case has also been studied through thyristor-based active protection scheme for comparison. With a simulation configuration shown in Figure 5.7, the fault can be detected in 6 cycles (0.1 s) as indicated in Figure 5.8.

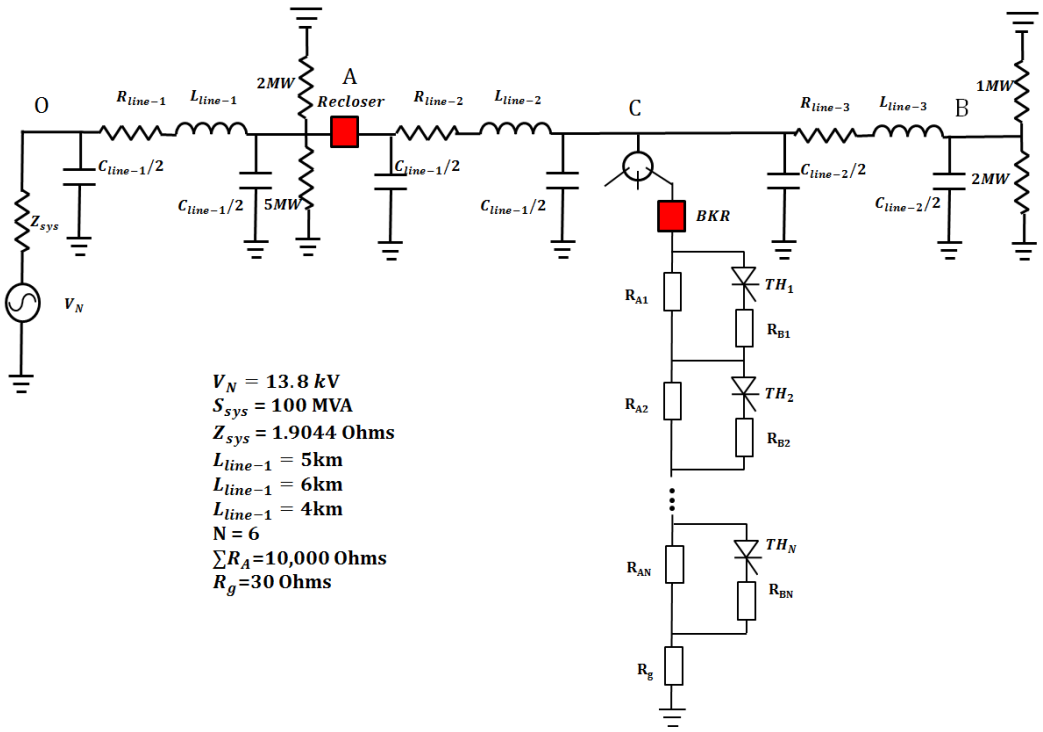

Figure 5.7 Simulation Configuration of Thyristor-Based Scheme in Studied Case

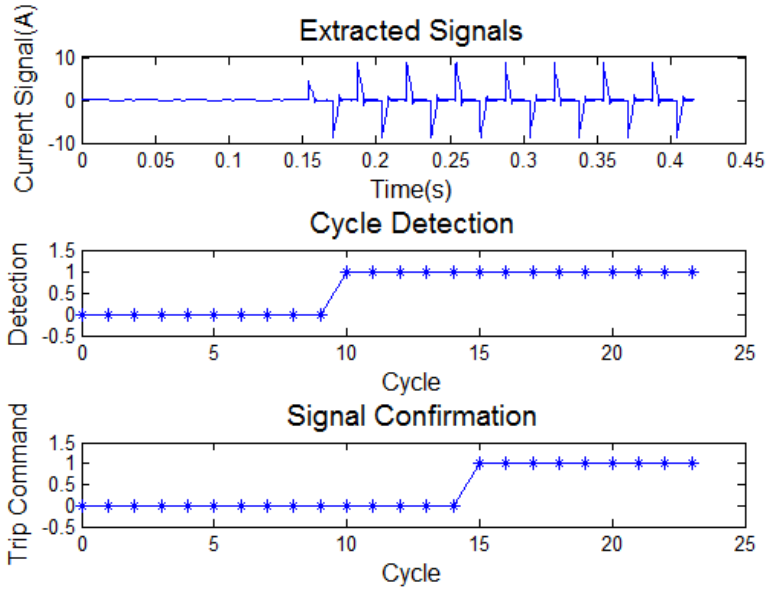

Figure 5.8 Detection Results of Thyristor-Based Scheme in Studied Case

With the variation of grounding resistance and load current as presented in Chapter 4, the proposed thyristor-based trip grounding method can effectively trip

the recloser within 6 to 9 cycles, which are 0.1 s and 0.15 s. This speed can be guaranteed even though the grounding resistance can be as large as 1000 ohms.

While diode-based active protection scheme consists of simple signal generators with small device size, and provides faster response within 4 cycles (0.0667 s), it has a disadvantage in restricted worksite condition and load transient cases. The reason is that once a large load disturbance occurred, a detection delay due to standard deviation filtering in "Zone_0", and waiting till stabilization in "Zone_1" and "Zone_2" may postpone the fault clearing time.

However, thyristor-based active protection scheme solves such issues using specific signal patterns, so that worksite can be protected in despite of extreme worksite condition. Moreover, in transient state, a shorter clearing time (0.1 s – 0.15 s) can still be fulfilled.

It is obvious that the proposed trip grounding scheme is more effective than the typical existing ones. The ability to perform speedy response of accidental worksite energization is one of the most interesting features of the proposed trip grounding method.

5.4 Effects of Capacitor Switching

Capacitor switching is a common operation in power distribution system. The transient current and voltage from capacitor switching may lead to false alarm in the proposed scheme. In order to estimate the effects of capacitor switching, simulation studies are conducted as following.

- ***Typical case of 1.5 MVar capacitor switching***

In order to investigate the detection performance under the biggest switching transient, simulations of a three-phrase 1.5 MVar capacitor bank connecting to the feeder is conducted Figure 5.9. System parameters are selected as the typical case in detection simulations.

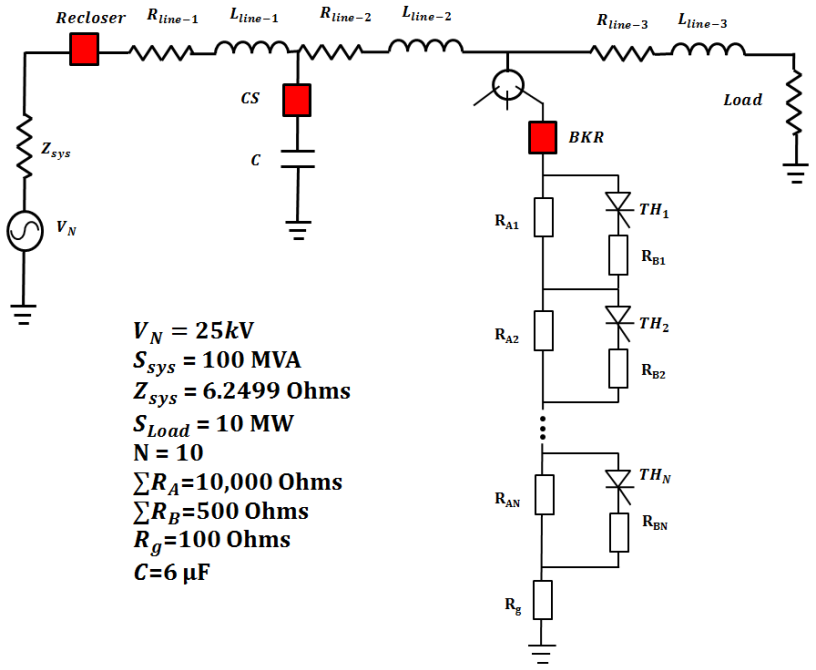

Figure 5.9 Single line diagram of 1.5 MVar capacitor switching case

Results capacitor current and voltage are shown in Figure 5.10. A maximum transient of 381.95 A is detected in capacitor current while the maximum transient in detected voltage reaches 27.67 kV. The detection results are shown in Figures 5.11.

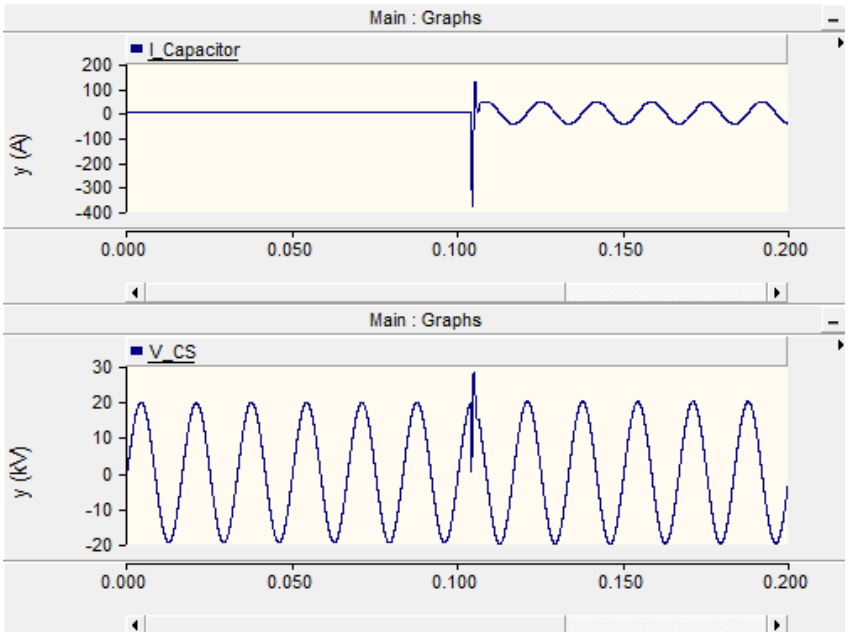

Figure 5.10 Capacitor transient current and voltage

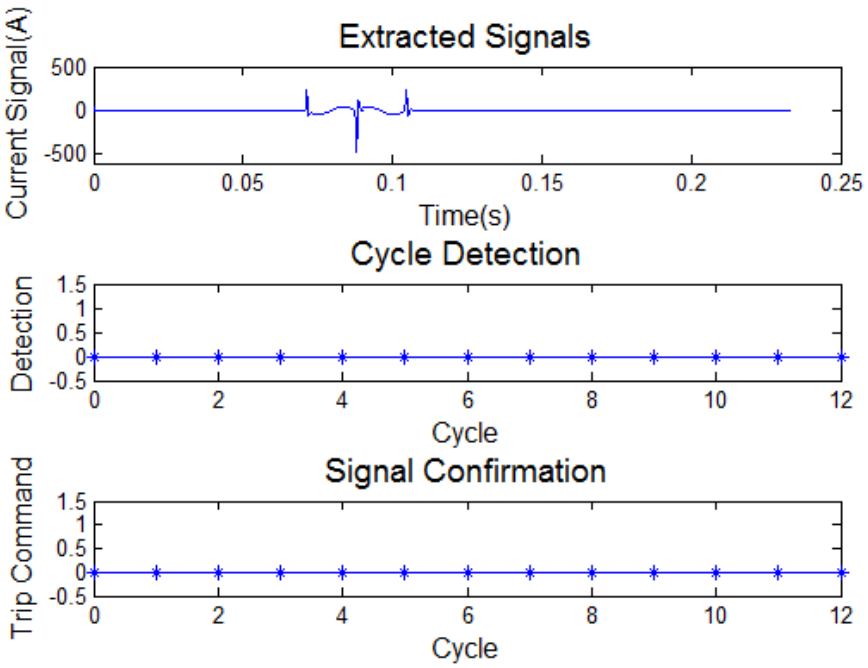

Figure 5.11 Detection results in typical capacitor switching

Based on simulation results, no false alarm has been found in the transient state, since 1) the transient current waveform cannot match the signal strength detection criterion; 2) transient signal peak is out of the detection zone. So no false alarm will be created by capacitor switching.

- ***Extreme case with large switching transient***

In the case where capacitor banks create a short circuit in the system, leading to the biggest switching transient, the detection performance is analyzed as following. Simulation diagram is shown in Figure 5.12.

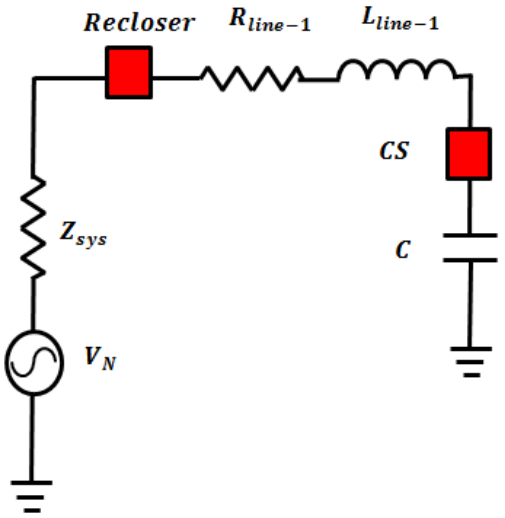

Figure 5.12 Simulation diagram of extreme case

The switching transient last for a couple cycles, and the capacitor current reaches 371.09 A, with a line voltage peak of 31.49 kV as shown in Figure 5.13. The detection results are shown in Figure 5.14.

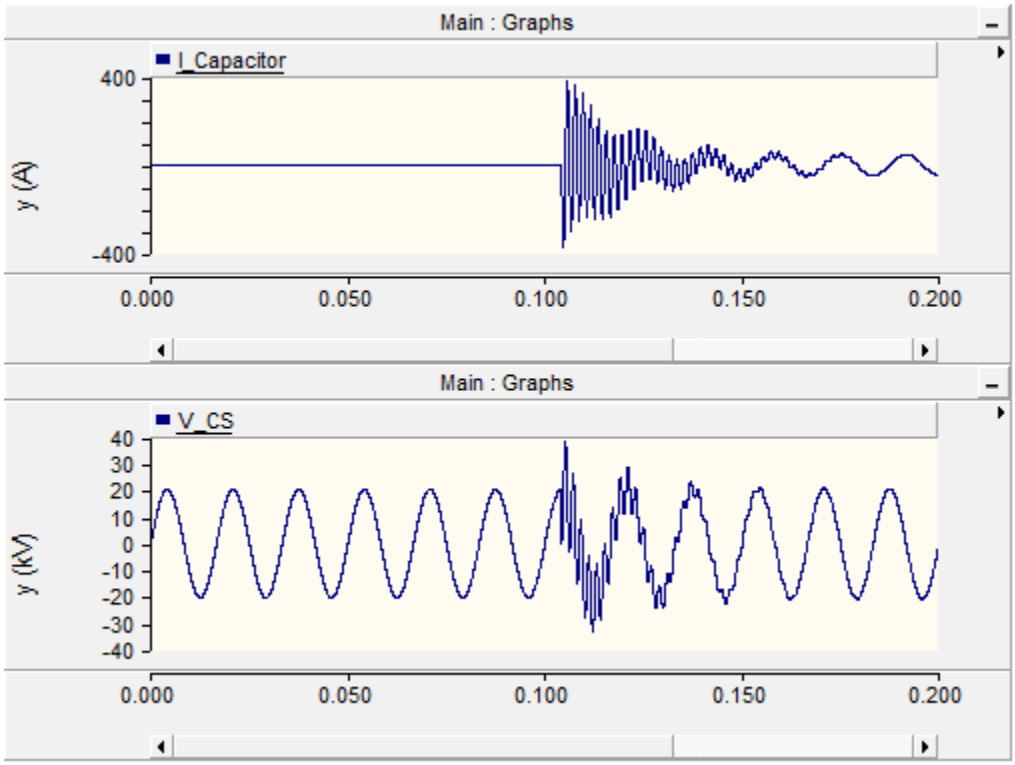

Figure 5.13 Capacitor transient current and voltage in extreme case

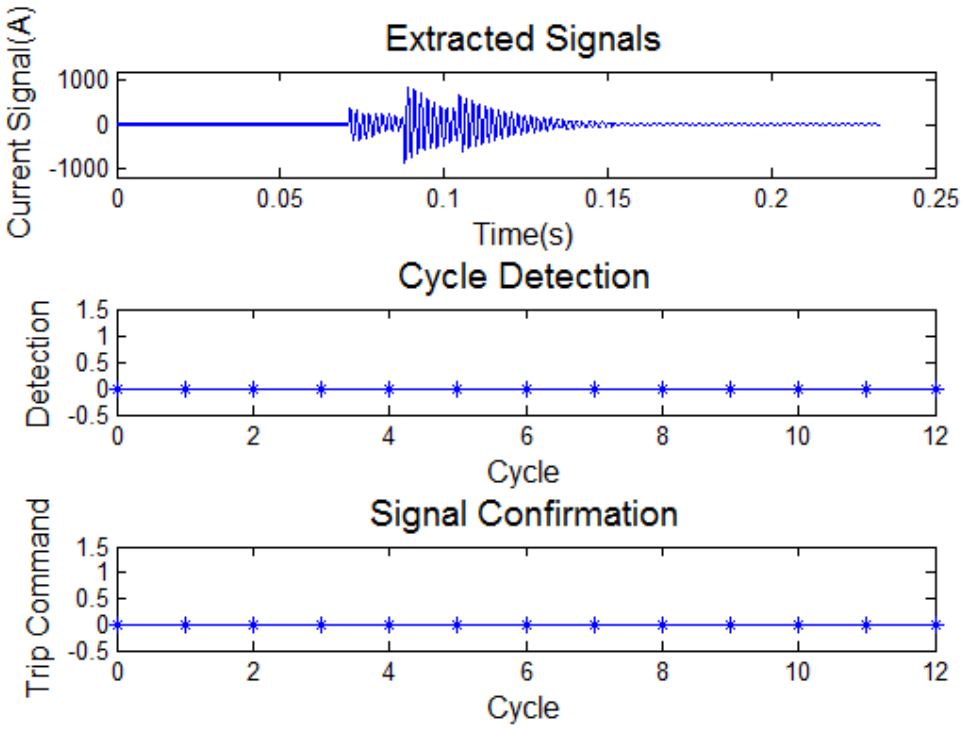

Figure 5.14 Detection results in extreme capacitor switching

Based on the simulation results, even in the extreme case with large switching transient, the detection of our proposed scheme will not be affected, and no false alarm will be given.

5.5 Effects of Arcing

It is also important to realize that the arc may appear during the worksite energization. Therefore, the effectiveness of proposed trip grounding method needs to be further investigated.

Based on the literature review and our experiment results summarized in Appendix A, the main characteristics of current waveform of arc path are

- **Current zero pause** indicating a particular distortion around the current's zero crossing point, as shown in Figure 5.9.

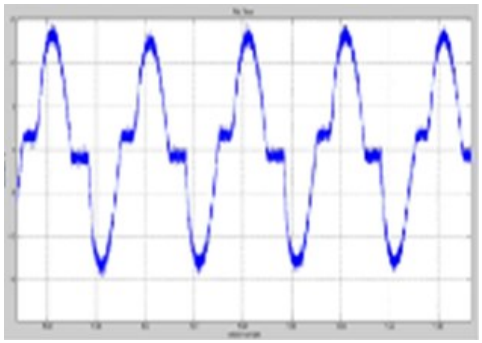

Figure 5.15 Current zero pause in arc [15]

- **Distortion** indicating the non-linearity of arc and ground resistance caused arcing current waveform distortion, as shown in Figure 5.10.

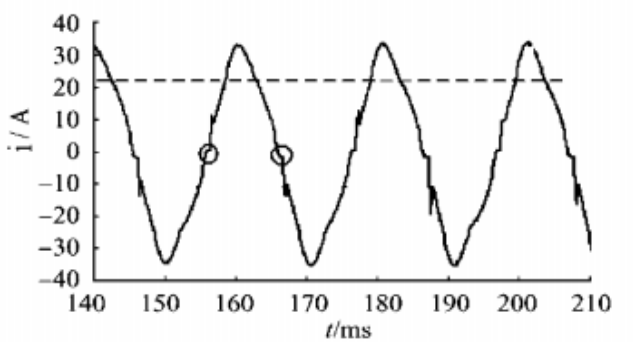

Figure 5.16 Distortion in arc [16]

- **Randomness** indicating arcing current is not behaving in exact periodic way and may vary in magnitude and/or distorted pattern to some extent, as shown in Figure 5.17.

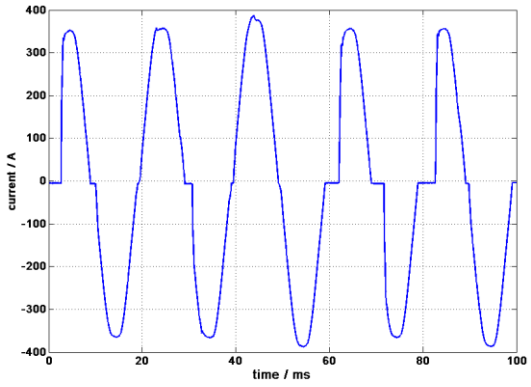

Figure 5.17 Randomness of arc waveforms [17]

- **Intermittency** indicating arc bursts and extinguishes with intermittent patterns, as shown in Figure 5.18.

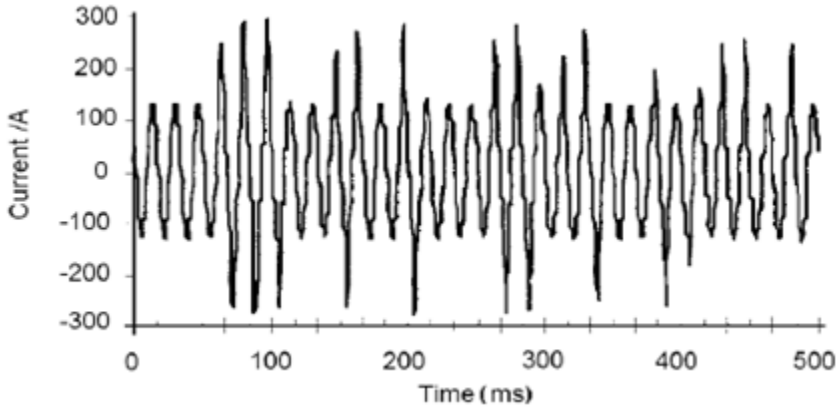

Figure 5.18 Intermittency of arc [18]

1) Current zero pause

The current zero pause as shown in Figure 5.15 impacts little on the signal generation. This is because the signal starts from 90 degree before zero-crossing point of the falling edge of voltage and ends at zero-crossing point of the falling edge of voltage. If arc exists in the signal path, only the tail of signal will be cut. As long as the arc current is periodic, the current zero pause will has no effect on the signal strength and little effect on the signal RMS value. So this is not conflict with the two criteria to identify the existence of signal. The difference of signal patterns with and without zero pause is compared in Figure 5.19.

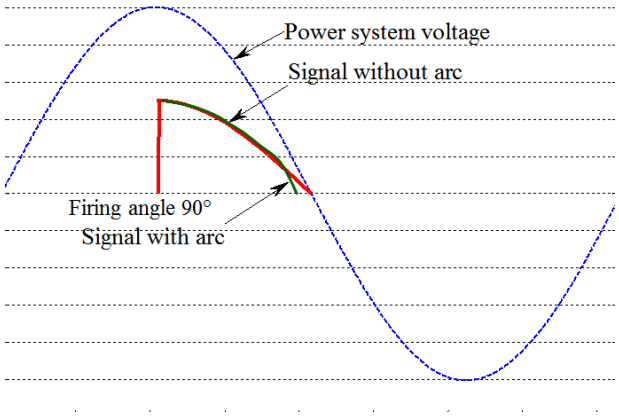

Figure 5.19 Comparison of signal patterns with and without zero pause

2) Current distortion

The periodically distorted current waveform will not impact the signal extraction results, as the load current is also distorted. The current waveform distortion can be eliminated though cycle-by-cycle subtraction.

3) Current randomness

The randomly distorted waveform may be a factor leading to the wrong signal extraction result, especially at the beginning of the contact. Our experiments using scaled down voltage and current show that when connecting two bare conductors as the scenarios of truck arm touching overhead line, the transient period will only last a few cycles, This may lead to a few cycle delays in detection. Experiment and detection results are shown in Figure 5.20.

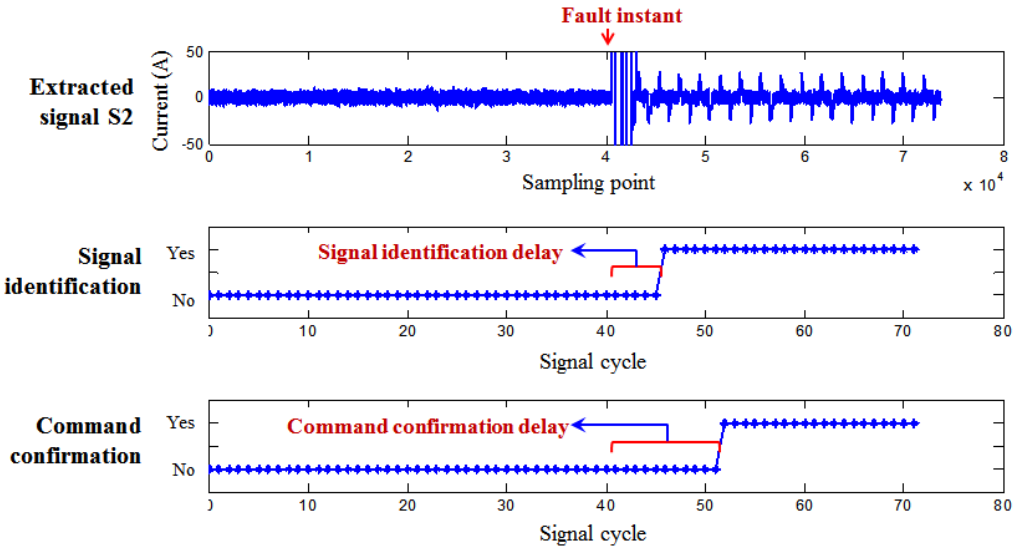

Figure 5.20 Effect of randomness of arcing current

4) Current intermittency

Intermittency of arc current can result in trip grounding signal missing during the arc extinction periods. In this case, the trip command will be delayed until the arc becomes stable. The intermittent arc always happens when the contact parts are not good inductive materials based on literature review [16]. However, the worksite equipment energization occurs always through a raised heavy metal part. When the metal part approaches close to the bare power line,

the two will immediately appeal to each other and positively conduct because of the electromagnetic force. Furthermore, our experiments also confirmed that the bare conductor contact resulted only for few cycles of arcing as shown in Figure 5.20 and no arc intermittency was observed.

Based on the above investigation, it can be concluded that, in most cases, arc fault happens when connecting two bare conductors is stable and constant. Therefore, when eliminated by cycle subtractions, arc fault will not have significant effects on signal detection and decision making process. Even if the arc may interrupt the signal detection occasionally because the significant randomness of arcing current waveform between one cycle and the next, the detection delay would only be less than 5 ~ 10 cycles.

Chapter 6
Conclusions and Future Work

6.1 Conclusions

This thesis discusses the electric hazards nearby medium voltage power lines at worksites. Shortcomings of traditional protection methods are reviewed and main causes of electric hazards nearby distribution power lines are investigated. To solve the challenges, this thesis develops an effective and economical power-electronics-based protection scheme to trip the upstream power supply and thus effectively ensure a safe condition for workers. The design of corresponding signal generator and detector as well as detection algorithms were presented in detail. The scheme was verified by simulations with sensitivity studies and field measurement data with specificity studies. Moreover, the comparison in the performance between traditional power line protection methods and proposed new strategies were conducted.

The key conclusions arising from this thesis are as follows:

- Traditional protection methods including insulation, isolation, equipotential bonding, and grounding may cause safety risks to the worksite personnel, and even produce a false and misleading signal of safety.

- An active signaling worksite protection scheme was proposed. A device was developed to perform the proposed strategy consisting of a portable signal generator equipped with several electronic devices, and a signal detector equipped with a low-cost microprocessor.They are installed between equipment and grounding rod at worksite and the closest recloser control, respectively. The communication path is established through the power line between the worksite and the closest recloser. In this way, the

protection coordination is no longer taken into consideration. Results show that the time required to clear fault was significantly improved.

- A diode-based signal generator module and its corresponding detection algorithms were designed. This signal generator produces half-cycle sinusoidal disturbance signals through the conducting and stopping characteristics of diodes. Meanwhile, the corresponding detector implemented at the upstream recloser was able to exclude current transient by a large standard deviation. And the detector was also able to recognize disturbance signals by the strengthened DC component in detected current and trip the recloser instantly to de-energize the worksite. The fault clearing time was limited within 4 cycles (0.0667 s) in the most of worksite conditions with decent grounding resistance and load current.

- A thyristor-based signal generator module with triggering control was developed to improve the feasibility of application in an extreme worksite condition and to ensure performance reliability. With this triggering control, signals with specific patterns were able to be achieved. By the new subtraction algorithms, signal strength was doubled in detection process. Therefore, the signal was much easier to be extracted and identified. The method was shown to be more effective with low-intense signals. The clearing time was 0.1 s ~ 0.15 s, as long as the load current was lower than 800 A for 25 kV feeders and 450 A for 13.8 kV feeders.

- The proposed scheme was useful and feasible in reality as practical challenges including portable size, signal strength, load transient, and grounding resistance were addressed by a proper parameter design in signal generator and detection algorithms in signal detector.

- Data from numerous simulations and field measurement verified the proposed scheme in both 25 kV and 13.8 kV distribution systems. Furthermore, as expected, sensitivity studies show that the major factors

influencing detecting time and accuracy are grounding resistance and load current.

- The proposed protection scheme dramatically shortened the fault clearing time compared to traditional relay protection methods. In addition, it was not dependent on the restriction of fault location and grounding resistance of the traditional method. The thyristor-based protection scheme even coped with issues of load transient. And it also resolved the high resistance-caused weak signals issues by using specific signal patterns. Hence, this device can be a potential alternative trip grounding device with more reliable and much faster response than traditional relay protection.

6.2 Future Work

The recommendations for future work are summarized as follows:

- The active protection scheme can be extended to other voltage levels by updating the signal generator parameter design and detection algorithms as required for the specific voltage level.

- The active protection scheme can be implemented in low voltage systems to improve cabinet enclosure grounding and other grounding scenarios.

- For simplicity and fast detection, we restricted firing angle to 90 degrees in the thyristor-based scheme in Chapter 4. In the future, this firing angle can be customized for conditions with sufficient time scenarios.

References

[1] J. Cawley, "White Paper on Occupational Electrical Accidents in the US 2003-2009," 2010.

[2] "Alberta municipal affairs, 'Statistics -- Electrical incidents in Alberta'. 2014.," 2014.

[3] "STATISTICS, Electrical incidents in Alberta, January 1 to December 31, 2013."

[4] "STATISTICS, Electrical incidents in Alberta, January 1 to December 31, 2014."

[5] NIOSH, "The National Institute for Occupational Safety and Health," 2013. [Online]. Available: http://www.cdc.gov/niosh/about.html.

[6] C. F. Dalziel, "Dangerous Electric Currents," *Am. Inst. Electr. Eng. Trans.*, vol. 65, no. 8, pp. 579–585, 1946.

[7] Dalziel Cf, "Electric shock hazard," *IEEE Spectr.*, vol. 9, no. 2, pp. 41–50, 1972.

[8] C. F. Dalziel and W. R. Lee, "Reevaluation of Lethal Electric Currents," *IEEE Trans. Ind. Gen. Appl.*, vol. IGA-4, no. 5, pp. 467–476, 1968.

[9] G. Biegelmeier and W. R. Lee, "New Considerations on the Threshold of Ventricular Fibrillation for a.c. Shocks at 50-60 Hz," *IEE Proceedings-A*, vol. 127, no. 2. pp. 103–110, 1980.

[10] IEEE Power and Energy Society, *IEEE Guide for Safety in AC Substation Grounding*, vol. 2000, no. February. 2013.

[11] J. Sverak, "Simplified Analysis of Electrical Gradients Above a Ground Grid-I How Good Is The Present IEEE Method? (A Special Report For WG 78.1)," *IEEE Trans. Power Appar. Syst.*, vol. PAS-103, no. 1, pp. 7–

25, 1984.

[12] J. A. Güemes-Alonso, F. E. Hernando-Fernández, F. Rodríguez-Bona, and J. M. Ruiz-Moll, "A practical approach for determining the ground resistance of grounding grids," *IEEE Trans. Power Deliv.*, vol. 21, no. 3, pp. 1261–1266, 2006.

[13] D. Prasad and H. C. Sharma, "SIGNIFICANCE OF STEP AND TOUCH VOLTAGES," *Int. J. Soft Comput. Eng. ISSN 2231-2307, Vol. Issue-5, Novemb. 2011*, no. 5, pp. 193–197, 2011.

[14] "Alberta Electrical Utility Code - 4th Edition, February 2013."

[15] CEE Relays Limited, "Application Guide for the Chioce of Protective Relay," *No*, 2000.

[16] J. C. Chen, B. T. Phung, D. M. Zhang, T. Blackburn, and E. Ambikairajah, "Study on High Impedance Fault Arcing Current Characteristics," *Power Eng. ...*, no. October, 2013

[17] R. Yu, Z. Fu, Q. Wang, S. Sun, H. Chen, Q. Xu, and X. Chen, "Modeling and simulation analysis of single phase arc grounding fault based on MATLAB," in *Proceedings of 2011 International Conference on Electronic & Mechanical Engineering and Information Technology*, 2011, vol. 9, pp. 4607–4610.

[18] P. Müller, "Characteristics of Series and Parallel Low Current Arc Faults in the Time and Frequency Domain," *... Contacts (HOLM), 2010 ...*, pp. 223–229, 2010.

[19] T. Cui, X. Dong, and Z. Bo, "Modeling study for high impedance fault detection in MV distribution system," *... , 2008. UPEC 2008. ...*, 2008.

[20] M. Michalik and W. Rebizant, "High-impedance fault detection in distribution networks with use of wavelet-based algorithm," *Power Deliv. ...*, vol. 21, no. 4, pp. 1793–1802, 2006.

[21] N. I. Elkalashy, M. Lehtonen, H. a. Darwish, M. a. Izzularab, and A. M. I. Taalab, “Modeling and experimental verification of high impedance arcing fault in medium voltage networks,” *IEEE Trans. Dielectr. Electr. Insul.*, vol. 14, no. 2, pp. 375–383, 2007.

[22] V. Torres, J. L. Guardado, H. F. Ruiz, and S. Maximov, “Modeling and detection of high impedance faults,” *Int. J. Electr. Power Energy Syst.*, vol. 61, pp. 163–172, 2014.

Appendix

Appendix A: Characteristics of Arcing

In the proposed scheme, all investigations are based on the assumption of a solid contact between signal generator and power grid. In reality, for some instances, the worksite equipment may not make a solid contact with energized power line. When the parts of equipment approach very close to the power line, the arc may already appear because of a significant difference in potential in the airgap. This appendix summarizes the characteristics of arc that may impact the performance of the proposed trip grounding method.

A.1 Characteristics of Arc Current

A typical arc characteristic and its underlying mechanisms can be summarized as follow.

(1) Current zero pause

A particular distortion around the current's zero crossing point is an evident feature of arc [19], [20]. The arc current as it approaches zero is slightly distorted from a true sinusoidal waveform due to the influence of arc voltage, which causes the current to flow in the opposite direction. Therefore the arc cannot be re-established immediately. Thus there is a finite time period when no current flows, which is generally referred to as the 'current zero pause'. This is an influencing factor in the detail distortions around the zero crossing points of the arc current waveform [21].

(2) Distortion and harmonics

In scope of each cycle, the waveform appears to be distorted by harmonics due to the ground resistance non-linearity and arcing phenomenon [18]. This can be explained by the change in the path resistance due to the thermal conditions. The more heat that is produced, the greater the conductance of the path would be [21].

(3) Randomness and intermittency

While in a longer time scale, arc bursts and extinguishes with intermittent patterns. This phenomenon can be due to environment temperature change, physical and chemical reactions of contact surfaces and moisture evaporation. Other facts like random swing of the conductor and motion of arc also contribute to arc's intermitting/random feature [19].

A.2 Review of the Appearance of Arc Current

Arc lasting time

One of the experiments is composed of alternating power supply (220V, 50 Hz), current sensor, digital filter and a part of model electrodes to simulate the arc's discharge, shown in Figure A.1 and results in Figure A.2.

Waveform 1 is normal current waveform, waveform 2 is arc current waveform, T1 is the waveform when the arc comes into being, T2 is the waveform when the arc is back to normal.

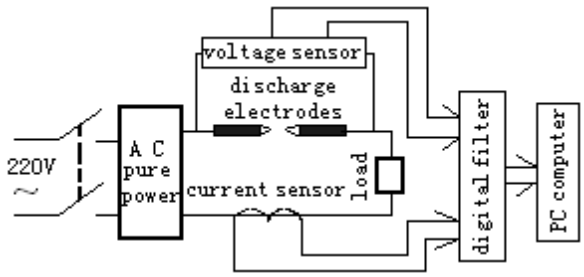

Figure A.1. Schematic diagram of experiment circuit

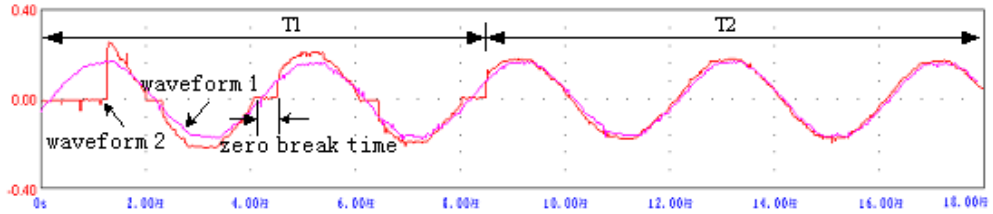

Figure A.2. Arc current waveform compared with natural current waveform

Arcing on different surfaces

Arcs were actually produced on different surfaces in the experiment. The applied voltage is 13.8 kV. Typical waveforms for each surface are shown in Figure A.3 ~ Figure A.6. The distortion is most evident around the zero crossings where the signal magnitude remains unchanged for a considerable time [15].

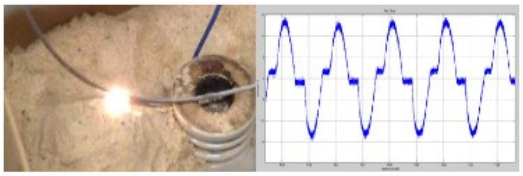

Figure A.3 Typical wet sand arc and waveform

Figure A.4 Typical soil arc and waveform

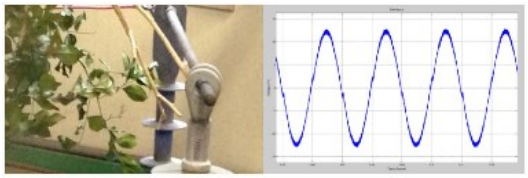

Figure A.5 Typical tree branch arc and waveform

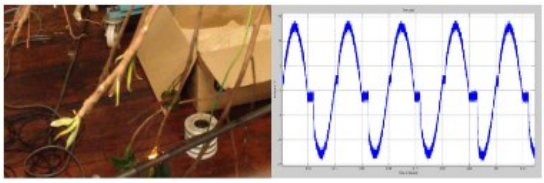

Figure A.6 Typical tree leaf arc and waveform

Comparison of series and parallel arc-fault

Peter M etc. [17] have investigated the difference between serial arc-fault and parallel arc-fault. The schematics of both experiments are shown in Figure A.7 and Figure A.8, and results are shown in Figure A.9 and Figure A.10.

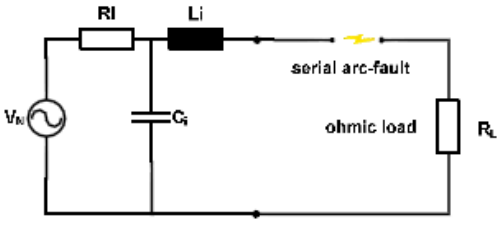

Figure A.7 Supply grid with ohmic load and arc fault in series to the connected

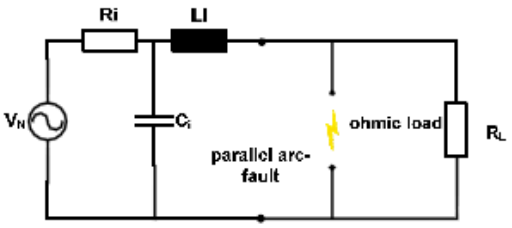

Figure A.8 Supply grid with arc in parallel to connected ohmic and inductive

load

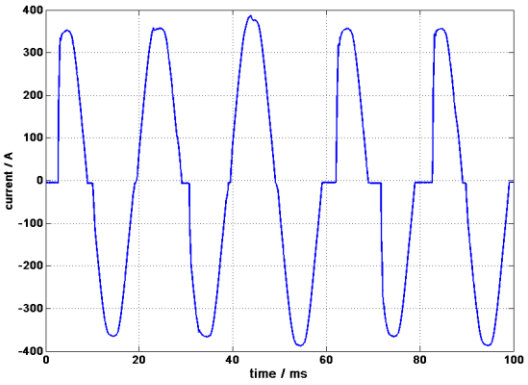

Figure A.9 Current measurement of series arc fault

load

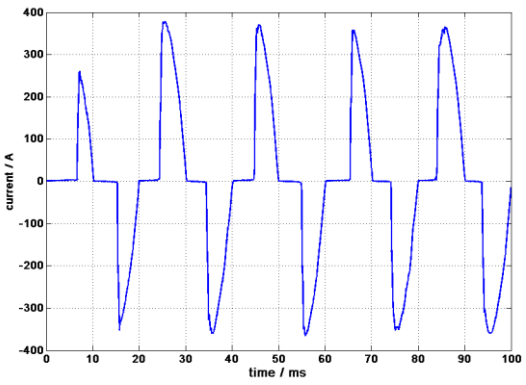

Figure A.10 Current measurement of parallel arc fault between two phases

In series arc fault, the current has gaps because the arc extinguishes after zero crossing. Due to molten copper, sometimes a conductive bridge forms, which prevents current interruption and arc re-ignition, such as the third positive half-wave in Figure A.9 [17]. The non-stable characteristic of arc extinguishing and re-ignition is more obvious in series arc fault, which is similar to the scenario of large grounding resistance.

For parallel arcs, the duration of the current gap is longer and occurs continuously after every current zero. Also the arc current is only limited by surface conditions of the failure region and the electrode. Therefore, the arc current might be much higher for parallel arcs than for series arcs, which is more similar to small grounding resistance scenario. The arc current and its characteristics are more stable and well defined in this circumstances [17].

Field test at 22 kV networks

Figure A.11 shows an ignition test undertaken by HRL at the TCA High Energy Facility at Lane Cove (NSW, Australia). Testing was carried out at 12,700 V (the conductor-to-earth voltage of Victoria's 22kV and SWER networks) at realistic fault currents ranging from 4.2 A to 1,000A.

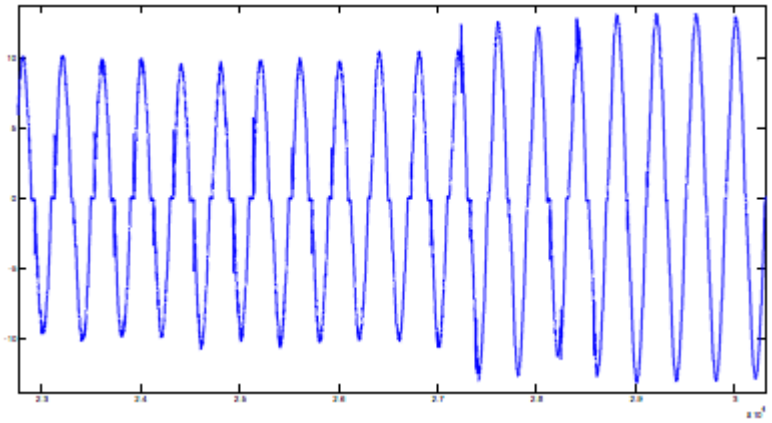

Figure A.11 Example of arc waveform

Field test at 10 kV networks

A measurement curve of arc current in the 10 kV voltage level is shown in Figure A.12. The arc current waveform is similar to sine wave, but it changes slowly in zero-current area, which characterized ‘zero-rest’ circled in the figure.

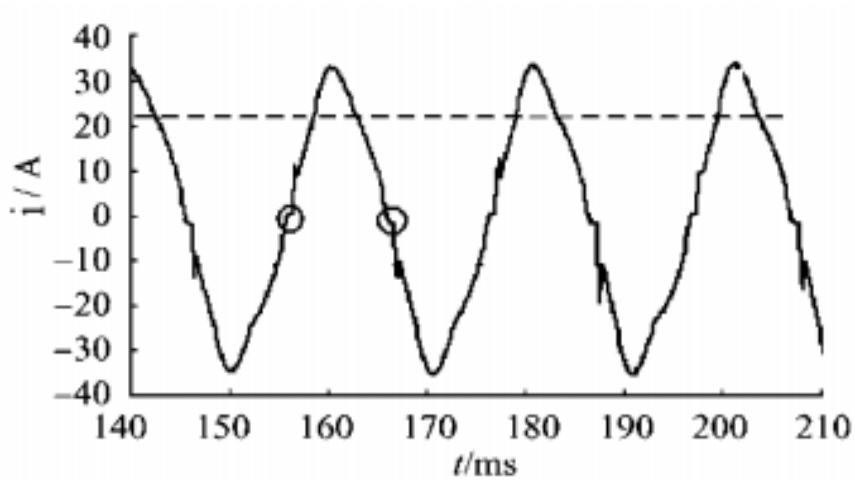

Figure A.12 Measured waveform of arc current [17]

The above figures of typical arc fault current clearly indicates different aspects of the arc features [18] : 1) The arc actually shapes the special details like the quench and re-ignition of fault current around zero-crossing point. 2) The waveform appears to be distorted by harmonics due to the ground resistance non-

linearity and arcing. 3) Arc bursts and extinguished with intermittent patterns, which can be explained by environment temperature change, physical and chemical reactions of contact surfaces and random swing of the conductor and motion of arc.

A.3 Bare Connection Experiments

Most of experiments above are done by connecting live line with conductive items. Since most equipment connecting to the live line are conductive, a series of arc experiments have been conducted to investigate the transient state of metal-to-metal contacts.

Bare connection between two metal conductors

Experiments were simulated by a normal 120 V AC source as the system, a suspended swing-free cable as overhead line, and a bare aluminum conductor moving close as worksite device. Experiment layout is shown in Figure A.13, and current of the cable has been recorded and shown in Figure A.14.

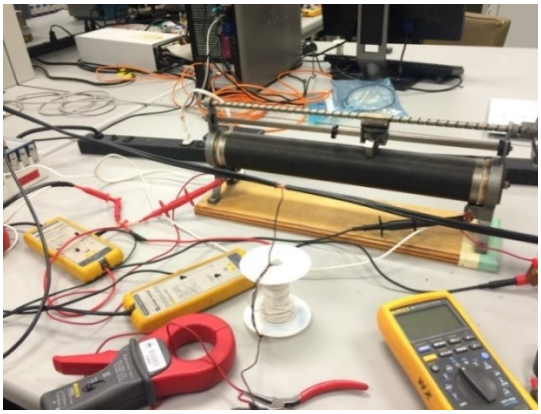

Figure A.13 Arc experiment layout

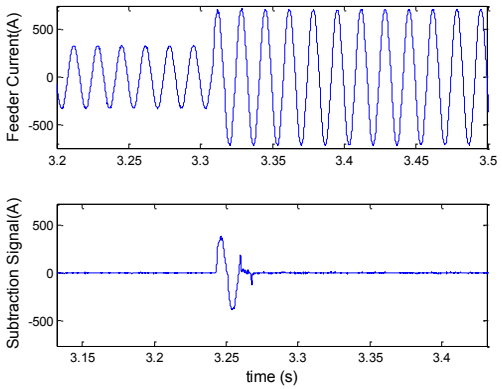

Figure A.14 Recorded feeder current and subtraction results

From the swinging of the freely suspended cable, we noticed a strong magnetic pull attracting the cable and aluminum conductor. As a result, a permanent fault was conducted due to this solid contact, which has been

confirmed from current waveforms. Furthermore, transient state of arc lasted for less than five cycles among all experiments, which indicates that the proposed scheme will only be affected in the first few cycles.

Bare connection through salted water

It might be possible that worksite was energized through conductive media but not direct contact, for example, when a worker used high pressure water jet to clean up an underground cable, the water may hit on some lacerations on cable skin, which leads to an accidental energization of cleaning devices and create hazards to workers. For these cases, experiments of connecting two bare conductors through salted water are conducted.

Bare conductor was oxidized immediately after connecting through water as shown in Figure A.15. Feeder current in Figure A.16 shows that feeder current increased by fault within the transient state as well as subtracted signals. Based on experiment results, connecting two bare conductors by conductive media can be regarded as connecting through impedance, in which a transient state will last for a few cycles.

Figure A.15 Experiment of connecting through salted water

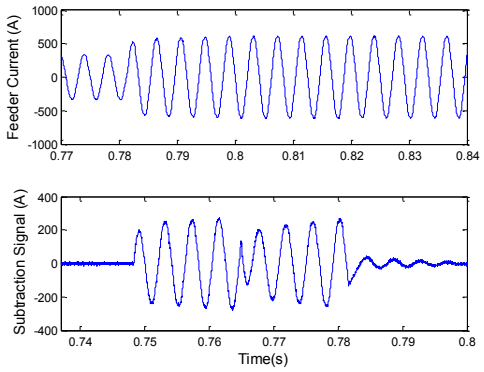

Figure A.16 Touching through heavily salted water